

# **For Reference**

---

**NOT TO BE TAKEN FROM THIS ROOM**



Ex LIBRIS  
UNIVERSITATIS  
ALBERTAENSIS







THE UNIVERSITY OF ALBERTA

RELEASE FORM

NAME OF AUTHOR: EDWARD S. KREBES

TITLE OF THESIS: SEISMIC BODY WAVES IN ANELASTIC MEDIA

DEGREE FOR WHICH THESIS WAS PRESENTED: Ph.D.

YEAR THIS DEGREE GRANTED: 1980

Permission is hereby granted to THE UNIVERSITY OF ALBERTA LIBRARY to reproduce single copies of this thesis and to lend or sell such copies for private, scholarly or scientific research purposes only.

The author reserves other publication rights, and neither the thesis nor extensive extracts from it may be printed or otherwise reproduced without the author's written permission.



THE UNIVERSITY OF ALBERTA

SEISMIC BODY WAVES IN ANELASTIC MEDIA

by



EDWARD S. KREBES

A THESIS

SUBMITTED TO THE FACULTY OF GRADUATE STUDIES AND RESEARCH  
IN PARTIAL FULFILMENT OF THE REQUIREMENTS FOR THE DEGREE  
OF DOCTOR OF PHILOSOPHY

DEPARTMENT OF PHYSICS

EDMONTON, ALBERTA

SPRING 1980



Digitized by the Internet Archive  
in 2020 with funding from  
University of Alberta Libraries

<https://archive.org/details/Krebes1980>



THE UNIVERSITY OF ALBERTA  
FACULTY OF GRADUATE STUDIES AND RESEARCH

The undersigned certify that they have read, and recommend to the Faculty of Graduate Studies and Research, for acceptance, a thesis entitled SEISMIC BODY WAVES IN ANELASTIC MEDIA submitted by EDWARD S. KREBES in partial fulfilment of the requirements for the degree of DOCTOR OF PHILOSOPHY.



## ABSTRACT

The linear theory of viscoelasticity is used to study the effects of anelasticity on seismic body waves propagating through a layered homogeneous isotropic medium. The mathematical formulation describing the propagation and attenuation of plane waves in a homogeneous isotropic linear viscoelastic medium is given. The particle motion associated with plane viscoelastic waves is examined, and is seen to be elliptical for P-SV waves and linear for SH waves. A conservation of energy equation for steady-state harmonic viscoelastic waves is derived from first principles and is used to calculate various time-averaged energy-related quantities such as energy fluxes, potential and kinetic energy densities, and dissipation rates. Reflection and transmission coefficients for plane waves impinging upon a plane boundary separating two linear viscoelastic media are calculated. The coefficients for SH waves are plotted and compared with the corresponding coefficients for the perfectly elastic case. Asymptotic ray theory is extended to homogeneous isotropic linear viscoelastic media, and the geometrical spreading factor for a given viscoelastic ray generated by a surface point source is calculated. Synthetic seismograms for SH body waves are computed for a plane-layered crustal model in both the elastic and anelastic cases, using a ray theory approach. Both the teleseismic case, and the case of a point source at the surface are





treated. The seismograms for the anelastic medium exhibit amplitude attenuation and waveform spreading.



## ACKNOWLEDGEMENTS

The author wishes to thank Prof. F. Hron for his guidance and advice throughout the course of this work.

The author also wishes to thank the Alberta Oil Sands Technology and Research Authority for awarding him an AOSTRA predoctoral scholarship.





# TABLE OF CONTENTS

CHAPTER	PAGE
1. INTRODUCTION	1
2. PLANE WAVE PROPAGATION AND ATTENUATION	4
3. PARTICLE MOTION AND ENERGY	11
3.1 Particle Motion	11
3.2 Energy	17
3.2.1 P Waves	22
3.2.2 SV Waves	29
3.2.3 SH Waves	32
4. REFLECTION AND TRANSMISSION AT A BOUNDARY	37
4.1 SH Waves	38
4.2 P-SV Waves	79
5. ASYMPTOTIC RAY THEORY FOR LINEAR VISCOELASTIC MEDIA	88
5.1 P Waves	93
5.2 S Waves	96
5.3 Geometrical Spreading	97
6. SYNTHETIC SEISMOGRAMS	106
6.1 Teleseismic Case	107
6.2 Surface Point Source Case	119
FOOTNOTES	132
REFERENCES	133
APPENDIX 1: FOURIER TRANSFORM OF $f(t) * dg(t)$	135
APPENDIX 2: THE INVERSE FOURIER TRANSFORM FOR A REAL RESPONSE	137



## LIST OF TABLES

TABLE	DESCRIPTION	PAGE
1	Crustal Model	108
2	Ray Codes for the Teleseismic Synthetic Seismograms	120
3	Ray Codes for the Surface Point Source Synthetic Seismograms	128





# LIST OF FIGURES

FIGURE	DESCRIPTION	PAGE
1	Incident, reflected and transmitted rays at a boundary separating two anelastic media	39
2	SH anelastic reflection coefficients illustrating jump discontinuities	48
3	Ray diagram illustrating an inhomogeneous elastic transmitted ray	58
4	H1H1 reflection coefficients	62
5	H1H2 transmission coefficients	66
6	H2H2 reflection coefficients	70
7	H2H1 transmission coefficients	74
8	Typical ray in a homogeneous layered medium	99
9	Ray tube between $K_0$ and $K$ for a homogeneous medium	100
10	Change in the cross-sectional area of the ray tube at an interface	102
11	Source pulse, and absolute value of spectrum	113
12	Synthetic seismograms for teleseismic SH body waves	116
13	Synthetic seismograms for SH body waves generated by a surface point source	122
14	H1H1 reflection coefficient for the perfectly elastic case.	130



# CHAPTER 1

## INTRODUCTION

It is becoming increasingly important to include the effects of anelasticity in the computation of synthetic seismograms and in other seismic modelling techniques. Anelastic effects such as the attenuation of seismic waves, are often modelled by the use of empirical laws deduced from seismic data. However, to facilitate the accurate interpretation of seismic field records, and to better understand the behaviour of seismic waves propagating in an anelastic medium, it is desirable to treat the anelasticity from a more physical viewpoint.

In this regard, a possible approach may be to use the linear theory of viscoelasticity to theoretically model the anelasticity. In this theory, an anelastic material is said to have "memory". In other words, the state of the material at a given time depends on the history of the material up to the given time. For instance, in the one-dimensional case, the stress on a solid at a given time  $t$  depends on all the strain forces that have acted on the solid in the past, up to the time  $t$ . In mathematical terms,

$$\sigma(t) = \int_{-\infty}^t r(t-\tau) \frac{de(\tau)}{d\tau} d\tau$$

where  $\sigma$  is the stress,  $e$  is the strain, and  $r$  is known as the relaxation function, and is a characteristic function of the solid. This equation is known as the Boltzman





after-effect equation. Various spring-dashpot models can be constructed to describe different types of viscoelastic solids. For each different model the relaxation function can be calculated, and the loss factors, which are measures of internal friction, can be calculated from the relaxation function. Detailed expositions of the linear theory of viscoelasticity can be found in such books as Fung (1965), Christensen (1971), Lockett (1972) and Flügge (1975).

The main purpose of this thesis is to examine the nature of seismic waves propagating in anelastic media and to investigate and develop methods of computing synthetic seismograms for plane layered anelastic media using a ray theory approach. The linear theory of viscoelasticity is used to model the anelasticity. The media are assumed to be homogeneous and isotropic. The numerical values of the loss factors (i.e., the reciprocal  $Q$ 's) for the various layers are assumed to be known, and are taken as input parameters in the calculations. The main advantage in this is that all calculations are then independent of any viscoelastic spring-dashpot model.

Since a ray theory approach is used, it is necessary to compute reflection and transmission coefficients for plane waves impinging upon a plane boundary separating two anelastic media. Some interesting aspects of the behaviour of plane waves propagating in layered anelastic materials are revealed by the examination of these coefficients and of the reflected and transmitted waves.



Synthetic seismograms are computed for both the teleseismic case, and the case of a point source at the surface. In the latter case, asymptotic ray theory is extended to include linear viscoelasticity and used to calculate the geometrical spreading factor for a given ray in a layered anelastic medium.

The results of the viscoelastic calculations are often compared with the analogous results for the perfectly elastic case, in order to better understand the effects of anelasticity. The elastic results are easily obtained since the theory of elasticity is contained within the theory of viscoelasticity as the special case of no dissipation.



## CHAPTER 2

### PLANE WAVE PROPAGATION AND ATTENUATION

In this chapter, we give the mathematical formulation necessary to describe the propagation and attenuation of plane seismic waves in a homogeneous isotropic linear viscoelastic medium (see Borchardt (1973, 1977), Silva (1976) and Buchen (1971a)).

The stress-strain relation for a homogeneous isotropic linear viscoelastic medium is given by

$$\begin{aligned}\sigma_{ij}(t) &= \delta_{ij} \int_{-\infty}^t \lambda(t-\tau) \frac{de_{kk}(\tau)}{d\tau} d\tau + 2 \int_{-\infty}^t \mu(t-\tau) \frac{de_{ij}(\tau)}{d\tau} d\tau \\ &= \delta_{ij} \lambda(t) * de_{kk}(t) + 2\mu(t) * de_{ij}(t)\end{aligned}\quad (2.1)$$

where the symbol  $*$  denotes the Stieltjes convolution (see, for example, Christensen (1971) and Fung (1965)).  $\lambda$  and  $\mu$  are the Lamé parameters, and  $e_{ij}$  is the strain tensor given by

$$e_{ij} = \frac{1}{2} (u_{i,j} + u_{j,i}) \quad (2.2)$$

where  $u_i$ ,  $i = 1, 2, 3$  is the displacement vector. The Einstein summation convention is used in (2.1), and in the equations that follow. As in the case of perfect elasticity, the viscoelastic stress-strain relation can be split into bulk and shear components as follows:





$$\sigma_{kk}(t) = 3\kappa(t) * de_{kk}(t) \quad (2.3)$$

$$\sigma_{ij}(t) = 2\mu(t) * de_{ij}(t), \quad i \neq j$$

where

$$\kappa(t) = \lambda(t) + \frac{2}{3}\mu(t) \quad (2.4)$$

Substituting (2.1) into the equation of motion

$$\sigma_{ij,j} = \rho \ddot{u}_i \quad (2.5)$$

yields, after some calculation,

$$[\lambda(t) + \mu(t)] * d(\nabla(\nabla \cdot \vec{u})) + \mu(t) * d(\nabla^2 \vec{u}) = \rho \ddot{\vec{u}} \quad (2.6)$$

in Cartesian coordinates. Taking the Fourier transform (see Appendix 1), we get

$$(\Lambda + M) \nabla(\nabla \cdot \vec{\bar{u}}) + M \nabla^2 \vec{\bar{u}} = -\rho \omega^2 \vec{\bar{u}} \quad (2.7)$$

where

$$\begin{aligned} \vec{\bar{u}} &= \int_{-\infty}^{\infty} \vec{u} e^{-i\omega t} dt \\ \Lambda &= \Lambda(\omega) = i\omega \int_0^{\infty} \lambda(t) e^{-i\omega t} dt \\ M &= M(\omega) = i\omega \int_0^{\infty} \mu(t) e^{-i\omega t} dt \end{aligned} \quad (2.8)$$



We can write  $\vec{u}$  in terms of Helmholtz potentials as

$$\vec{u} = \nabla \bar{\phi} + \nabla \times \vec{\bar{\psi}} \quad (2.9)$$

and inserting this in (2.7) gives

$$\begin{aligned} \nabla^2 \bar{\phi} + k_P^2 \bar{\phi} &= 0 \\ \nabla^2 \vec{\bar{\psi}} + k_S^2 \vec{\bar{\psi}} &= 0 \end{aligned} \quad (2.10)$$

where

$$\begin{aligned} k_P^2 &= \omega^2 / \alpha^2, \quad \alpha^2 = (\Lambda + 2M) / \rho \\ k_S^2 &= \omega^2 / \beta^2, \quad \beta^2 = M / \rho \end{aligned} \quad (2.11)$$

and where  $\rho$  is the density. We can see that the P and S velocities  $\alpha$  and  $\beta$  are now complex, and frequency-dependent.

The general Helmholtz equation can be written as

$$\nabla^2 \vec{F} + k^2 \vec{F} = 0 \quad (2.12)$$

which applies to both P waves ( $k = k_P$ ,  $\vec{F} = \bar{\phi}$ ) and S waves ( $k = k_S$ ,  $\vec{F} = \vec{\bar{\psi}}$ ). Its solution is a general plane wave given by

$$\vec{F} = \vec{F}_O e^{-\vec{A} \cdot \vec{r}} e^{-i\vec{P} \cdot \vec{r}} = \vec{F}_O e^{-i\vec{k} \cdot \vec{r}} \quad (2.13)$$



where

$$\vec{k} = \vec{P} - i\vec{A}. \quad (2.14)$$

$\vec{P}$  is the propagation vector, and is perpendicular to the planes of constant phase defined by  $\vec{P} \cdot \vec{r} = \text{constant}$ .  $\vec{A}$  is the attenuation vector and is perpendicular to the planes of constant amplitude defined by  $\vec{A} \cdot \vec{r} = \text{constant}$ . The velocity of the planes of constant phase is given by

$$\vec{v} = \frac{\omega}{|\vec{P}|} \hat{P} \quad (2.15)$$

where  $\hat{P}$  is a unit vector in the direction of  $\vec{P}$ .

From (2.14) we have

$$k^2 = \vec{k} \cdot \vec{k} = P^2 - A^2 - 2i \vec{P} \cdot \vec{A} \quad (2.16)$$

where

$$\vec{P} \cdot \vec{A} = PA \cos \gamma \quad (2.17)$$

where  $\gamma$  is the angle between  $\vec{P}$  and  $\vec{A}$ , and  $P$  and  $A$  are the magnitudes of  $\vec{P}$  and  $\vec{A}$ . If  $\vec{P}$  and  $\vec{A}$  are parallel ( $\gamma = 0$ ), the wave is called homogeneous. If  $\vec{P}$  and  $\vec{A}$  are not parallel ( $\gamma \neq 0$ ), the wave is called inhomogeneous. To ensure that the amplitude of the wave does not increase in the direction of propagation, we must have, in general,





$$0 \leq |\gamma| \leq \frac{\pi}{2} \quad (2.18)$$

Solving (2.16) and (2.17) for P and A, we get

$$P^2 = \frac{1}{2} \left( \text{Re}(k^2) + \{ [\text{Re}(k^2)]^2 + \frac{[\text{Im}(k^2)]^2}{\cos^2 \gamma} \}^{\frac{1}{2}} \right) \quad (2.19)$$

$$A^2 = \frac{1}{2} \left( -\text{Re}(k^2) + \{ [\text{Re}(k^2)]^2 + \frac{[\text{Im}(k^2)]^2}{\cos^2 \gamma} \}^{\frac{1}{2}} \right)$$

We can also express P and A in a more amenable form in terms of the loss factors and homogeneous phase speeds of the medium, which are assumed to be known, as shown below.

Following Borchardt (1973), we define the loss factor for P and S waves as

$$Q^{-1} = \begin{cases} Q_S^{-1} = \text{Im}(M)/\text{Re}(M), & \text{S waves} \\ Q_P^{-1} = \text{Im}(\Lambda+2M)/\text{Re}(\Lambda+2M), & \text{P waves.} \end{cases} \quad (2.20)$$

$k^2$  can then be written in terms of  $Q^{-1}$  as

$$k^2 = \frac{\omega^2}{v_H^2} \left[ \frac{2(1-iQ^{-1})}{1+\sqrt{1+Q^{-2}}} \right] \quad (2.21)$$

for both P and S waves (i.e.,  $k=k_S$ ,  $Q=Q_S$ ,  $v_H=v_{HS}$  for S waves, and  $k=k_P$ ,  $Q=Q_P$ ,  $v_H=v_{HP}$  for P waves), where  $v_H$  is the homogeneous phase speed of the wave. Substituting (2.21) into (2.19) yields



$$\begin{aligned}
P^2 &= \frac{\omega^2}{v_H^2} \left( \frac{1 + \sqrt{1+Q^{-2}/\cos^2 \gamma}}{1 + \sqrt{1+Q^{-2}}} \right) \\
A^2 &= \frac{\omega^2}{v_H^2} \left( \frac{-1 + \sqrt{1+Q^{-2}/\cos^2 \gamma}}{1 + \sqrt{1+Q^{-2}}} \right)
\end{aligned}
\tag{2.22}$$

for both P and S waves.

If the medium is non-dissipative ( $\text{Im}(k^2) = 0$ ), equation (2.17) shows that either  $\vec{A} = 0$  or  $\gamma = \pm \pi/2$ . Conversely, if  $\vec{A} = 0$  or  $\gamma = \pm \pi/2$  the medium is non-dissipative. Hence, we can say that the medium is dissipative if and only if  $\vec{A} \neq 0$  and  $\gamma \neq \pm \pi/2$  (i.e.,  $|\gamma| < \pi/2$ ). This shows that the only type of inhomogeneous plane wave that propagates in a non-dissipative medium (i.e., the wave with  $\vec{A} \neq 0$  and  $\gamma = \pm \pi/2$ ) does not propagate in a dissipative medium, and vice versa. This is a basic difference between the theories of elasticity and viscoelasticity.

Using the subscripts "IH" for "inhomogeneous" and "H" for "homogeneous", we can see from equations (2.15) and (2.19) or (2.22) that

$$\begin{aligned}
|\vec{v}_{IH}| &< |\vec{v}_H| \\
|\vec{A}_{IH}| &> |\vec{A}_H|
\end{aligned}
\tag{2.23}$$

i.e., the phase speed of an inhomogeneous wave is less than that of a homogeneous wave, and the maximum attenuation of an inhomogeneous wave is greater than that of a homogeneous



wave.

P and A can be calculated uniquely from the medium parameters, for a specified  $\gamma$ , from (2.19) or (2.22). However, the velocity and attenuation of an inhomogeneous wave in a non-dissipative medium ( $A \neq 0$ ,  $\gamma = \pm \pi/2$ ) cannot be uniquely determined from (2.19) or (2.22). They can only be determined once the boundary conditions have been specified. For an example of this non-uniqueness in the case of elasticity, consider the following two waves: an interface P-wave generated by an SV wave incident on a plane interface at an angle greater than the P-critical angle, and a Rayleigh wave on an elastic half-space. Both waves have  $\gamma = \pi/2$ , but their phase velocities are different.



## CHAPTER 3

### PARTICLE MOTION AND ENERGY

#### 3.1 Particle Motion

Borcherdt (1973) and Buchen (1971a) have shown that the particle motion for P-SV steady-state harmonic plane viscoelastic waves is elliptical, rather than linear as in the case of perfect elasticity.

This is demonstrated as follows. First, let us employ the usual steady-state harmonic condition on the displacement,

$$\vec{u} = \vec{U} e^{i\omega t} \quad (3.1)$$

and insert this into the time-domain equation of motion (2.6). We obtain

$$(\Lambda + M) \nabla (\nabla \cdot \vec{u}) + M \nabla^2 \vec{u} = \rho \ddot{\vec{u}} \quad (3.2)$$

where  $\Lambda$  and  $M$  are given by (2.8). Writing  $\vec{u}$  in terms of Helmholtz potentials

$$\vec{u} = \nabla \phi + \nabla \times \vec{\psi} \quad (3.3)$$

and inserting this into (3.2) yields





$$\nabla^2 \phi + k_P^2 \phi = 0 \quad (3.4)$$

$$\nabla^2 \vec{\psi} + k_S^2 \vec{\psi} = 0$$

where  $k_P$  and  $k_S$  are given by (2.11).

For P waves, the solution for  $\phi$  is given by

$$\phi = B e^{i(\omega t - \vec{k} \cdot \vec{r})} \quad (3.5)$$

where  $B$  is a complex constant,  $\vec{k} = \vec{P} - i\vec{A}$ , and where the subscript "P" has been suppressed in all the parameters. The displacement field is then given by

$$\begin{aligned} \vec{u} &= \nabla \phi \\ &= -i\vec{k}B e^{i(\omega t - \vec{k} \cdot \vec{r})} \\ &= -ie^{-\vec{A} \cdot \vec{r}} (kB) \frac{\vec{k}}{k} e^{i(\omega t - \vec{P} \cdot \vec{r})} \\ &= C \frac{\vec{k}}{k} e^{i\zeta(t)} \end{aligned} \quad (3.6)$$

where

$$C = |kB| e^{-\vec{A} \cdot \vec{r}} \quad (3.7)$$

$$\zeta(t) = \omega t - \vec{P} \cdot \vec{r} + \arg(kB) - \pi/2$$

The quantity  $\vec{k}/k$  can be written as



$$\frac{\vec{k}}{k} = \frac{\vec{P} - i\vec{A}}{k_R + ik_I} = \vec{\xi}_1 - i\vec{\xi}_2 \quad (3.8)$$

where

$$\vec{\xi}_1 = \frac{k_R \vec{P} - k_I \vec{A}}{|k|^2}, \quad \vec{\xi}_2 = \frac{k_I \vec{P} + k_R \vec{A}}{|k|^2} \quad (3.9)$$

The subscripts "R" and "I" refer to real and imaginary parts. Inserting these in (3.6), and taking the real part of  $\vec{u}$  to get the actual physical motion, yields

$$\vec{u}_R = C [\vec{\xi}_1 \cos \zeta(t) + \vec{\xi}_2 \sin \zeta(t)] \quad (3.10)$$

Also, using (2.16) and some rules of complex algebra, it is easy to show that

$$\vec{\xi}_1 \cdot \vec{\xi}_2 = 0 \quad (3.11)$$

$$\xi_1^2 - \xi_2^2 = 1$$

Hence  $\vec{\xi}_1$  and  $\vec{\xi}_2$  are perpendicular, and  $\xi_1 > \xi_2 \geq 0$ .

Setting

$$\begin{aligned} x &= \frac{\vec{u}_R \cdot \vec{\xi}_1}{C \xi_1} = \xi_1 \cos \zeta(t) \\ y &= \frac{\vec{u}_R \cdot \vec{\xi}_2}{C \xi_2} = \xi_2 \sin \zeta(t) \end{aligned} \quad (3.12)$$



reveals that

$$\left(\frac{x}{\xi_1}\right)^2 + \left(\frac{y}{\xi_2}\right)^2 = 1 \quad (3.13)$$

which is an ellipse with major axis  $\xi_1$ , and minor axis  $\xi_2$ . The motion is in the plane of  $\vec{P}$  and  $\vec{A}$ , and the direction of rotation is from  $\vec{P}$  to  $\vec{A}$ . For a homogeneous P wave ( $\gamma = 0$ ), it is easy to show that  $\xi_1 = 1$  and  $\xi_2 = 0$ , hence, the elliptical particle motion degenerates to straight-line or linear motion of a longitudinal nature, i.e. parallel to the direction of propagation  $\vec{P}$ .

A similar calculation can be performed for the SV wave, with similar results. The solution to (3.4) for  $\vec{\psi}$  representing the SV case is given by

$$\vec{\psi} = \vec{B} e^{i(\omega t - \vec{k} \cdot \vec{r})} \quad (3.14)$$

where  $\vec{B} = B\hat{n}$  with  $B$  a complex constant and  $\hat{n}$  a real unit vector, and where the subscript "S" has been suppressed in all the parameters. The subsidiary condition

$$\nabla \cdot \vec{\psi} = 0 \quad (3.15)$$

implies that

$$\vec{k} \cdot \vec{B} = (\vec{P} - i\vec{A}) \cdot \vec{B} = 0 \quad (3.16)$$



Hence,  $\hat{n}$  is perpendicular to  $\vec{P}$  and  $\vec{A}$ . The displacement field is given by

$$\begin{aligned}
 \vec{u} &= \nabla \times \vec{\psi} \\
 &= -i (\vec{k} \times \vec{B}) e^{i(\omega t - \vec{k} \cdot \vec{r})} \\
 &= -ie^{-\vec{A} \cdot \vec{r}} (kB) \frac{\vec{k}}{k} \times \hat{n} e^{i(\omega t - \vec{P} \cdot \vec{r})} \\
 &= C \frac{\vec{k}}{k} \times \hat{n} e^{i\zeta(t)} \tag{3.17}
 \end{aligned}$$

where

$$C = |kB| e^{-\vec{A} \cdot \vec{r}} \tag{3.18}$$

$$\zeta(t) = \omega t - \vec{P} \cdot \vec{r} + \arg(kB) - \pi/2$$

Following the same procedure as for P waves, using

$$\vec{u}_R = \text{Re}(\nabla \times \vec{\psi}) \tag{3.19}$$

we again obtain equations (3.10) - (3.13), where for SV waves,

$$\frac{\vec{k}}{k} \times \hat{n} = \vec{\xi}_1 - i\vec{\xi}_2 \tag{3.20}$$

with





$$\vec{\xi}_1 = \frac{(\mathbf{k}_R \vec{P} - \mathbf{k}_I \vec{A}) \times \hat{n}}{|\mathbf{k}^2|} \quad (3.21)$$

$$\vec{\xi}_2 = \frac{(\mathbf{k}_I \vec{P} + \mathbf{k}_R \vec{A}) \times \hat{n}}{|\mathbf{k}^2|}$$

For homogeneous waves,  $\xi_1 = 1$  and  $\xi_2 = 0$ , so the particle motion degenerates to linear transverse motion, perpendicular to  $\vec{P}$ .

Anelastic P-SV waves exhibit elliptical particle motion. However, for anelastic SH waves, Borchardt (1977) has shown that the particle motion is linear in the direction perpendicular to the plane containing  $\vec{P}$  and  $\vec{A}$ , i.e., the  $x_2$  or  $y$  direction, if we assume  $\vec{P}$  and  $\vec{A}$  lie in the  $x_1$ - $x_3$  or  $x$ - $z$  plane. This is the same motion as in the case of perfect elasticity. The solution to (3.4) for  $\vec{\psi}$  representing the SH case is given by

$$\vec{\psi} = \vec{B} e^{i(\omega t - \vec{k} \cdot \vec{r})} \quad (3.22)$$

where

$$\vec{B} = z_1 \hat{x}_1 + z_3 \hat{x}_3 \quad (3.23)$$

where  $z_1, z_3$  are arbitrary complex numbers, and  $\hat{x}_1, \hat{x}_3$  are real unit vectors in the  $x_1$  and  $x_3$  directions. Calculating the displacement field, we obtain



$$\begin{aligned}
\vec{u} &= \nabla \times \vec{\psi} \\
&= -i (\vec{k} \times \vec{B}) e^{i(\omega t - \vec{k} \cdot \vec{r})} \\
&= D e^{i(\omega t - \vec{k} \cdot \vec{r})} \hat{x}_2
\end{aligned} \tag{3.24}$$

where

$$D = (z_3 \hat{x}_1 - z_1 \hat{x}_3) \cdot (\vec{A} + i\vec{P}) \tag{3.25}$$

Taking the real part of  $\vec{u}$  to obtain the actual physical motion, yields

$$\vec{u}_R = |D| e^{-\vec{A} \cdot \vec{r}} \cos(\omega t - \vec{P} \cdot \vec{r} + \arg(D)) \hat{x}_2 \tag{3.26}$$

which represents a linear motion in the  $x_2$  direction.

### 3.2 Energy

In this section, we calculate various energy-related quantities such as kinetic and potential energy densities, dissipation rates, and energy fluxes for steady-state harmonic plane waves propagating in a linear viscoelastic medium. Such energy calculations have been carried out previously by Borchardt (1973) and Buchen (1971a), who used two different approaches. The calculations in this section combine the general aspects of these two papers to produce



a more general approach to the calculation of energy-related quantities. The approach is also different from the above-mentioned papers in that the equation for the conservation of energy is calculated from first principles.

The stress tensor for the steady-state harmonic case is obtained by substituting (3.1) into (2.1). The result is

$$\sigma_{ij} = \Lambda(\omega) \theta \delta_{ij} + 2M(\omega) e_{ij} \quad (3.27)$$

where

$$\theta = e_{kk} = \nabla \cdot \vec{u} \quad (3.28)$$

To obtain an equation for the conservation of energy, we begin by considering the power  $P$ , or rate of work done on a volume  $V$  with boundary  $S$ . Neglecting body forces,  $P$  is given by

$$P = \int_S \vec{t}_R \cdot \vec{v}_R \, dS \quad (3.29)$$

where  $\vec{t}$  is the traction and  $\vec{v}$  is the velocity. The traction is given by

$$\vec{t} = \vec{\sigma} \cdot \vec{v} \quad (3.30)$$

where  $\vec{\sigma}$  is the stress dyad and  $\vec{v}$  is a unit vector normal to



the boundary. Using the symmetry of the stress tensor, i.e.,

$$\sigma_{ij} = \sigma_{ji} \quad (3.31)$$

and the dyad-vector rules

$$\begin{aligned} (\vec{X} \cdot \vec{Y})_i &= \sum_j X_{ij} Y_j \\ (\vec{Y} \cdot \vec{X})_i &= \sum_j Y_j X_{ji} \end{aligned} \quad (3.32)$$

and Gauss's theorem, we have

$$\begin{aligned} p &= \int_S (\vec{\sigma}_R \cdot \vec{v}) \cdot \dot{\vec{u}}_R \, dS = \int_S \sigma_{ijR} v_j \dot{u}_{iR} \, dS \\ &= \int_S (\vec{\sigma}_R \cdot \dot{\vec{u}}_R) \cdot \vec{v} \, dS = \int_V \nabla \cdot (\vec{\sigma}_R \cdot \dot{\vec{u}}_R) \, dV \\ &= \int_V (\sigma_{ijR} \dot{u}_{iR})_{,j} \, dV \\ &= \int_V [\sigma_{ij,jR} \dot{u}_{iR} + \sigma_{ijR} \dot{u}_{i,jR}] \, dV \end{aligned} \quad (3.33)$$

Using the equation of motion (2.5), and the easily demonstrated fact

$$\sigma_{ijR} \dot{u}_{i,jR} = \sigma_{ijR} \dot{e}_{ijR} \quad (3.34)$$





equation (3.33) becomes

$$\begin{aligned}
 P &= \int_V [\rho \dot{u}_{iR} \ddot{u}_{iR} + \sigma_{ijR} \dot{e}_{ijR}] dV \\
 &= \frac{\partial}{\partial t} \left[ \int_V \frac{1}{2} \rho \dot{u}_{iR} \dot{u}_{iR} dV \right] + \int_V \sigma_{ijR} \dot{e}_{ijR} dV \quad (3.35)
 \end{aligned}$$

Using (3.33), we then obtain

$$\frac{\partial}{\partial t} \left[ \int_V \frac{1}{2} \rho \dot{u}_{iR} \dot{u}_{iR} dV \right] + \int_V \sigma_{ijR} \dot{e}_{ijR} dV = - \int_S \left[ -\vec{\sigma}_R \cdot \dot{\vec{u}}_R \right] \cdot \vec{n} dS \quad (3.36)$$

where

$$\frac{1}{2} \rho \dot{u}_{iR} \dot{u}_{iR} = \text{kinetic energy density} = \text{KED}$$

$$\sigma_{ijR} \dot{e}_{ijR} = \text{rate of change of strain energy density} \quad (3.37)$$

$$\left[ -\vec{\sigma}_R \cdot \dot{\vec{u}}_R \right] = \text{energy flux vector, or intensity} \equiv \vec{I}$$

Using (3.27), (3.32) and the dyad rule

$$(\nabla \vec{u})_{ij} = \frac{\partial}{\partial x_i} u_j \equiv \partial_i u_j = u_{j,i} \quad (3.38)$$

the rate of change of strain energy density, and the intensity  $\vec{I}$  can be expanded and expressed in terms of  $\Lambda$ ,  $M$  and the displacements. When this is done, (3.36) finally



becomes, after some algebra,

$$\frac{\partial}{\partial t} \left[ \int_V (\text{KED} + \text{PED}) \, dV \right] + \int_V \mathcal{D} \, dV = - \int_S \vec{I} \cdot \vec{\nu} \, dS \quad (3.39)$$

This is the equation expressing the conservation of energy for steady-state harmonic viscoelastic waves. KED is the kinetic energy density and PED is the potential energy density.  $\mathcal{D}$  is the rate of energy dissipation per unit volume.  $\vec{I} = \vec{I}_1 + \vec{I}_2$  is the energy flux, where  $\vec{I}_1$  is the rate at which the material inside (outside) the surface  $S$  is doing work on the material outside (inside), and  $\vec{I}_2$  is the rate at which energy is convected across the surface  $S$ . The mathematical expressions for these terms are

$$\begin{aligned} \text{KED} &= \frac{1}{2} \rho \dot{\vec{u}}_R^2 \\ \text{PED} &= \frac{1}{2} \Lambda_R \theta_R^2 + M_R e_{ijR} e_{ijR} \\ \mathcal{D} &= \frac{1}{\omega} [\Lambda_I \dot{\theta}_R^2 + 2M_I \dot{e}_{ijR} \dot{e}_{ijR}] \\ \vec{I} &= - \vec{\sigma}_R \cdot \dot{\vec{u}}_R = \vec{I}_1 + \vec{I}_2, \text{ where} \\ \vec{I}_1 &= -[\Lambda_R \theta_R \dot{\vec{u}}_R + M_R (\dot{\vec{u}}_R \cdot \nabla \vec{u}_R + \nabla \vec{u}_R \cdot \dot{\vec{u}}_R)] \\ \vec{I}_2 &= - \frac{1}{\omega} [\Lambda_I \dot{\theta}_R \dot{\vec{u}}_R + M_I (\dot{\vec{u}}_R \cdot \nabla \dot{\vec{u}}_R + \nabla \dot{\vec{u}}_R \cdot \dot{\vec{u}}_R)] \end{aligned} \quad (3.40)$$



We now calculate the time averages of several quantities for P, SV and SH waves, making use of the well known facts

$$\begin{aligned}
 \langle \cos^2 [\omega t - f(\vec{r})] \rangle &= 1/2 \\
 \langle \sin^2 [\omega t - f(\vec{r})] \rangle &= 1/2 \\
 \langle \sin [\omega t - f(\vec{r})] \cos [\omega t - f(\vec{r})] \rangle &= 0
 \end{aligned} \tag{3.41}$$

where  $\langle \dots \rangle$  denotes the time average over one cycle.

### 3.2.1 P Waves

The scalar potential  $\phi$  for P waves is given by (3.5), where  $\vec{k} = \vec{P} - i\vec{A}$ . The displacement is then given by

$$\vec{u} = \nabla \phi = -i\vec{k}B e^{i(\omega t - \vec{k} \cdot \vec{r})} \tag{3.42}$$

From (3.27), we obtain

$$\sigma_{ij} = -B\zeta_{ij} e^{i(\omega t - \vec{k} \cdot \vec{r})} \tag{3.43}$$

where

$$\zeta_{ij} = \Lambda k^2 \delta_{ij} + 2Mk_i k_j \tag{3.44}$$



The subscript  $i$  ( $i=1,2,3$ ) is not to be confused with the complex number  $i$ . The mean energy flux is then given by

$$\langle I_i \rangle = - \langle \sigma_{ijR} \dot{u}_{jR} \rangle \quad (3.45)$$

Using (3.41) - (3.43), this becomes, after some algebra,

$$\langle I_i \rangle = \frac{1}{2} \omega |B|^2 e^{-2\vec{A} \cdot \vec{r}} \text{Re}[\zeta_{ij} k_j^*] \quad (3.46)$$

where the superscript  $*$  denotes the complex conjugate.

Using

$$\Lambda k^2 = \rho \omega^2 - 2Mk^2 \quad (3.47)$$

$\zeta_{ij}$  can be written as

$$\zeta_{ij} = \rho \omega^2 \delta_{ij} + 2M(k_i k_j - k^2 \delta_{ij}) \quad (3.48)$$

Hence

$$\zeta_{ij} k_j^* = \rho \omega^2 k_i^* + 2M(k_i k_j - k^2 \delta_{ij}) k_j^* \quad (3.49)$$

It can be shown that

$$\begin{aligned} (k_i k_j - k^2 \delta_{ij}) k_j^* &= 2(A_j + iP_j)(P_i A_j - P_j A_i) \\ &= [2(\vec{A} \times \vec{P}) \times (\vec{A} + i\vec{P})]_i \end{aligned} \quad (3.50)$$





Using (3.49) and (3.50) in (3.46), we finally obtain for the mean energy flux,

$$\langle \vec{I} \rangle = \frac{1}{2} \omega |\mathbf{B}|^2 e^{-2\vec{A} \cdot \vec{r}} [\rho \omega^2 \vec{P} + 4(\vec{P} \times \vec{A}) \times (M_I \vec{P} - M_R \vec{A})] \quad (3.51)$$

For homogeneous waves ( $\vec{P} \times \vec{A} = 0$ ), this reduces to

$$\langle \vec{I} \rangle_H = \frac{1}{2} \rho \omega^3 |\mathbf{B}|^2 e^{-2\vec{A} \cdot \vec{r}} \vec{P} \quad (3.52)$$

and for a perfectly elastic material ( $M_I = 0$ ,  $\vec{P} \cdot \vec{A} = 0$ ), it reduces to

$$\langle \vec{I} \rangle_{el} = \frac{1}{2} \omega |\mathbf{B}|^2 e^{-2\vec{A} \cdot \vec{r}} [\rho \omega^2 + 4M_R A^2] \vec{P} \quad (3.53)$$

where the vector identity

$$(\vec{P} \times \vec{A}) \times \vec{A} = (\vec{P} \cdot \vec{A}) \vec{A} - (\vec{A} \cdot \vec{A}) \vec{P} \quad (3.54)$$

was used. From (3.51) - (3.53) we see that the direction of the mean energy flux is not, in general, the same as the direction of propagation, except for anelastic homogeneous waves, and elastic waves.

Next, we calculate the mean kinetic energy density. Using (3.41) and (3.42), it is easily calculated, and is given by



$$\begin{aligned}
\langle \text{KED} \rangle &= \left\langle \frac{1}{2} \rho \dot{u}_{iR} \dot{u}_{iR} \right\rangle \\
&= \frac{1}{4} \rho \omega^2 |B|^2 e^{-2\vec{A} \cdot \vec{r}} (P^2 + A^2)
\end{aligned} \tag{3.55}$$

The calculation of the mean potential energy density is more complicated. Using the expression given for PED in (3.40), and using (3.41) and (3.42), we obtain, after some algebra,

$$\begin{aligned}
\langle \text{PED} \rangle &= \left\langle \frac{1}{2} \Lambda_R \theta_R^2 + M_R e_{ijR} e_{ijR} \right\rangle \\
&= |B|^2 e^{-2\vec{A} \cdot \vec{r}} \left[ \frac{1}{4} \Lambda_R |k^2|^2 + \frac{1}{2} M_R (P^2 + A^2)^2 \right]
\end{aligned} \tag{3.56}$$

Equation (3.47) implies

$$\begin{aligned}
\Lambda_R &= \rho \omega^2 \text{Re} (1/k^2) - 2M_R \\
&= \rho \omega^2 \frac{(k^2)_R}{|k^2|^2} - 2M_R
\end{aligned} \tag{3.57}$$

Hence,

$$\begin{aligned}
\Lambda_R |k^2|^2 &= \rho \omega^2 (k^2)_R - 2M_R |k^2|^2 \\
&= \rho \omega^2 (P^2 - A^2) - 2M_R |k^2|^2
\end{aligned} \tag{3.58}$$

and so  $\langle \text{PED} \rangle$  becomes



$$\langle \text{PED} \rangle = \frac{1}{4} |B|^2 e^{-2\vec{A} \cdot \vec{r}} [\rho \omega^2 (P^2 - A^2) + 2M_R \{ (P^2 + A^2)^2 - |k^2|^2 \}] \quad (3.59)$$

Using (2.16), one can show that

$$(P^2 + A^2)^2 - |k^2|^2 = 4 |\vec{P} \times \vec{A}|^2 \quad (3.60)$$

Hence, we finally obtain

$$\langle \text{PED} \rangle = \frac{1}{4} |B|^2 e^{-2\vec{A} \cdot \vec{r}} [\rho \omega^2 (P^2 - A^2) + 8M_R |\vec{P} \times \vec{A}|^2] \quad (3.61)$$

Note that  $\langle \text{PED} \rangle \neq \langle \text{KED} \rangle$  unless  $A = 0$  which occurs only for homogeneous waves in elastic media. Using (3.55) and (3.61), we can also obtain the total mean energy density  $\langle E \rangle$  :

$$\begin{aligned} \langle E \rangle &= \langle \text{KED} \rangle + \langle \text{PED} \rangle \\ &= \frac{1}{2} |B|^2 e^{-2\vec{A} \cdot \vec{r}} [\rho \omega^2 P^2 + 4M_R |\vec{P} \times \vec{A}|^2] \end{aligned} \quad (3.62)$$

We can now derive an interesting relationship between  $\langle E \rangle$  and  $\langle \vec{I} \rangle$ . Using the vector identity

$$\vec{A} \cdot (\vec{B} \times \vec{C}) = \vec{B} \cdot (\vec{C} \times \vec{A}) = \vec{C} \cdot (\vec{A} \times \vec{B}) \quad (3.63)$$

we can show that



$$\vec{P} \cdot \{ (\vec{P} \times \vec{A}) \times (M_I \vec{P} - M_R \vec{A}) \} = M_R |\vec{P} \times \vec{A}|^2 \quad (3.64)$$

Using this in (3.51) gives

$$\langle E \rangle = \frac{1}{\omega} \vec{P} \cdot \langle \vec{I} \rangle \quad (3.65)$$

i.e., the mean total energy density is proportional to the component of the mean energy flux along the direction of propagation.

Finally, we calculate the mean rate of energy dissipation per unit volume  $\langle \mathcal{D} \rangle$ . We could use the expression for  $\mathcal{D}$  in (3.40), but there is an easier way. First, we write (3.39) in differential form

$$\frac{\partial}{\partial t} (KED + PED) + \mathcal{D} = - \nabla \cdot \vec{I} \quad (3.66)$$

We have

$$\frac{\partial}{\partial t} (KED + PED) = \rho \dot{u}_{iR} \ddot{u}_{iR} + \Lambda_R \theta_R \dot{\theta}_R + 2M_R e_{ijR} \dot{e}_{ijR} \quad (3.67)$$

Now, it is easy to show that

$$\langle \text{Re} (g) \text{Re} (\dot{g}) \rangle = 0 \quad (3.68)$$

where  $g = G(\omega, \vec{r}) e^{i\omega t}$ , with  $G$  complex. Using this result, we have





$$\langle \frac{\partial}{\partial t} (\text{KED} + \text{PED}) \rangle = 0 \quad (3.69)$$

Hence, using (3.51),

$$\begin{aligned} \langle \mathcal{D} \rangle &= - \nabla \cdot \langle \vec{I} \rangle \\ &= 2\vec{A} \cdot \langle \vec{I} \rangle \end{aligned} \quad (3.70)$$

Evaluating this, using (3.63) to show that

$$\vec{A} \cdot \{ (\vec{P} \times \vec{A}) \times (M_I \vec{P} - M_R \vec{A}) \} = M_I |\vec{P} \times \vec{A}|^2 \quad (3.71)$$

we finally obtain

$$\langle \mathcal{D} \rangle = \omega |\mathbf{B}|^2 e^{-2\vec{A} \cdot \vec{r}} [\rho \omega^2 (\vec{P} \cdot \vec{A}) + 4M_I |\vec{P} \times \vec{A}|^2] \quad (3.72)$$

Equation (3.70) shows that the mean rate of energy dissipation per unit volume is proportional to the component of the mean energy flux along  $\vec{A}$ . For homogeneous waves, we have

$$\langle \mathcal{D} \rangle_H = \rho \omega^3 |\mathbf{B}|^2 e^{-2\vec{A} \cdot \vec{r}} \text{PA} \quad (3.73)$$

and for elastic waves ( $M_I = 0$ ,  $\vec{P} \cdot \vec{A} = 0$ ), we have

$$\langle \mathcal{D} \rangle_{el} = 0 \quad (3.74)$$



### 3.2.2 SV Waves

We now calculate the same quantities for SV waves. The potential  $\vec{\psi}$  for SV waves is given by (3.14), with  $\vec{k} = \vec{P} - i\vec{A}$  as usual. Using (3.17), the displacement is given by

$$\vec{u} = \nabla \times \vec{\psi} = -iB \vec{m} e^{i(\omega t - \vec{k} \cdot \vec{r})} \quad (3.75)$$

where

$$\vec{m} = \vec{k} \times \hat{n} \quad (3.76)$$

Noting that

$$\theta = \nabla \cdot \vec{u} = \nabla \cdot (\nabla \times \vec{\psi}) = 0 \quad (3.77)$$

equation (3.27) gives

$$\sigma_{ij} = -MB (k_i m_j + k_j m_i) e^{i(\omega t - \vec{k} \cdot \vec{r})} \quad (3.78)$$

To obtain the mean energy flux, we start by using (3.41), (3.75) and (3.78) to obtain

$$\begin{aligned} \langle I_i \rangle &= - \langle \sigma_{ijR} \dot{u}_{jR} \rangle \\ &= \frac{1}{2} \omega |B|^2 e^{-2\vec{A} \cdot \vec{r}} \text{Re}[M(k_i m_j + k_j m_i) m_j^*] \end{aligned}$$



$$= \frac{1}{2} \omega |B|^2 e^{-2\vec{A} \cdot \vec{r}} \text{Re}[M\{(\vec{m} \cdot \vec{m}^*)\vec{k} + (\vec{k} \cdot \vec{m}^*)\vec{m}\}] \quad (3.79)$$

Using (2.16), (3.16) and standard vector identities involving dot and cross products, we get, after some tedious algebra,

$$\vec{m} \cdot \vec{m}^* = P^2 + A^2 \quad (3.80)$$

$$(\vec{k} \cdot \vec{m}^*)\vec{m} = -2(\vec{P} \times \vec{A}) \times (\vec{A} + i\vec{P})$$

Using (3.80), we have

$$\text{Re}[M(\vec{m} \cdot \vec{m}^*)\vec{k}] = [M_R(P^2 + A^2)]\vec{P} + [M_I(P^2 + A^2)]\vec{A} \quad (3.81)$$

From (2.11) we obtain

$$\rho \omega^2 = M k^2 \quad (3.82)$$

and taking the real and imaginary parts of this equation, we get

$$M_R(P^2 - A^2) + 2M_I(\vec{P} \cdot \vec{A}) = \rho \omega^2 \quad (3.83)$$

$$-2M_R(\vec{P} \cdot \vec{A}) + M_I(P^2 - A^2) = 0$$

We now rewrite these as



$$M_R(P^2+A^2) = \rho\omega^2 + 2M_RA^2 - 2M_I(\vec{P}\cdot\vec{A}) \quad (3.84)$$

$$M_I(P^2+A^2) = 2M_R(\vec{P}\cdot\vec{A}) + 2M_I A^2$$

Substituting them into (3.81), and using standard vector identities, we obtain

$$\text{Re}[M(\vec{m}\cdot\vec{m}^*)\vec{k}] = \rho\omega^2\vec{P} + 2(\vec{P}\times\vec{A}) \times (M_I\vec{P} - M_R\vec{A}) \quad (3.85)$$

We also easily obtain

$$\text{Re}[M(\vec{k}\cdot\vec{m}^*)\vec{m}] = 2(\vec{P}\times\vec{A}) \times (M_I\vec{P} - M_R\vec{A}) \quad (3.86)$$

Hence, using (3.85) and (3.86) in (3.79), we finally obtain

$$\langle\vec{I}\rangle = \frac{1}{2} \omega |B|^2 e^{-2\vec{A}\cdot\vec{r}} [\rho\omega^2 \vec{P} + 4(\vec{P}\times\vec{A}) \times (M_I\vec{P} - M_R\vec{A})] \quad (3.87)$$

which has the same form as the mean energy flux for P waves. Using (3.70), this means that  $\langle\mathcal{D}\rangle$  will also have the same form as the  $\langle\mathcal{D}\rangle$  for P waves.

Only KED and PED remain. The mean kinetic energy density is easily calculated to be

$$\begin{aligned} \langle\text{KED}\rangle &= \left\langle \frac{1}{2} \rho \dot{u}_{iR} \dot{u}_{iR} \right\rangle \\ &= \frac{1}{4} \rho\omega^2 |B|^2 e^{-2\vec{A}\cdot\vec{r}} \text{Re}[\vec{m}\cdot\vec{m}^*] \end{aligned}$$





$$= \frac{1}{4} \rho \omega^2 |B|^2 e^{-2\vec{A} \cdot \vec{r}} (P^2 + A^2) \quad (3.88)$$

where (3.80) has been used. This again has the same form as the  $\langle KED \rangle$  for P waves. Hence, we can conclude that  $\langle PED \rangle$  will have the same form as  $\langle PED \rangle$  for P waves. Also, all of the results pertaining to the time-averaged quantities for P waves will also hold for SV waves.

### 3.2.3 SH Waves

Finally, we calculate the energy-related quantities for SH waves. The potential  $\vec{\psi}$  for SH waves is given by (3.22) and (3.23) with  $\vec{k} = \vec{P} - i\vec{A}$  as always. The displacement is given by (3.24) and (3.25). Taking equation (3.77) into account, the stress tensor becomes

$$\sigma_{ij} = -iMD (\delta_{i2}k_j + \delta_{j2}k_i) e^{i(\omega t - \vec{k} \cdot \vec{r})} \quad (3.89)$$

Applying this to the calculation of  $\langle \vec{I} \rangle$ , we get, using (3.24), (3.25) and (3.41),

$$\begin{aligned} \langle I_i \rangle &= - \langle \sigma_{ijR} \dot{u}_{jR} \rangle \\ &= \frac{1}{2} \omega |D|^2 e^{-2\vec{A} \cdot \vec{r}} \text{Re}[M \delta_{j2} (\delta_{i2}k_j + \delta_{j2}k_i)] \\ &= \frac{1}{2} \omega |D|^2 e^{-2\vec{A} \cdot \vec{r}} \text{Re}[M k_i] \\ &= \frac{1}{2} \omega |D|^2 e^{-2\vec{A} \cdot \vec{r}} (M_{R^P i} + M_{I^A i}) \end{aligned} \quad (3.90)$$



where we have used the fact that  $k_2 = P_2 - iA_2 = 0$ . Hence

$$\langle \vec{I} \rangle = \frac{1}{2} \omega |D|^2 e^{-2\vec{A} \cdot \vec{r}} (M_R \vec{P} + M_I \vec{A}) \quad (3.91)$$

We can rewrite this in a form similar to the P-SV case.

Equations (3.81) and (3.85) imply

$$(P^2 + A^2) (M_R \vec{P} + M_I \vec{A}) = \rho \omega^2 \vec{P} + 2(\vec{P} \times \vec{A}) \times (M_I \vec{P} - M_R \vec{A}) \quad (3.92)$$

hence

$$\langle \vec{I} \rangle = \frac{1}{2} \omega \frac{|D|^2}{h} e^{-2\vec{A} \cdot \vec{r}} [\rho \omega^2 \vec{P} + 2(\vec{P} \times \vec{A}) \times (M_I \vec{P} - M_R \vec{A})] \quad (3.93)$$

where

$$h \equiv P^2 + A^2 \quad (3.94)$$

Comparing (3.93) with the P-SV result, we see that it differs by a factor of 2 in the second vector term. As will be seen, this is also true for  $\langle \text{PED} \rangle$ ,  $\langle E \rangle$  and  $\langle D \rangle$ .

We can also relate D to B: using the vector identity

$$|\vec{X} \times \vec{Y}|^2 = (XY)^2 - (\vec{X} \cdot \vec{Y})^2 \quad (3.95)$$

and the fact that the condition  $\nabla \cdot \vec{\psi} = 0$  implies

$$\vec{B} \cdot \vec{A} = \vec{B} \cdot \vec{P} = 0$$



we obtain, after some algebra,

$$\begin{aligned}
 |D|^2 &= (|\vec{B}_R|^2 + |\vec{B}_I|^2) (P^2 + A^2) = (\vec{B} \cdot \vec{B}^*) (P^2 + A^2) \\
 \Rightarrow \frac{|D|^2}{h} &= \vec{B} \cdot \vec{B}^*
 \end{aligned} \tag{3.96}$$

The mean kinetic energy density can again be easily computed to be

$$\begin{aligned}
 \langle \text{KED} \rangle &= \langle \frac{1}{2} \rho \dot{u}_{iR} \dot{u}_{iR} \rangle \\
 &= \frac{1}{4} \rho \omega^2 \left( \frac{|D|^2}{h} \right) e^{-2\vec{A} \cdot \vec{r}} (P^2 + A^2)
 \end{aligned} \tag{3.97}$$

For the mean potential energy density, we again use (3.77), and obtain

$$\begin{aligned}
 \langle \text{PED} \rangle &= \langle M_R e_{ijR} e_{ijR} \rangle \\
 &= \frac{1}{4} \left( \frac{|D|^2}{h} \right) e^{-2\vec{A} \cdot \vec{r}} [M_R (P^2 + A^2)^2]
 \end{aligned} \tag{3.98}$$

We can again rewrite this in a form similar to the P-SV case: equation (3.60) implies

$$M_R (P^2 + A^2)^2 = 4M_R |\vec{P} \times \vec{A}|^2 + M_R |k^2|^2 \tag{3.99}$$

Using the equation  $Mk^2 = \rho\omega^2$ , we have



$$M_R = \rho \omega^2 \operatorname{Re} (1/k^2) = \rho \omega^2 (P^2 - A^2)/|k^2|^2$$

$$\Rightarrow M_R |k^2|^2 = \rho \omega^2 (P^2 - A^2) \quad (3.100)$$

Using this in (3.99) and (3.98), we finally obtain

$$\langle \text{PED} \rangle = \frac{1}{4} \left( \frac{|D|^2}{h} \right) e^{-2\vec{A} \cdot \vec{r}} [\rho \omega^2 (P^2 - A^2) + 4M_R |\vec{P} \times \vec{A}|^2] \quad (3.101)$$

The mean total energy density can now be calculated, and it is again given by the equation

$$\langle E \rangle = \frac{1}{\omega} \vec{P} \cdot \langle \vec{I} \rangle \quad (3.102)$$

The mean rate of energy dissipation per unit volume is easily computed to be

$$\begin{aligned} \langle \mathcal{D} \rangle &= 2\vec{A} \cdot \langle \vec{I} \rangle \\ &= \omega \left( \frac{|D|^2}{h} \right) e^{-2\vec{A} \cdot \vec{r}} [\rho \omega^2 (\vec{P} \cdot \vec{A}) + 2 M_I |\vec{P} \times \vec{A}|^2] \end{aligned} \quad (3.103)$$

In summary, the following general conclusions can be drawn:

- (a)  $\langle \vec{I} \rangle$  is not, in general, in the same direction as  $\vec{P}$ , except for elastic waves, and anelastic homogeneous waves





- (b)  $\langle \text{PED} \rangle \neq \langle \text{KED} \rangle$  except for homogeneous waves in a perfectly elastic medium
- (c)  $\langle E \rangle$  is proportional to the component of  $\langle \vec{I} \rangle$  along  $\vec{P}$
- (d)  $\langle D \rangle$  is proportional to the component of  $\langle \vec{I} \rangle$  along  $\vec{A}$ .



## CHAPTER 4

### REFLECTION AND TRANSMISSION AT A BOUNDARY

In this chapter, we treat the problem of the reflection and transmission of harmonic plane waves at a plane boundary separating two homogeneous isotropic linear viscoelastic materials. Previous treatments of this problem include papers by Lockett (1962), Cooper and Reiss (1966), Cooper (1967), Shaw and Bugl (1969), Schoenberg (1971) and Borchardt (1977). The classical problem of a line source situated at a finite distance from a plane interface separating two linear viscoelastic solids has been examined by Buchen (1971b).

The treatment of plane wave reflection and transmission by Borchardt (1977) is the most recent and the most general, and provides part of the theoretical framework for the computation of reflection and transmission coefficients in this chapter. In the first section, we treat the problem of the reflection and transmission of SH waves in detail, and examine some of the interesting characteristics exhibited by viscoelastic waves which are not exhibited in the perfectly elastic case. We then discuss the computation of reflection and transmission coefficients and present some examples to illustrate the differences between elasticity and viscoelasticity. The treatment of the P-SV case is very similar to the SH case, and is outlined in the second section.



#### 4.1 SH Waves

Figure 1 shows the incident, reflected and transmitted waves at a boundary separating two viscoelastic media  $V$  and  $V'$ . The complex propagation vectors  $\vec{k}$  for the incident and reflected waves can be written as

$$\vec{k}_{Sj} = k_{Sx} \hat{x} + (-1)^j d_{\beta} \hat{z} \quad (j=1,2) \quad (4.1)$$

where

$$d_{\beta} = \pm \text{p.v.} \sqrt{k_S^2 - k_{Sx}^2} \quad (4.2)$$

and where  $j=1$  denotes the incident wave, and  $j=2$  the reflected wave, and  $\hat{x}$  and  $\hat{z}$  are unit vectors in the  $x$  and  $z$  directions. For the transmitted wave, we have

$$\vec{k}'_S = k_{Sx} \hat{x} - d'_{\beta} \hat{z} \quad (4.3)$$

where

$$d'_{\beta} = \pm \text{p.v.} \sqrt{k_S'^2 - k_{Sx}^2} \quad (4.4)$$

The symbol p.v. denotes the principal value of the complex square root, i.e., the complex root for which  $-90^\circ < \eta \leq +90^\circ$ , where  $\eta$  is the angle that the root makes in the complex plane. The choice of sign for  $d_{\beta}$  and  $d'_{\beta}$  will be discussed further on in this section.

In these equations, we have set

$$k_{Sx}(\text{inc.}) = k_{Sx}(\text{refl.}) = k_{Sx}(\text{transm.}) \equiv k_{Sx} \quad (4.5)$$



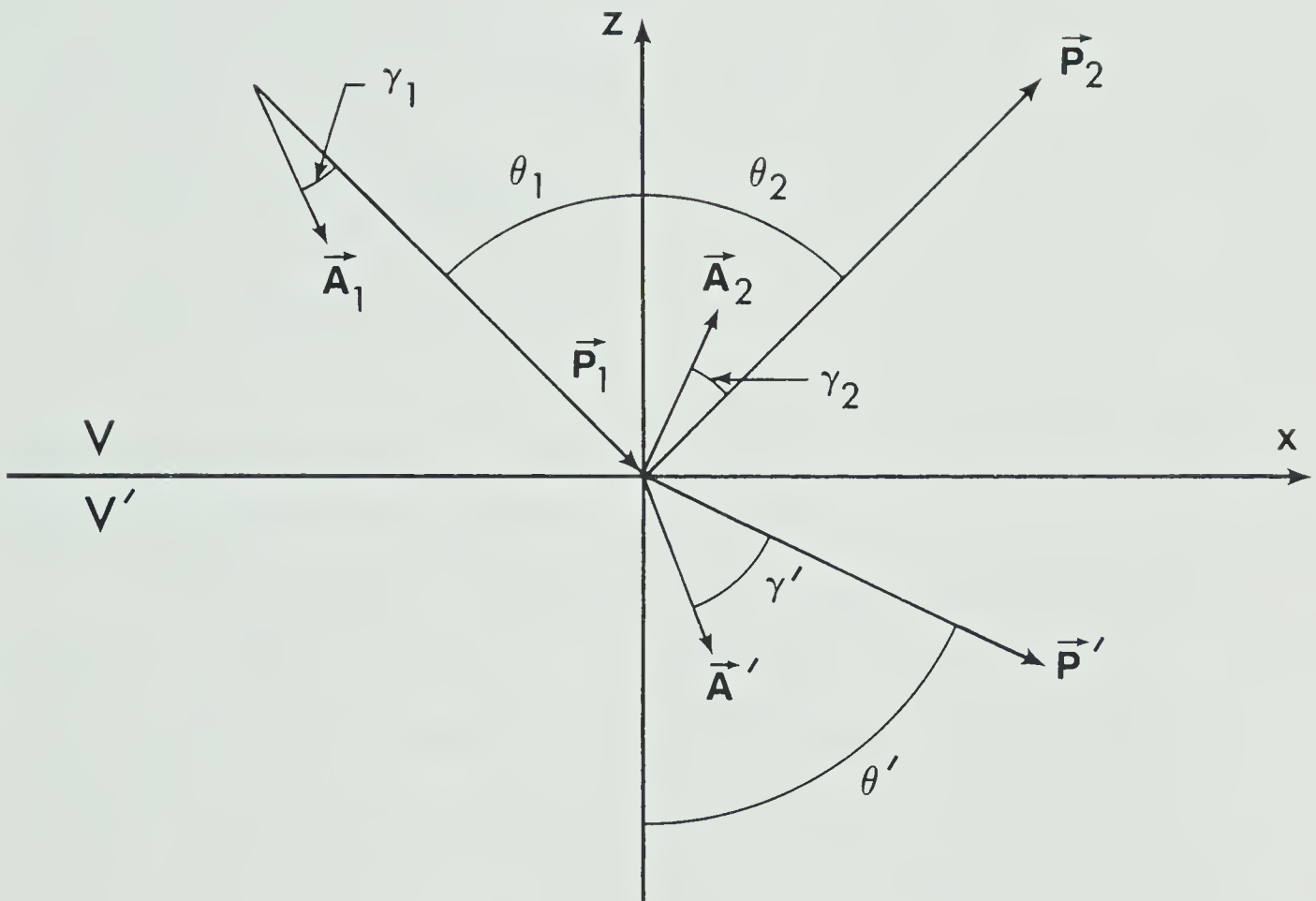


FIGURE 1: Incident, reflected and transmitted rays at a boundary separating two anelastic media. The angles  $\gamma$  lie between  $-90^\circ$  and  $+90^\circ$ . They are positive as shown.





in anticipation, since this will be the condition required to satisfy the boundary conditions of this problem.

From the equations  $\vec{k}_S = \vec{p}_S - i\vec{A}_S$ , we can calculate the propagation and attenuation vectors for the three waves. Suppressing the subscript "S" from hereon in, we obtain

$$\left. \begin{aligned} \vec{p}_j &= k_{xR} \hat{x} + (-1)^j d_{\beta R} \hat{z} \\ \vec{A}_j &= -k_{xI} \hat{x} + (-1)^{j+1} d_{\beta I} \hat{z} \end{aligned} \right\} \quad j=1,2$$

$$\vec{p}' = k_{xR} \hat{x} - d'_{\beta R} \hat{z}$$

$$\vec{A}' = -k_{xI} \hat{x} + d'_{\beta I} \hat{z}$$
(4.6)

where the subscripts "R" and "I" stand for the real and imaginary parts, as before.

To obtain the reflection and transmission coefficients (by which we mean the complex relative wave amplitudes of reflection and transmission, and not the squares of their magnitudes), we assume the two media are in welded contact, which means we require the stress and displacement to be continuous across the boundary. The stress and displacement for SH waves are given by (3.89) and (3.24) respectively. Hence, we have at  $z=0$ ,

$$\vec{u} = \vec{u}'$$
(4.7)

$$\sigma_{32} = \sigma'_{32} \quad (\sigma_{31} = \sigma_{33} = 0)$$

where



$$\vec{u} = \sum_{j=1}^2 D_j e^{i(\omega t - \vec{k}_j \cdot \vec{r})} \hat{y} \quad (4.8)$$

$$\vec{u}' = D' e^{i(\omega t - \vec{k}' \cdot \vec{r})} \hat{y}$$

Assuming, for the moment, that the three  $k_x$ 's are unequal, equations (4.7) lead to

$$\begin{aligned} D_1 e^{-ik_{x1}x} + D_2 e^{-ik_{x2}x} &= D' e^{-ik'_x x} \\ Md_{\beta 1} D_1 e^{-ik_{x1}x} - Md_{\beta 2} D_2 e^{-ik_{x2}x} &= M'd'_{\beta} D' e^{-ik'_x x} \end{aligned} \quad (4.9)$$

Since the complex amplitudes  $D_1$ ,  $D_2$  and  $D'$  are independent of the spatial coordinates  $x$ ,  $y$  and  $z$ , equation (4.9) implies

$$k_{x1} = k_{x2} = k'_x \equiv k_x \quad (4.10)$$

which is the equivalent of equation (4.5). Equation (4.5) (or (4.10)) leads to the anelastic form of Snell's law, as we shall see below. Equations (4.9) now become

$$D_1 + D_2 = D' \quad (4.11)$$

$$Md_{\beta} (D_1 - D_2) = M'd'_{\beta} D'$$

and the solutions are

$$\begin{aligned} \frac{D_2}{D_1} &= \frac{Md_{\beta} - M'd'_{\beta}}{Md_{\beta} + M'd'_{\beta}} \\ \frac{D'}{D_1} &= \frac{2Md_{\beta}}{Md_{\beta} + M'd'_{\beta}} \end{aligned} \quad (4.12)$$



The first equations in (4.12) gives the reflection coefficient, and the second gives the transmission coefficient.

The SH reflection coefficient at a free surface is easily obtained from (4.11) by equating the stress at the surface to zero, which yields  $D_1 = D_2$ , i.e.,  $(D_2/D_1) = 1$ .

As mentioned above, equation (4.5) leads to Snell's law for viscoelastic media. Since  $k_x = P_x - iA_x$ , there are now two parts to Snell's law, i.e.  $A_x$ , as well as  $P_x$ , must be continuous across the boundary. Referring to Figure 1, this implies

$$\begin{aligned} P_1 \sin\theta_1 &= P_2 \sin\theta_2 = P' \sin\theta' = k_{xR} \\ A_1 \sin(\theta_1 - \gamma_1) &= A_2 \sin(\theta_2 - \gamma_2) = A' \sin(\theta' - \gamma') \\ &= -k_{xI} \end{aligned} \tag{4.13}$$

This is the anelastic version of Snell's law. If

$|\vec{v}| = \omega/|\vec{P}|$  is substituted into the first equation of (4.13), it takes the form

$$\frac{\sin\theta_1}{|\vec{v}_1|} = \frac{\sin\theta_2}{|\vec{v}_2|} = \frac{\sin\theta'}{|\vec{v}'|} \tag{4.14}$$

where  $|\vec{v}_1|$ ,  $|\vec{v}_2|$  and  $|\vec{v}'|$  are the phase speeds of the incident, reflected and transmitted waves. From Chapter 2, we see that the phase speeds depend on  $\gamma_1$ ,  $\gamma_2$  and  $\gamma'$  respectively, and since  $\gamma'$  will generally depend on the angle of incidence  $\theta_1$ , the phase velocity of the trans-



mitted wave will also depend on  $\theta_1$ .

Equations (4.6) show that  $|\vec{P}_1| = |\vec{P}_2|$  and  $|\vec{A}_1| = |\vec{A}_2|$ , hence equations (4.13) show that  $\theta_1 = \theta_2$  and  $\gamma_1 = \gamma_2$ .

A critical angle for the transmitted SH wave is defined as an angle of incidence for which the transmitted SH wave propagates parallel to the interface. The following theorems, originally due to Borchardt (1977), show that critical angles for viscoelastic media differ in nature from those for elastic media.

Theorem 1: If medium V is perfectly elastic, and medium V' anelastic, then there are no critical angles for the transmitted SH wave.

Proof: Suppose  $\theta_1$  is a critical angle for the transmitted SH wave, i.e.  $\theta' = \pi/2$ , and  $\vec{P}'$  is in the x direction. Since V is perfectly elastic,  $A_1 = 0$  and (4.13) shows that  $k_{xI} = 0$ . Hence, from (4.6),  $\vec{A}'$  is in the z direction, which means  $\gamma' = \pm \pi/2$ , i.e.  $\vec{P}' \cdot \vec{A}' = 0$ . But we know from Chapter 2 that such a wave cannot propagate in an anelastic medium. Hence, there are no critical angles in this case.

Theorem 2: If medium V is anelastic and  $\theta_1$  is a critical angle for the transmitted SH wave ( $\theta_1 \neq \pi/2$ ), then

$$\sin \theta_1 \sin(\theta_1 - \gamma_1) = \xi \cos \gamma_1 \quad (4.15)$$

where





$$\xi = \frac{(k'^2)_I}{(k^2)_I} = \frac{k'_R k'_I}{k_R k_I} \quad (4.16)$$

Proof: If  $\theta_1$  is a critical angle for the transmitted SH wave, then the equation for  $\vec{P}'$  in (4.6) implies  $d'_{\beta R} = 0$ , which implies

$$2d'_{\beta R} d'_{\beta I} = \text{Im}[d'^2_{\beta}] = (k'^2)_I - (k^2_x)_I = 0 \quad (4.17)$$

Now using (4.13) and (2.16), we have

$$\begin{aligned} (k^2_x)_I &= \text{Im}[(k_{xR} + ik_{xI})^2] = 2k_{xR}k_{xI} \\ &= -2P_1 A_1 \sin \theta_1 \sin(\theta_1 - \gamma_1) \\ &= \frac{(k^2)_I}{\cos \gamma_1} \sin \theta_1 \sin(\theta_1 - \gamma_1) \end{aligned}$$

Using this in (4.17) gives the required relation (4.15).

The above theorem is stated and proved in a form slightly different from that of Borchardt (1977).

Corollary 2.1: If  $V$  is anelastic and  $V'$  elastic, then there exists at most one critical angle, namely  $\theta_1 = \gamma_1$ .

Proof: If  $V'$  is elastic, then  $(k'^2)_I = 0$ , hence  $\xi = 0$ , and (4.15) becomes

$$\sin \theta_1 \sin(\theta_1 - \gamma_1) = 0 \quad (4.18)$$

Hence, if  $\theta_1$  is critical, then  $\theta_1 = \gamma_1$ .



Theorem 2 shows that critical angles can exist only when (4.15) is satisfied, i.e., for distinct values of  $\theta_1$  and  $\gamma_1$ . This means that critical angles in viscoelastic media are discrete. In other words, if  $\theta_c$  is a critical angle and  $\theta_1$  is increased beyond  $\theta_c$ , then  $\theta_1$  is no longer a critical angle, i.e. the transmitted propagation vector  $\vec{P}'$  is no longer parallel to the interface.  $\vec{P}'$  is parallel to the interface only for  $\theta_1 = \theta_c$ . This result represents a significant deviation from perfect elasticity theory. Cooper (1967) obtained the same result. Note that Theorem 2 does not imply that every solution  $\theta_1$  of (4.15) is a critical angle;  $\theta_1$  could be an angle for which  $\vec{A}'$ , rather than  $\vec{P}'$ , is parallel to the interface.

For two anelastic media, the quantities pertaining to the transmission medium, i.e.  $P'$ ,  $A'$ ,  $\theta'$  and  $\gamma'$ , can be calculated as follows. First of all, we assume that  $\theta_1$  and  $\gamma_1$  are initially known, along with the medium parameters, i.e. the densities, homogeneous phase speeds, and loss factors.  $P_1$ ,  $A_1$  and hence  $k_x$  can then be calculated.  $k^2$  and  $k'^2$  can be calculated solely from the medium parameters. We can then see from (4.6) that the magnitudes of the transmitted propagation and attenuation vectors  $\vec{P}'$  and  $\vec{A}'$  are given by

$$\begin{aligned} P' &= \sqrt{k_{xR}^2 + d_{\beta R}'^2} \\ A' &= \sqrt{k_{xI}^2 + d_{\beta I}'^2} \end{aligned} \tag{4.19}$$



The angle of transmission,  $\theta'$ , is obviously given by

$$\theta' = \tan^{-1} \left( \frac{k_{xR}}{d'_{\beta R}} \right) \quad (4.20)$$

Once  $P'$ ,  $A'$  and  $\theta'$  are known,  $\gamma'$  can then be calculated from (4.13). Since  $Q$  is, in general, frequency-dependent, velocities and angles will also, in general, depend on frequency.

Equation (4.20) shows that  $\theta'$  depends on  $d'_{\beta R}$ , and as mentioned earlier, there is a choice of sign to be considered in the calculation of  $d'_{\beta}$ , i.e., a choice of which of the two square roots to use (see (4.4)). Intuitively, one would expect that the "+" sign would always be chosen, because this would make  $d'_{\beta R}$  always positive, and hence from (4.6)  $\vec{P}'$  would always point in the proper direction, i.e. it would always point into the transmission medium. However, such a choice of sign has been found to introduce errors in the computation of the reflection and transmission coefficients at and beyond the critical angle (if one exists). For example, assuming that a critical angle  $\theta_c$  for the transmitted SH wave exists, let us consider an angle of incidence  $\theta_1$  slightly less than  $\theta_c$ , and suppose that  $d'_{\beta}$ , for this angle of incidence  $\theta_1$ , lies in the 4th quadrant of the complex plane, near the imaginary axis. In other words,  $d'_{\beta}$  makes an angle slightly greater than  $-90^\circ$  in the complex plane, i.e.  $d'_{\beta}$  is almost purely imaginary (it is often the case that  $d'_{\beta R} \geq 0$  and  $d'_{\beta I} \leq 0$  for



$0 \leq \theta_1 < \theta_c$ ). For the critical angle  $\theta_c$ ,  $\vec{P}'$  is in the x direction, i.e. parallel to the interface, hence (4.6) implies  $d'_{\beta R} = 0$  and that  $d'_\beta$  is purely imaginary, i.e.,  $d'_\beta = \pm \text{p.v.} \sqrt{k'^2 - k_x^2} = \pm ia$ , where "a" is a constant. If we choose the "+" sign, i.e. the "positive" root, then, due to the definition of the principal value,  $d'_{\beta I}$  undergoes a sudden change of sign, from negative for  $\theta_1 < \theta_c$ , to positive for  $\theta_1 = \theta_c$ . As we can see from (4.12), this would correspondingly introduce a sudden change in the reflection and transmission coefficients at the critical angle, i.e. a jump discontinuity at  $\theta_c$  (see Figure 2a).<sup>†</sup> To avoid this, we must choose the "-" sign at  $\theta_c$ . For super-critical incident angles, the same problem occurs since  $d'^2_\beta$ , which lies along the negative real axis of the complex plane for  $\theta_1 = \theta_c$ , moves upwards, in this particular example, into the 2nd quadrant for  $\theta_1 > \theta_c$ , which means that choosing the "+" sign for  $d'_\beta$ , i.e. the "positive" root, would again cause the same sudden change of sign (- to +) in  $d'_{\beta I}$ , due to the definition of the principal value. Hence, to eliminate the jump discontinuities in the reflection and transmission coefficients, i.e. to obtain smooth continuous curves, we must choose the sign of  $d'_\beta$  appropriately. In this example, choosing the "+" sign for  $\theta_1 < \theta_c$  and the "-" sign for  $\theta_1 \geq \theta_c$  will ensure that  $d'_\beta$  will pass smoothly from the 4th quadrant for  $\theta_1 < \theta_c$  into the 3rd quadrant for  $\theta_1 \geq \theta_c$  (rather than the 1st), of the complex plane, and hence no





FIGURE 2: SH anelastic reflection coefficients illustrating jump discontinuities. The top curve in each diagram is the relative amplitude and the bottom is the relative phase. The loss factors for the media of incidence and transmission are  $RQ1$  and  $RQ2$ , respectively.  $DEN1$  and  $DEN2$  are the densities in g/cc.  $VH1$  and  $VH2$  are the homogeneous phase speeds in km/s. The data, taken from Silva (1976), represent highly attenuative soil layers. The incident attenuation angle  $\gamma_1$  is  $40^\circ$  for all three diagrams. The jump discontinuities occur because of a wrong choice of sign for  $d_\beta'$ :

- (a) the positive principal value in equation (4.4) is chosen for all angles of incidence. A jump discontinuity is produced at the critical angle  $\theta_c = 55.53^\circ$ .
- (b) The sign of  $d_\beta'$  is chosen by requiring the mean energy flux of the transmitted ray to always point away from the boundary, for all angles of incidence. The jump discontinuity occurs at the angle of incidence for which the mean energy flux of the transmitted ray is parallel to the interface.
- (c) The sign of  $d_\beta'$  is chosen correctly, hence no jump discontinuity is produced and the curves are continuous.



H1H1

RQ1=0.20000

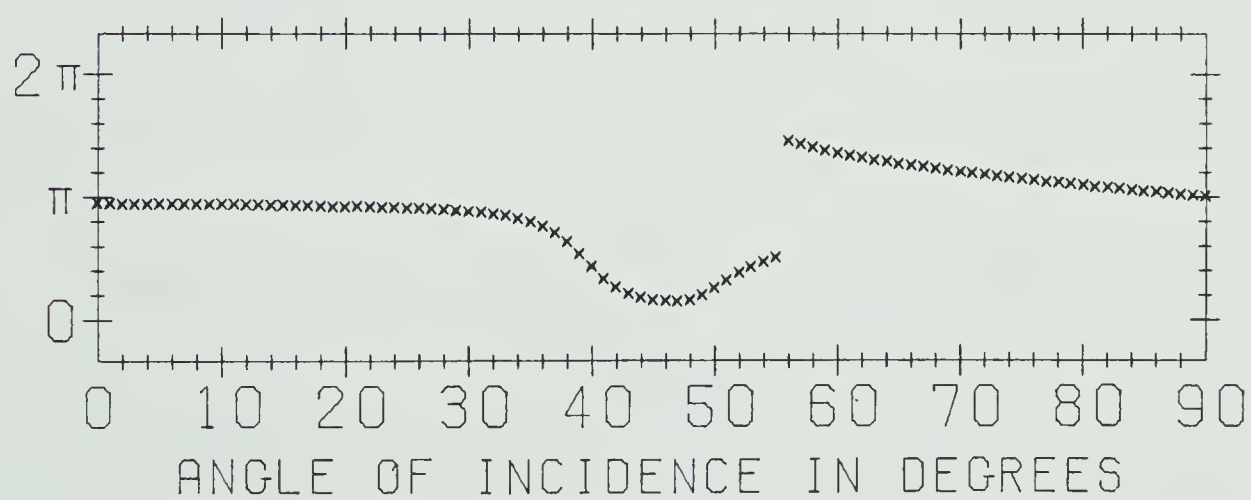
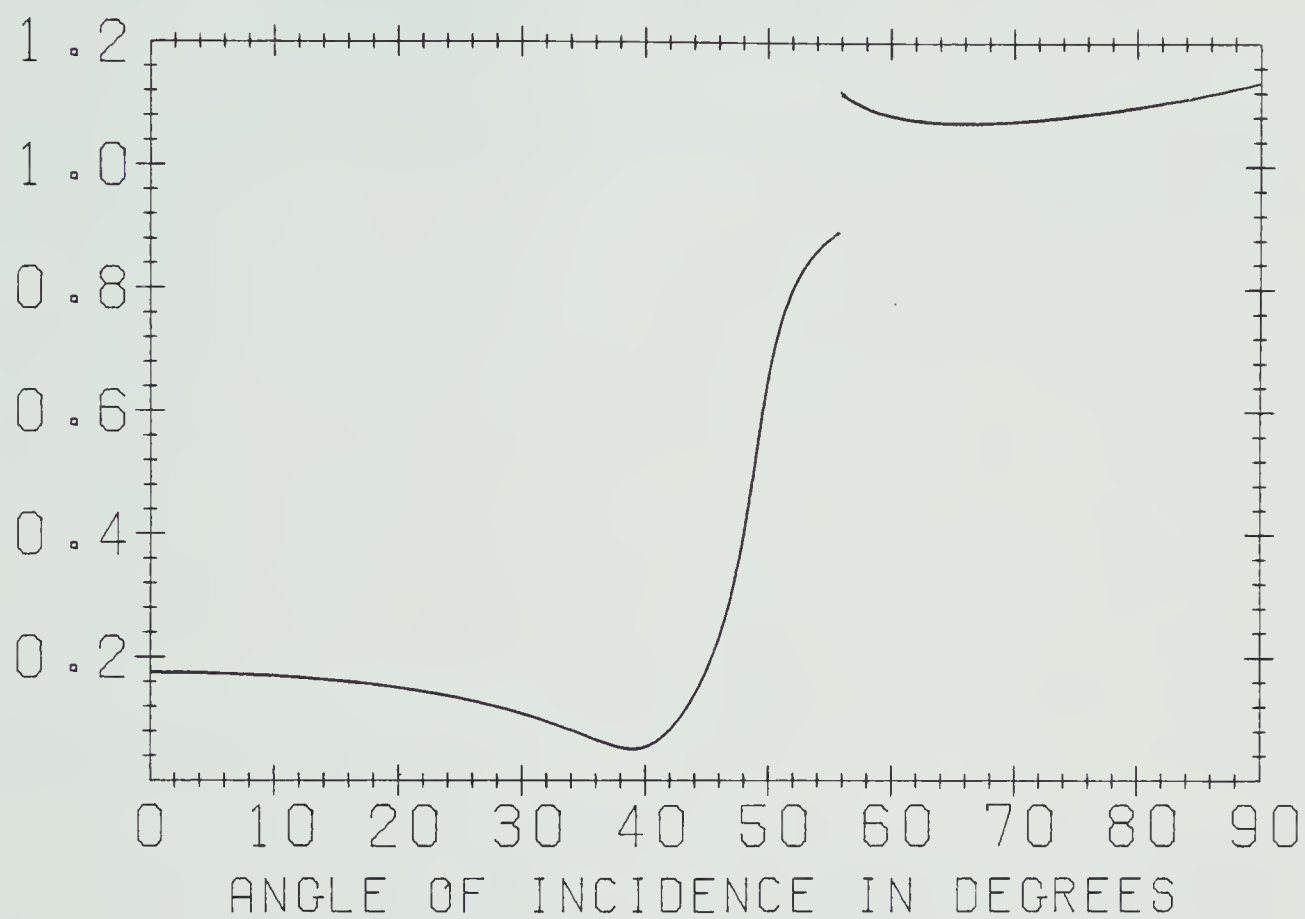
RQ2=0.10000

DEN1=1.920

DEN2=2.050

VH1=0.323

VH2=0.427



(a)



H1H1

RQ1=0.20000

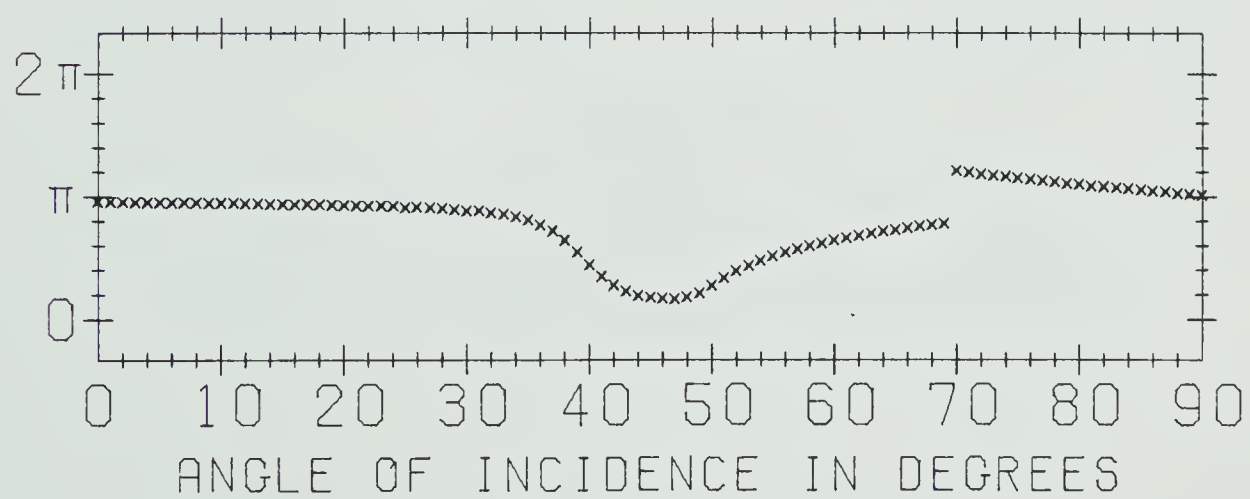
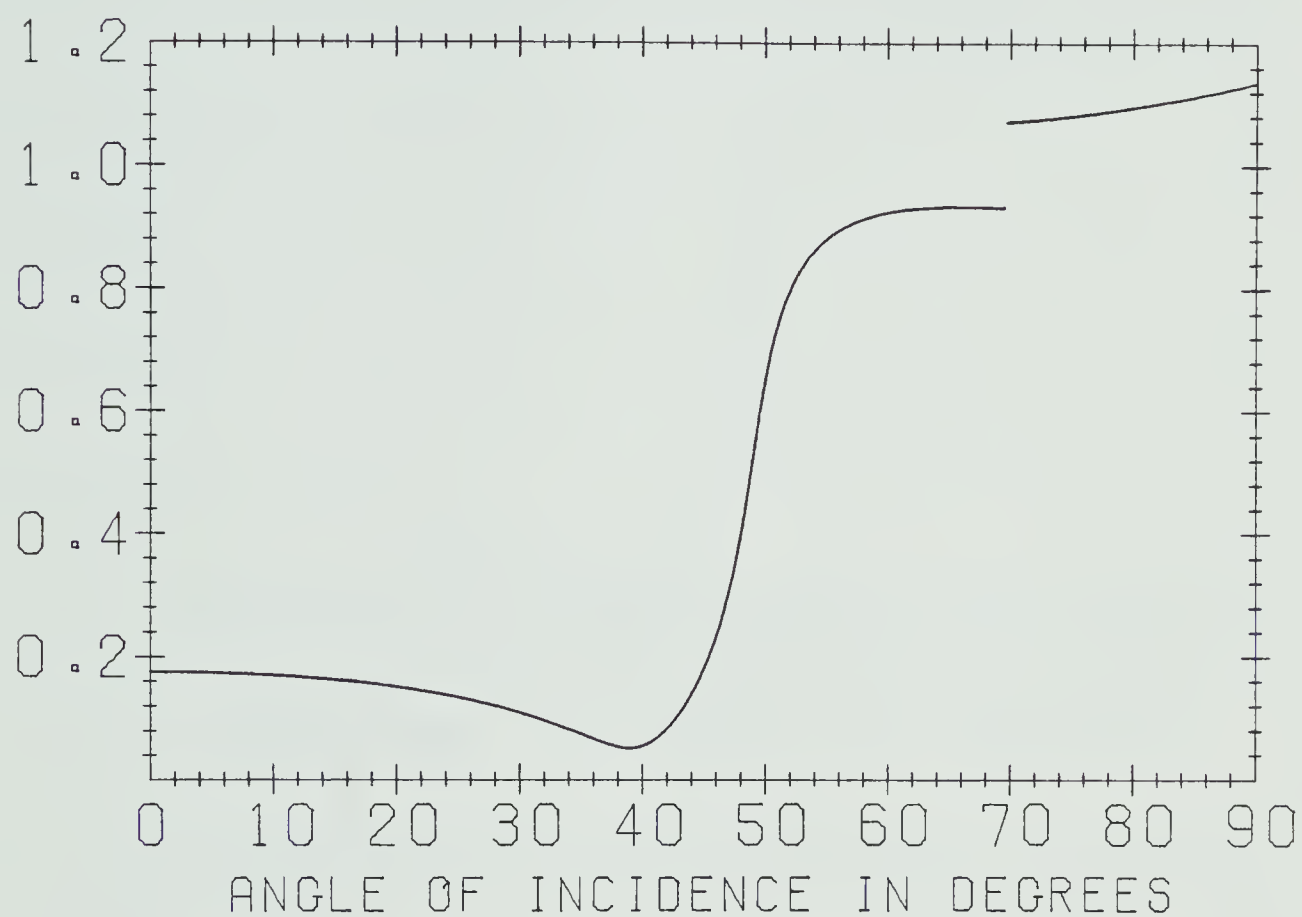
RQ2=0.10000

DEN1=1.920

DEN2=2.050

VH1=0.323

VH2=0.427



(b)



H1H1

RQ1=0.20000

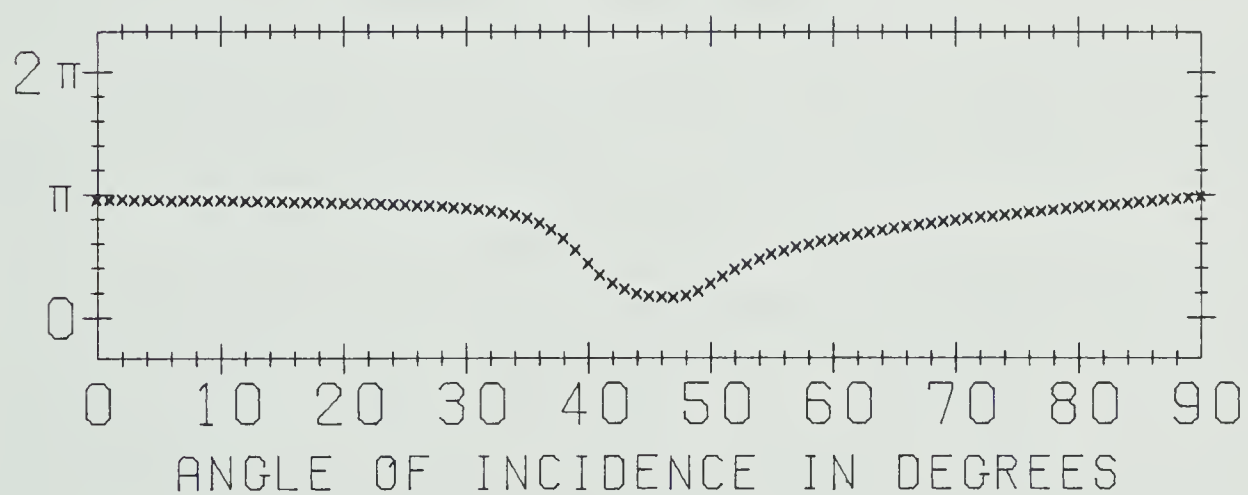
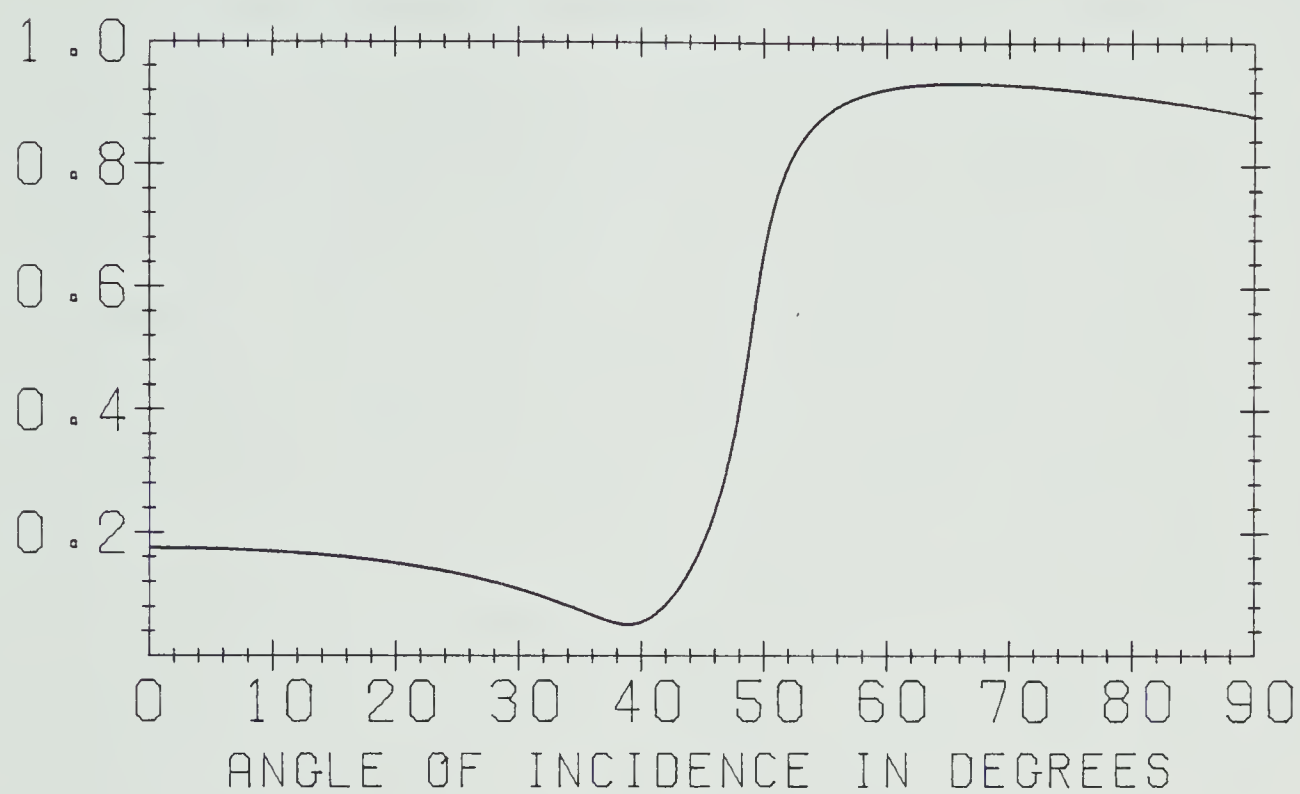
RQ2=0.10000

DEN1=1.920

DEN2=2.050

VH1=0.323

VH2=0.427



(c)





jump discontinuities will occur (see Figure 2c).

The same arguments can be applied when  $d'_{\beta I} \geq 0$  for  $0 \leq \theta_1 < \theta_c$ . In these cases, we must choose the "+" sign for  $\theta_1 \leq \theta_c$  and "-" sign for  $\theta_1 > \theta_c$ .

Alternatively, Borcherdt (1977) has suggested that the signs of  $d_\beta$  and  $d'_\beta$  be determined by requiring that the mean energy fluxes associated with the incident and transmitted waves point, respectively, toward and away from the boundary. From a theoretical viewpoint, this seems like a very natural, physically realistic criterion. However, as it turns out, this criterion also produces jump discontinuities in the reflection and transmission curves, although not necessarily at the critical angle, for which  $\vec{P}'$  is parallel to the interface, rather, at the angle at which the mean energy flux of the transmitted wave,  $\langle \vec{I}' \rangle$ , is parallel to the interface (see Figure 2b).

Apparently, we must accept the criterion proposed above, involving the reversal of the sign of  $d'_\beta$  at  $\theta_1 = \theta_c$ . However, while this criterion does eliminate the jump discontinuities, it also introduces conceptual problems involving the transmitted wave. For instance, the angle of transmission is given by (4.20). However, when  $\theta_1 > \theta_c$ , we have  $d'_{\beta R} < 0$ , according to the above criterion, hence  $\theta'$  is apparently negative. Actually this is not the case: what we must do is use the branch of the arctangent function immediately above the principal branch, i.e.,



$$\theta' = \tan^{-1} \left( \frac{k_{xR}}{d'_{\beta R}} \right) = \pi + \text{p.v.} [\tan^{-1} \left( \frac{k_{xR}}{d'_{\beta R}} \right)] \quad (4.21)$$

where p.v. is the principal value of the arctangent, i.e. the value on the principal branch. This means that for  $\theta_1 > \theta_c$ , we have  $\theta' > 90^\circ$ . This interpretation is consistent with equation (4.6) which shows that  $\vec{P}'$  points into the incidence medium when  $d'_{\beta R} < 0$ . This seemingly strange situation must be accepted if we are to avoid jump discontinuities at  $\theta_c$  in the reflection and transmission coefficients. We have already shown in the discussion of Theorem 2 that  $\vec{P}'$  must move away from the interface for  $\theta_1 > \theta_c$ , and so the situation is not really that surprising. The only surprise is that  $\vec{P}'$  must move into the incidence medium rather than back into the transmission medium. However, it usually does not move very far into the incidence medium, i.e.  $\theta'$  usually exceeds  $90^\circ$  by only a very small amount, on the order of a fraction of a degree, on the average.

One might think that this situation occurs because of the plane-wave assumption. However, Buchen (1971b) has reached the same conclusions in his treatment of the classical problem of a line source radiating cylindrical waves, situated at a finite distance from a plane interface separating two viscoelastic media. He suggests that no true ray path can be associated with this transmitted wave beyond the critical angle because it does not satisfy Fermat's principle.



One should interpret the transmitted wave with  $\theta' > 90^\circ$  not as an actual ray, but rather as representing a small energy flux across the interface from  $V'$  to  $V$  for  $\theta_1 > \theta_c$ . This does not occur in the perfectly elastic case. Borchardt (1977) has obtained results concerning energy flow across the interface which support this notion. He has shown, for SH viscoelastic waves, that the normal component of the total mean energy flux (i.e., the flux for the total wave field) is continuous across the plane boundary separating  $V$  and  $V'$ . The proof of this rests on the fact that the  $z$  component of the mean energy flux can be shown to be proportional to  $\sigma_{32}$ , which, according to (4.7), must be continuous across the boundary. In mathematical terms, we have

$$(\langle \vec{I}_1 \rangle + \langle \vec{I}_2 \rangle + \langle \vec{I}_{12} \rangle + \langle \vec{I}_{21} \rangle) \cdot \hat{z} = \langle \vec{I}' \rangle \cdot \hat{z} \quad (4.22)$$

where  $\langle \vec{I}_1 \rangle$  and  $\langle \vec{I}_2 \rangle$  are the mean energy fluxes associated with the incident and reflected waves,  $\langle \vec{I}' \rangle$  is the mean energy flux associated with the transmitted wave, and  $\langle \vec{I}_{12} \rangle$  ( $\langle \vec{I}_{21} \rangle$ ) is the mean energy flux due to the velocity field of the incident (reflected) wave interacting with the stress field of the reflected (incident) wave.  $\langle \vec{I}_{12} \rangle$  and  $\langle \vec{I}_{21} \rangle$  do not occur in the perfectly elastic case. If we define

$$\begin{aligned} R &\equiv |\langle \vec{I}_2 \rangle \cdot \hat{z} / \langle \vec{I}_1 \rangle \cdot \hat{z}| \\ T &\equiv \langle \vec{I}' \rangle \cdot \hat{z} / \langle \vec{I}_1 \rangle \cdot \hat{z} \\ IC_{ij} &\equiv - \langle \vec{I}_{ij} \rangle \cdot \hat{z} / \langle \vec{I}_1 \rangle \cdot \hat{z} \end{aligned} \quad (4.23)$$



then equation (4.22) can be written as

$$R + T + IC_{12} + IC_{21} = 1 \quad (4.24)$$

which states that energy is conserved at the boundary. In the perfectly elastic case,  $IC_{12} + IC_{21} = 0$  and (4.24) simplifies to the familiar form  $R + T = 1$ .

Theorem 2 shows that it is possible that two critical angles for the transmitted SH wave may exist, since (4.15) can have two solutions for  $\theta_1$ . Numerical computations verify that such situations do, in fact, exist in certain instances. In these cases, the transmitted angle  $\theta'$  behaves in the following way for monotonically increasing  $\theta_1$ : let  $\theta_{c1}$  and  $\theta_{c2}$  be the two critical angles, such that  $\theta_{c1} < \theta_{c2}$ . For  $\theta_1 < \theta_{c1}$ , we have  $\theta' < 90^\circ$ . After the first critical angle  $\theta_{c1}$  is achieved,  $\theta'$  exceeds  $90^\circ$ , reaches a maximum value, decreases back to  $90^\circ$  for the second critical angle  $\theta_{c2}$ , and then continues to slowly decrease, remaining near  $90^\circ$ , until  $\theta_1$  is parallel to the interface.

Concerning the choice of sign for  $d_\beta$  in equation (4.2), we assume that  $\theta_1$  always satisfies  $0 \leq \theta_1 < 90^\circ$ . Hence (4.6) implies  $d_{\beta R}$  is always  $> 0$ . This means that the "+" sign is always chosen for  $d_\beta$ .

We can see from the above discussions that if we restrict our calculations to sub-critical regions, i.e.  $\theta_1 < \theta_c$ , then the calculations are substantially simplified, since we do not need to worry about choosing the correct





sign for  $d'_\beta$ , or computing  $\theta'$  correctly, etc. However, to obtain a more thorough understanding of viscoelastic reflection and transmission, it is necessary to examine the super-critical behaviour of viscoelastic waves.

In the following chapters, synthetic seismograms will be computed for layered anelastic media. A ray theory approach will be used, which means that, for a given ray, it will be necessary to compute reflection and transmission coefficients at all the interfaces which the ray encounters. In order to be able to compute synthetic seismograms for a general layered medium, which may contain perfectly elastic layers embedded among anelastic layers, we must be able to compute reflection and transmission coefficients for two half-spaces separated by a boundary, where each half-space may be either elastic or anelastic. In order to do this effectively, we divide the calculations of reflection and transmission coefficients into six separate cases:

- (1)  $\begin{cases} Q^{-1} \neq 0 & , \text{ anelastic incident rays} \\ Q'^{-1} \neq 0 & , \text{ anelastic transmitted rays} \end{cases}$
- (2)  $\begin{cases} Q^{-1} \neq 0 & , \text{ anelastic incident rays} \\ Q'^{-1} = 0 & , \text{ inhomogeneous elastic ("IEL") } \\ & \text{transmitted rays } (\gamma' = \pm 90^\circ) \end{cases}$
- (3)  $\begin{cases} Q^{-1} = 0 & , \text{ IEL incident rays } (\gamma_1 = \pm 90^\circ) \\ Q'^{-1} \neq 0 & , \text{ anelastic transmitted rays} \end{cases}$



- (4)  $\begin{cases} Q^{-1}=0 & , \text{ IEL incident rays} \\ Q'^{-1}=0 & , \text{ IEL transmitted rays} \end{cases}$
- (5)  $\begin{cases} Q^{-1}=0 & , \text{ elastic incident rays} \\ Q'^{-1} \neq 0 & , \text{ anelastic transmitted rays} \end{cases}$
- (6)  $\begin{cases} Q^{-1}=0 & , \text{ elastic incident rays} \\ Q'^{-1}=0 & , \text{ elastic transmitted rays} \end{cases}$

Case 1 involves two anelastic media, and critical angles can be determined by solving (4.15) for  $\theta_1$  and checking to see if  $\theta_1$  is a critical angle (i.e. if  $\theta'=90^\circ$ ).

Case 2 shows that if  $V$  is anelastic and  $V'$  elastic, the transmitted rays must be inhomogeneous elastic ("IEL") rays (see Figure 3). This can be demonstrated as follows. Since  $A_1 \sin(\theta_1 - \gamma_1)$  is not, in general, equal to zero, equation (4.13) implies that  $A'$  is also not zero, in general, and since  $V'$  is elastic, we know that  $\vec{P}'$  and  $\vec{A}'$  must be perpendicular to each other. Also,  $A_x$  must be continuous across the interface. Hence, the general situation is shown in Figure 3. We see that the continuity of  $A_x$  can lead to a situation in which the transmitted wave is damped toward the interface, rather than away from it. This can also happen in the other cases. Such situations have also been found by other authors such as Cooper and Reiss (1966), Cooper (1967) and Buchen (1971b). Corollary 2.1 shows that if a critical angle exists, it satisfies  $\theta_1 = \theta_c = \gamma_1$ .



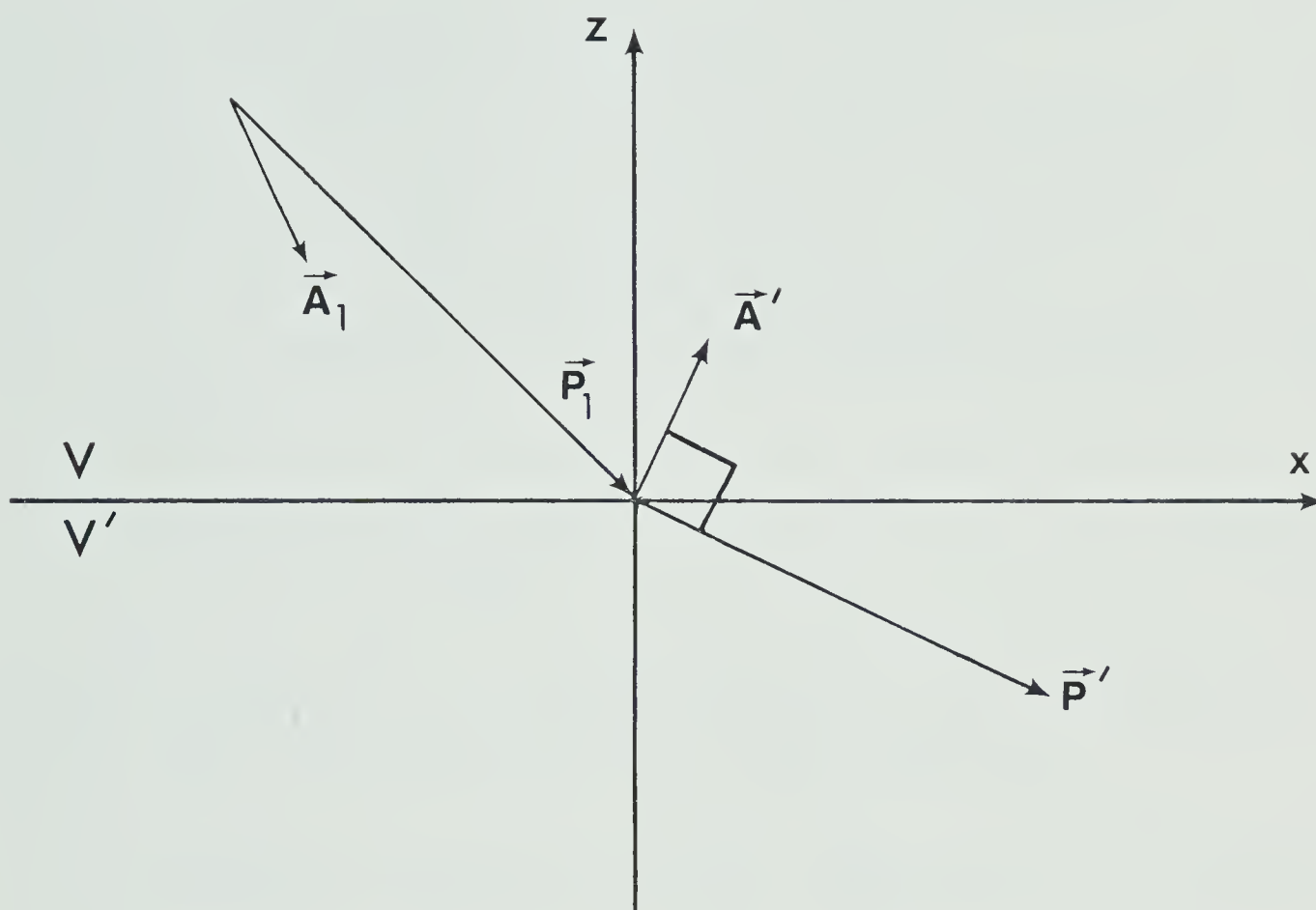


FIGURE 3: Ray diagram illustrating the appearance of an inhomogeneous elastic ("IEL") transmitted ray in  $V'$ , for the case in which  $V$  is anelastic and  $V'$  elastic.



Cases 3 and 4 are treated in order to cover the possibility of the transmitted IEL ray of Case 2 in turn being an incident ray for another interface. These cases were not treated by Borchardt (1977).

For case 3, we can prove a theorem concerning critical angles similar to Theorems 1 and 2.

Theorem 3: Suppose  $V$  is an elastic medium in which IEL incident rays ( $\gamma_1 = \pm 90^\circ$ ) propagate, and  $V'$  is anelastic. Then, if  $\gamma_1 = +90^\circ$ , there are no critical angles. If  $\gamma_1 = -90^\circ$ , and  $\theta_1$  is a critical angle for the transmitted SH wave, then  $\theta_1$  satisfies

$$\sin 2\theta_1 = - \frac{(k'^2)_I}{P_1 A_1} \quad (4.25)$$

Proof: Assume  $\theta_1$  is a critical angle for the transmitted wave. Then (4.6) implies  $d'_{\beta R} = 0$ , which implies

$$2d'_{\beta R} d'_{\beta I} = \text{Im}(d'^2_{\beta}) = (k'^2)_I - (k^2_x)_I = 0 \quad (4.26)$$

Now, using (4.13), (2.16) and the fact that  $\gamma_1 = \pm 90^\circ$ , we have

$$\begin{aligned} (k^2_x)_I &= 2k_{xR} k_{xI} \\ &= -2P_1 A_1 \sin \theta_1 \sin[\theta_1 - (\pm 90^\circ)] \\ &= \pm 2P_1 A_1 \sin \theta_1 \cos \theta_1 \\ &= \pm P_1 A_1 \sin 2\theta_1 \end{aligned} \quad (4.27)$$

Hence, (4.26) implies





$$\sin 2\theta_1 = \pm \frac{(k'^2)_I}{P_1 A_1}$$

If  $\gamma_1 = +90^\circ$ , then since  $(k'^2)_I$  is negative,  $\theta_1$  must lie in the range  $\pi/2 \leq \theta_1 \leq \pi$ , which is unphysical. So  $\theta_1$  cannot be a critical angle if  $\gamma_1 = +90^\circ$ . For  $\gamma_1 = -90^\circ$ , we obtain equation (4.25).

Note that Theorem 3 shows that there can possibly be two critical angles for the transmitted SH wave, since (4.25) yields two solutions for  $\theta_1$ , as for Theorem 2.

For Case 4, the necessary continuity of  $A_x$  across the interface shows that incident rays which are IEL, in general must produce transmitted rays which are also IEL. Concerning critical angles for Case 4, we have

Theorem 4: If  $V$  and  $V'$  are elastic media in which IEL rays propagate, then there are no critical angles for the transmitted SH wave.

Proof: Assume  $\theta_1$  is a critical angle for the transmitted SH wave. Hence (4.6) implies  $d'_{\beta R} = 0$ , which in turn implies equation (4.26). Since  $V'$  is elastic, we have  $(k'^2)_I = 0$ . Equation (4.26) thus implies  $(k_x^2)_I = 0$ . Hence (4.27) then yields  $\theta_1 = 0, \pi/2, \dots$ , which is unphysical for a critical angle. Therefore, no critical angles exist.

For Case 5, Theorem 1 shows that there are no critical angles for the transmitted SH wave.

Case 6 is simply the case for two perfectly elastic half-spaces.



Cases 1-6 are all the possible cases. For instance, the case

$$\begin{cases} Q^{-1}=0 & , \text{ IEL incident rays} \\ Q'^{-1}=0 & , \text{ elastic transmitted rays} \end{cases}$$

is NOT possible. The transmitted rays have to be IEL rays.

In order to get an idea of what anelastic reflection and transmission coefficients look like, we plot some examples of anelastic reflection and transmission amplitudes and phases. Figures 4-7 are plots of reflection and transmission coefficients, the top graph being the amplitude, and the bottom graph being the phase, for SH waves impinging upon a boundary separating two anelastic media 1 and 2. The parameters for each medium are the S wave loss factor  $Q^{-1}$ , the density  $\rho$ , and the homogeneous phase speed  $v_H$ , and they are shown at the top of each figure. The densities (DEN1 and DEN2) are in g/cc and the homogeneous phase speeds (VH1 and VH2) are in km/s. The medium parameters used are the parameters of the first two layers of a crustal model used to compute synthetic seismograms in the following chapters. The coefficient notation is such that H1H2, for example, denotes the transmission coefficient for an incident SH ray in medium 1 and a transmitted SH ray in medium 2.

Each plot shows curves (#2, 3 and 4) for different values of  $\gamma_{inc}$ , as well as the curve (#1) for the perfectly elastic case ( $\gamma_{inc}$  denotes the value of the attenuation angle for the incident ray - it corresponds to  $\gamma_1$  in



FIGURE 4: HlHl reflection coefficients. Curve #1 is for the perfectly elastic case. Curves #2, 3 and 4 correspond to

(a)  $\gamma_{\text{inc}} = -40^\circ, -60^\circ$  and  $-80^\circ$ , respectively

(b)  $\gamma_{\text{inc}} = 20^\circ, 0^\circ$  and  $-20^\circ$ , respectively

(c)  $\gamma_{\text{inc}} = 40^\circ, 60^\circ$  and  $80^\circ$ , respectively

where  $\gamma_{\text{inc}}$  is the attenuation angle for the incident ray. The phase curves correspond to amplitude curves #3, i.e., to  $\gamma_{\text{inc}} = -60^\circ, 0^\circ$  and  $60^\circ$  in diagrams (a), (b) and (c) respectively.



H1H1

RQ1= 0.03333

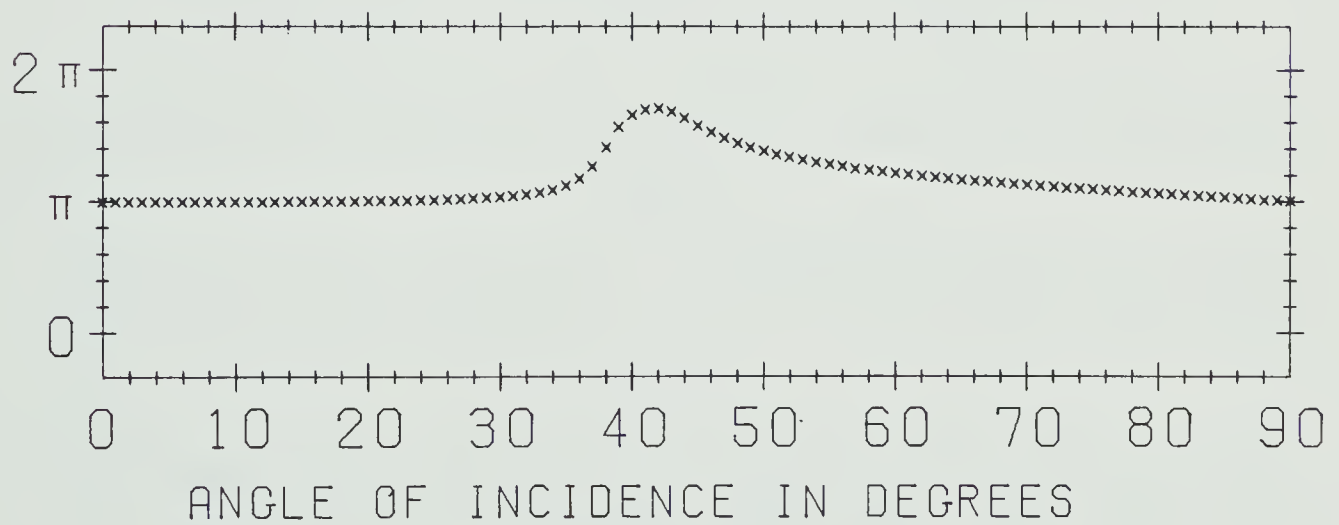
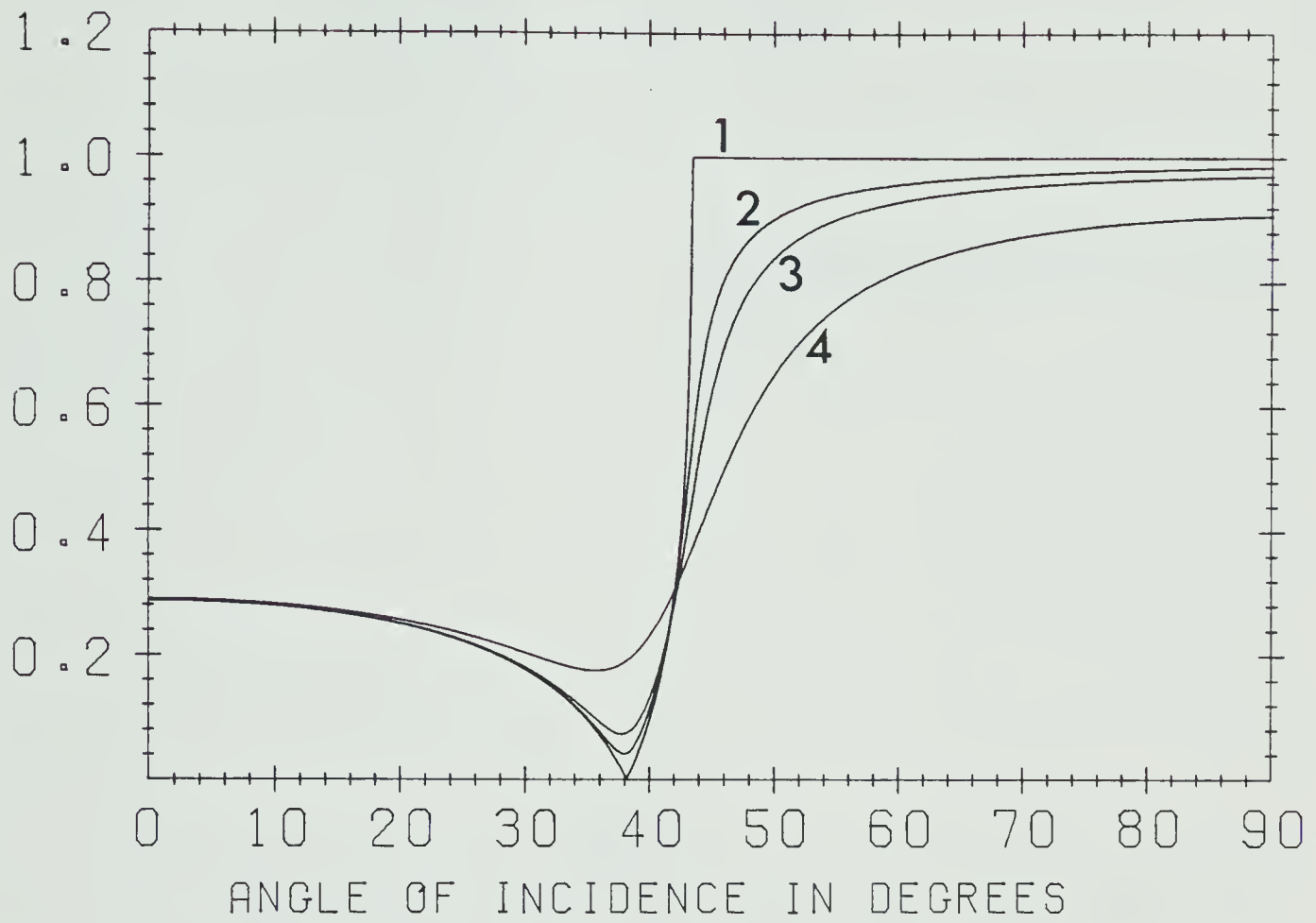
RQ2= 0.02222

DEN1= 2.100

DEN2= 2.600

VH1= 2.400

VH2= 3.500



(a)





H1H1

RQ1= 0.03333

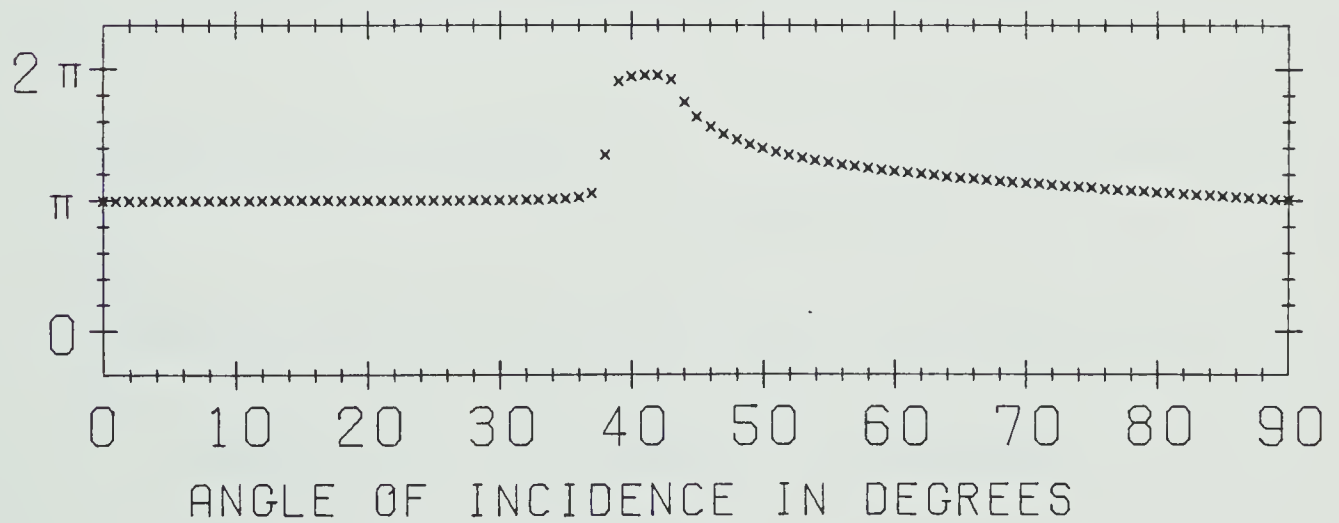
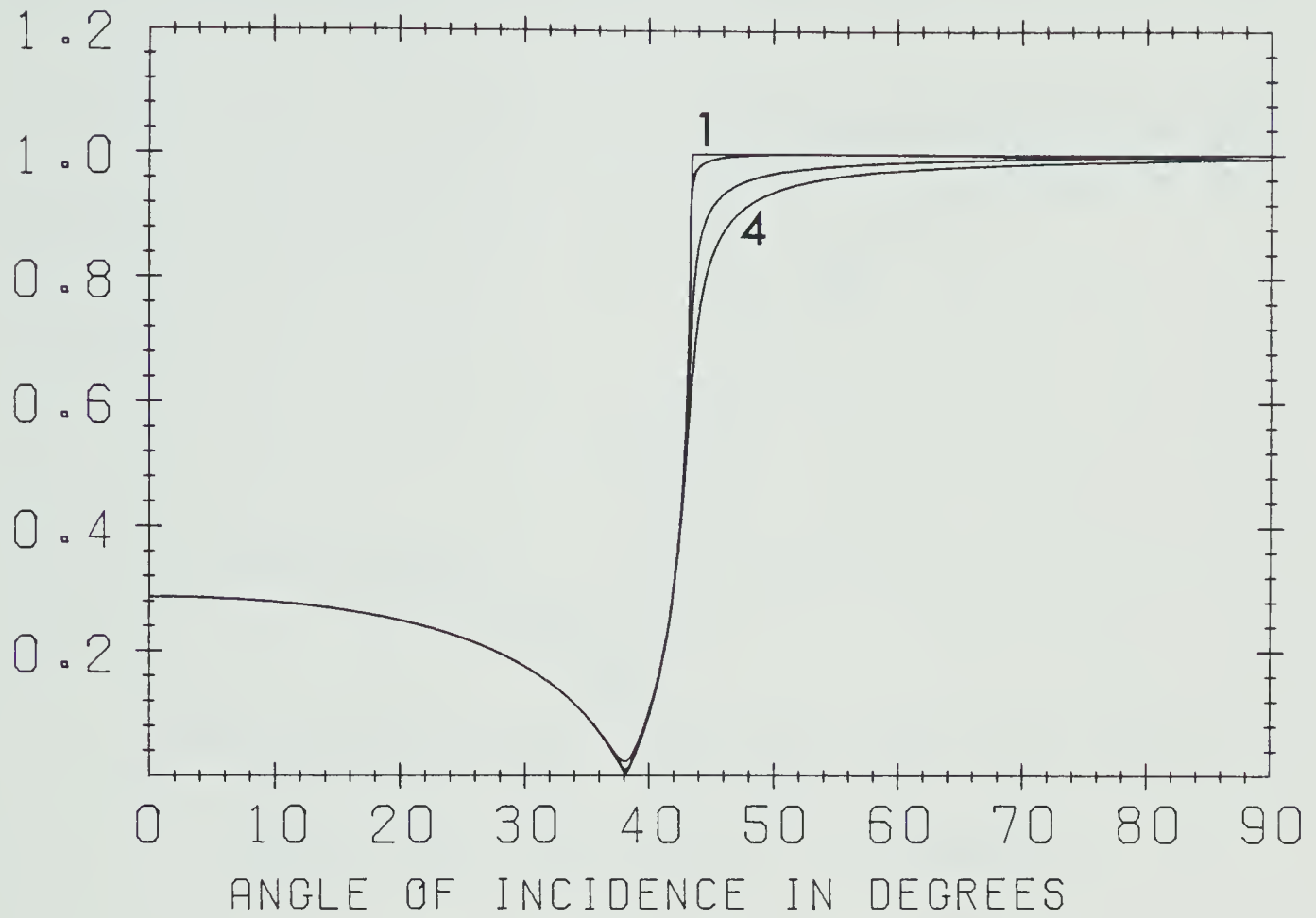
RQ2= 0.02222

DEN1= 2.100

DEN2= 2.600

VH1= 2.400

VH2= 3.500



(b)



H1H1

RQ1= 0.03333

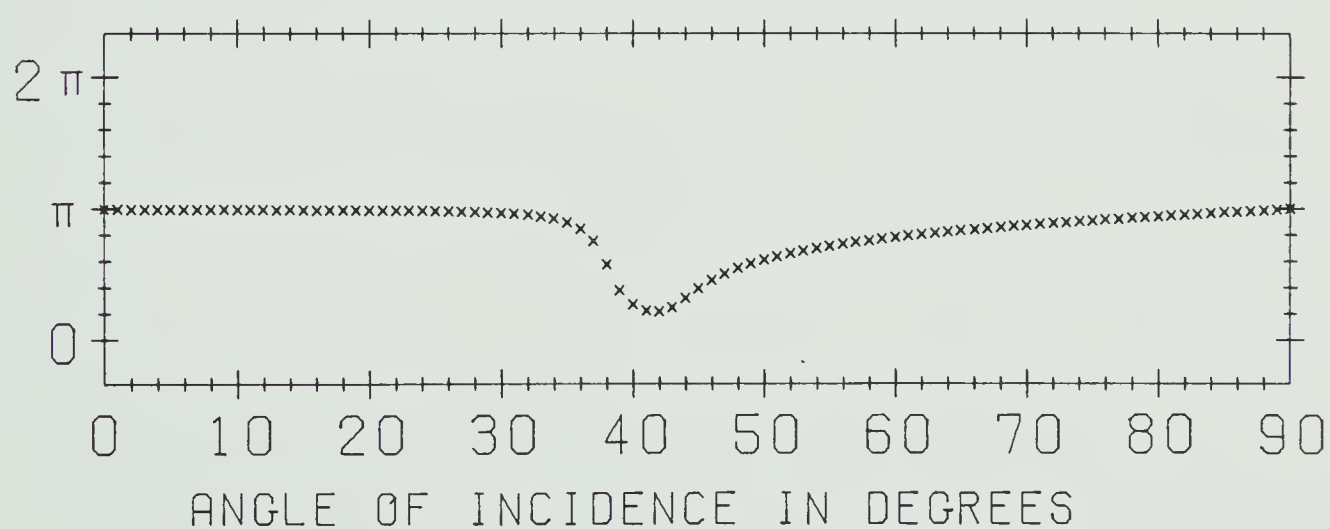
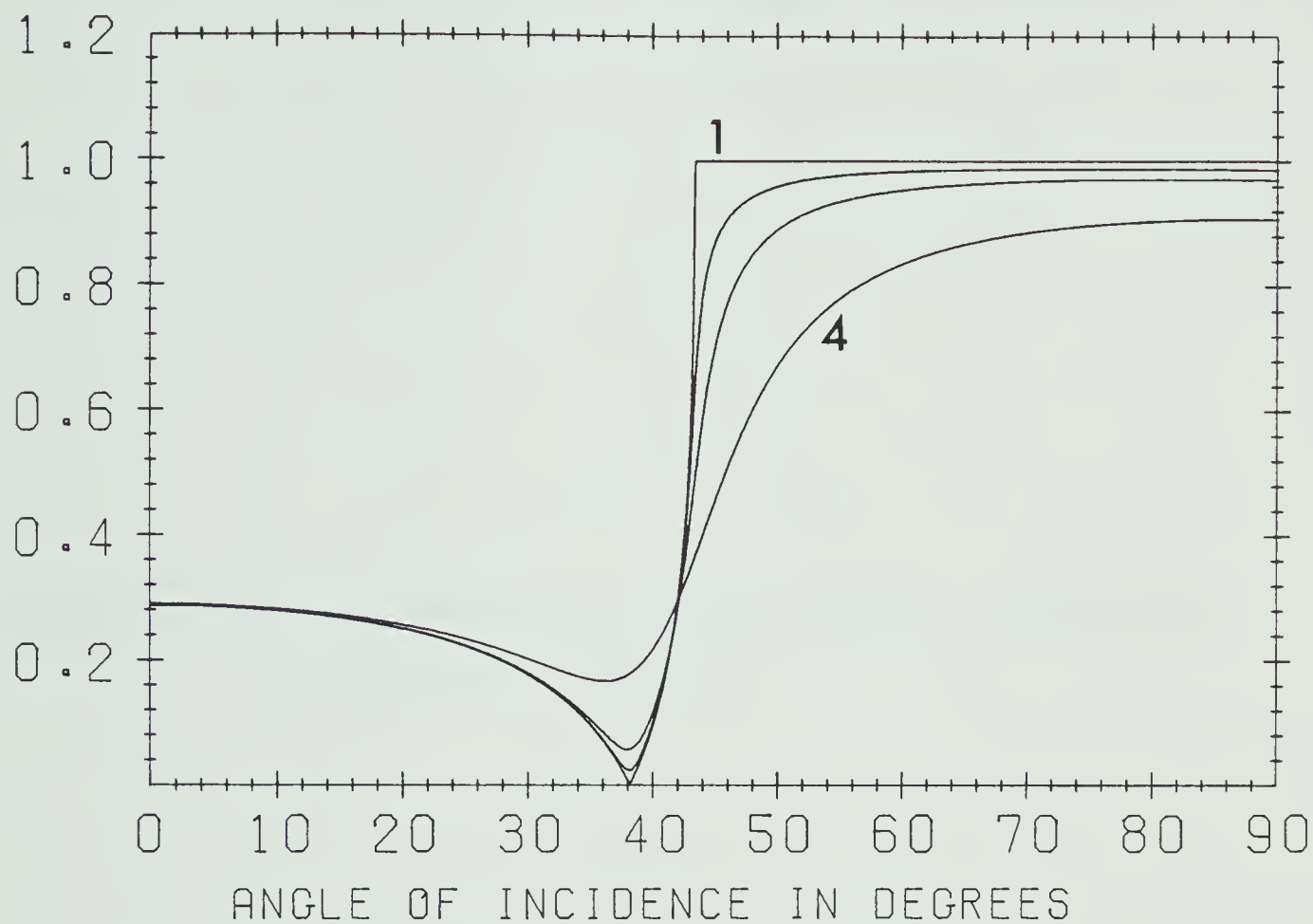
RQ2= 0.02222

DEN1= 2.100

DEN2= 2.600

VH1= 2.400

VH2= 3.500



(c)



FIGURE 5: H1H2 transmission coefficients. For details,  
see caption of Figure 4.



H1H2

RQ1= 0.03333

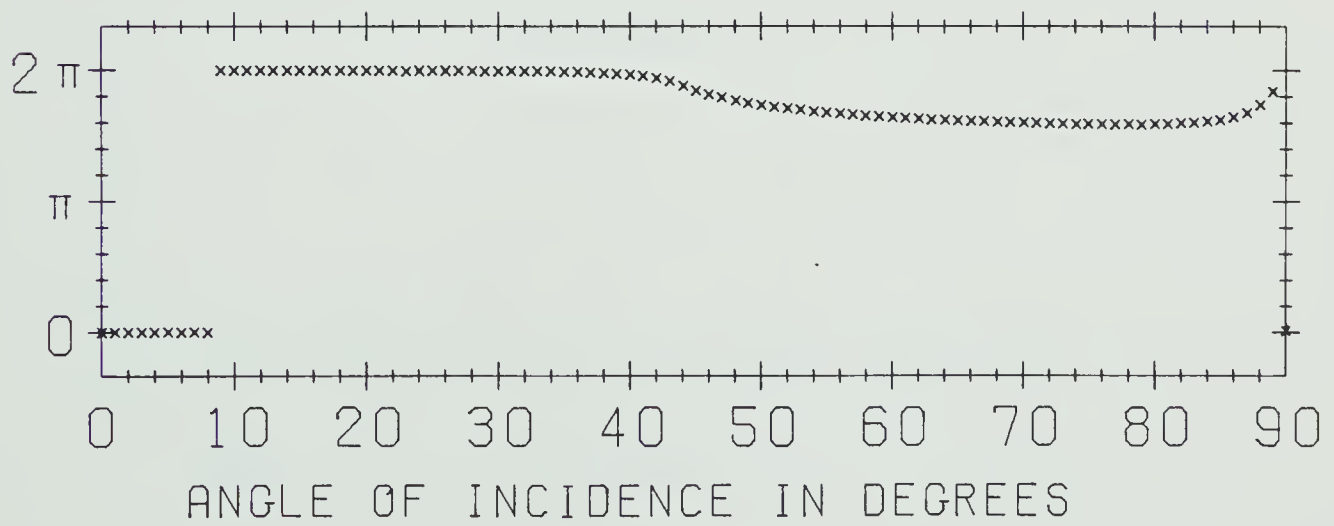
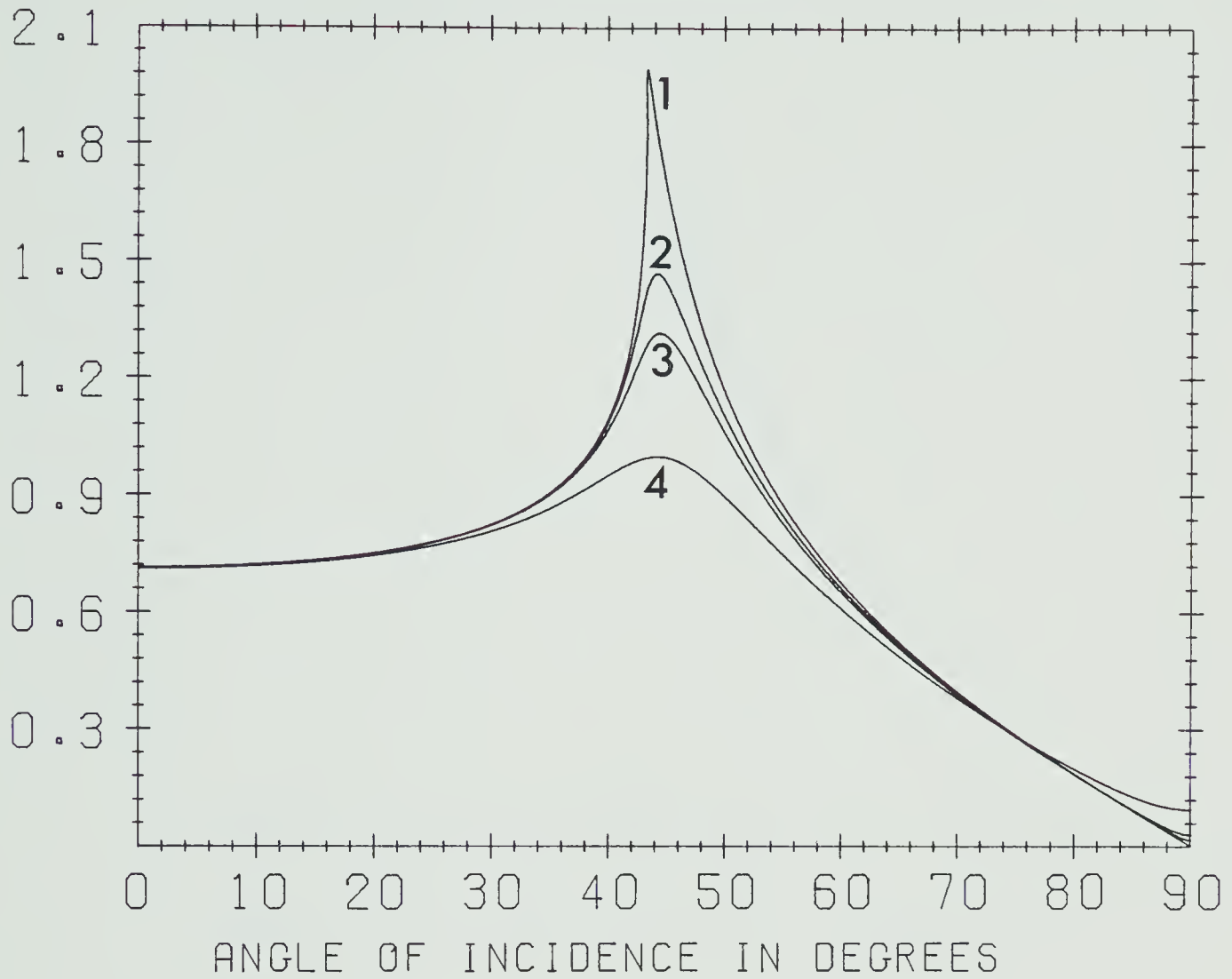
RQ2= 0.02222

DEN1= 2.100

DEN2= 2.600

VH1= 2.400

VH2= 3.500



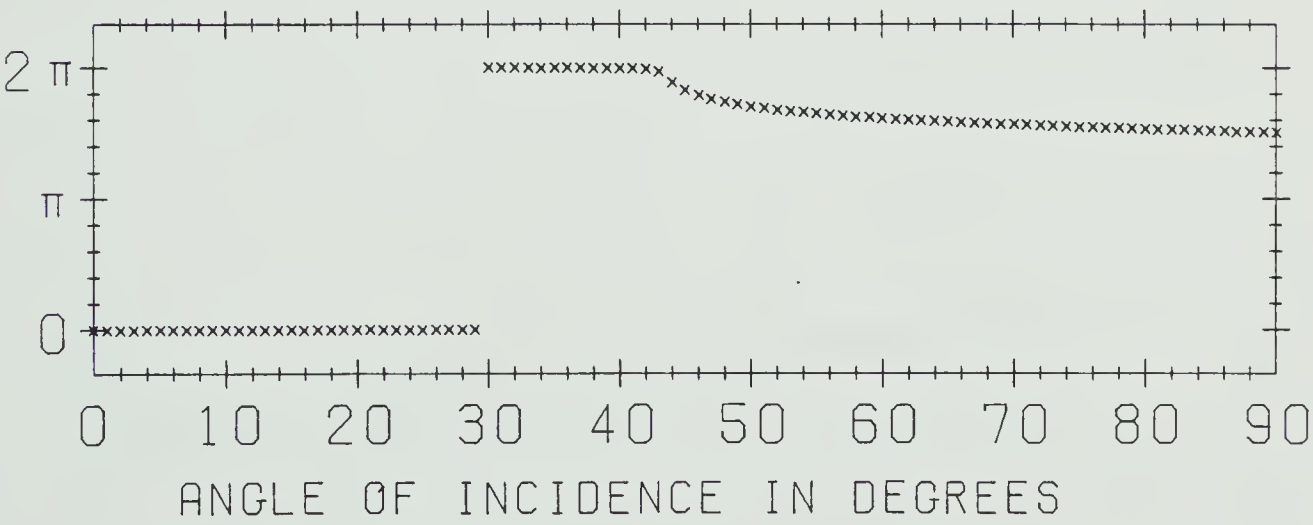
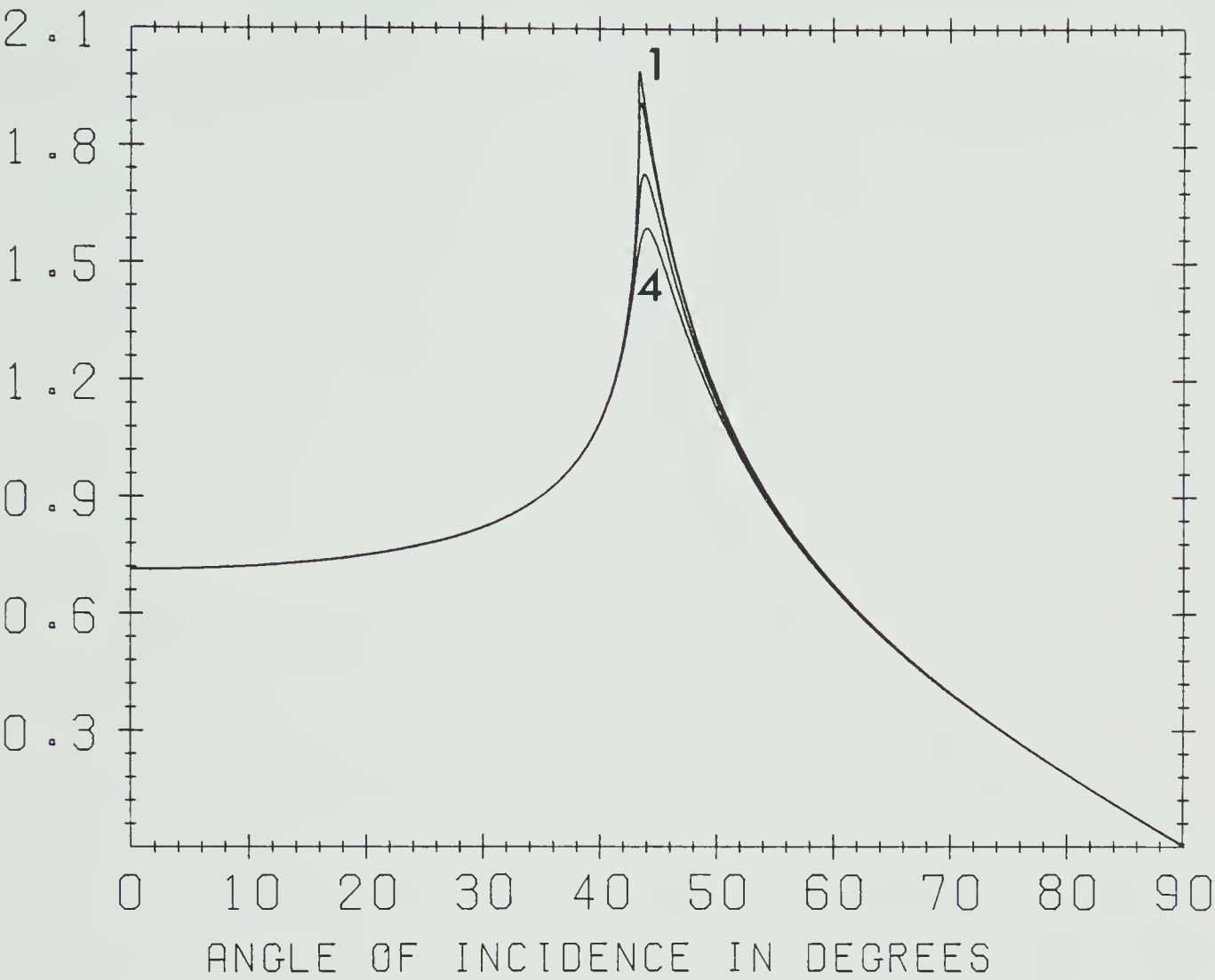
(a)





H1H2

RQ1= 0.03333	RQ2= 0.02222
DEN1= 2.100	DEN2= 2.600
VH1= 2.400	VH2= 3.500



(b)



H1H2

RQ1= 0.03333

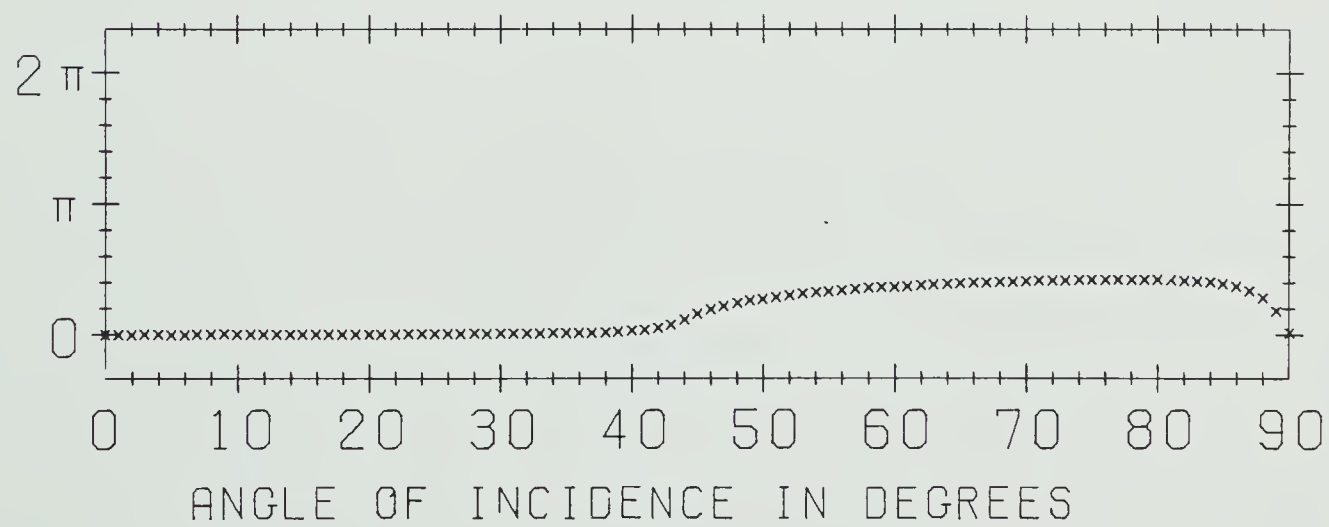
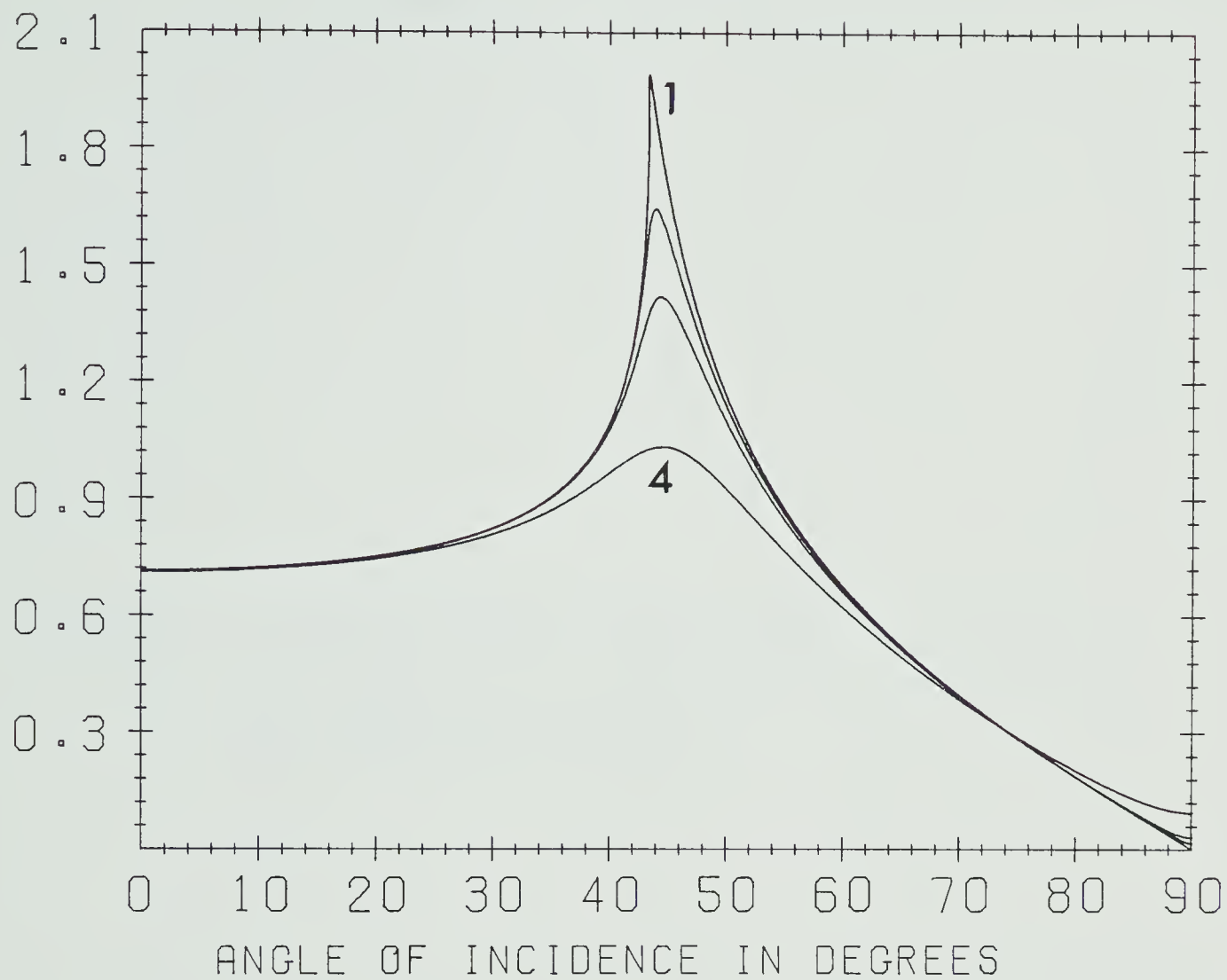
RQ2= 0.02222

DEN1= 2.100

DEN2= 2.600

VH1= 2.400

VH2= 3.500



(c)



FIGURE 6: H<sub>2</sub>H<sub>2</sub> reflection coefficients. For details,  
see caption of Figure 4.



H2H2

RQ1= 0.03333

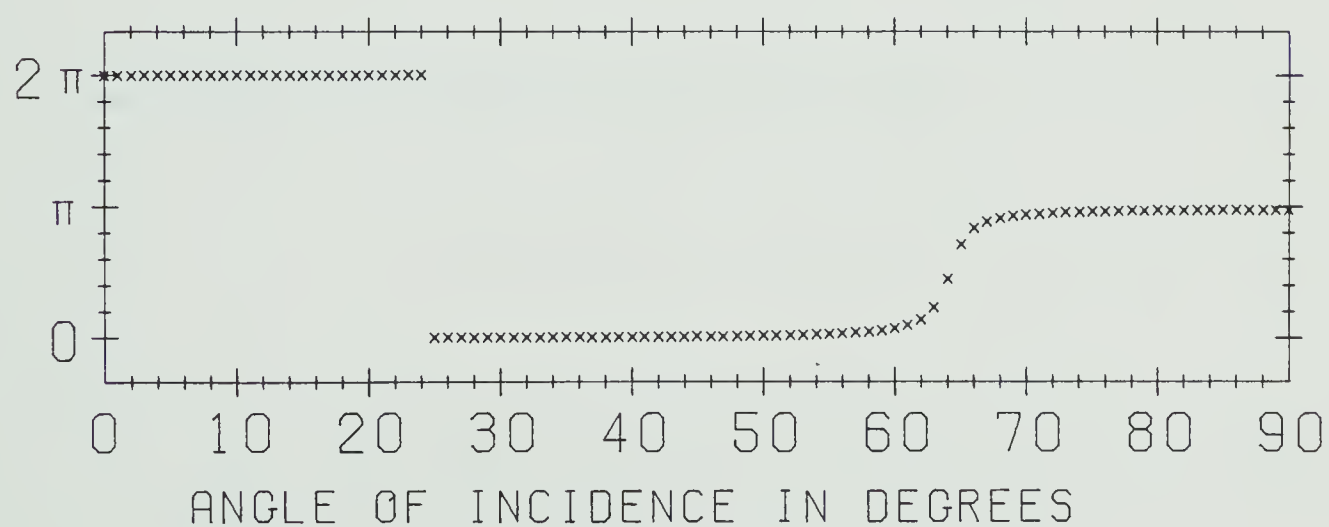
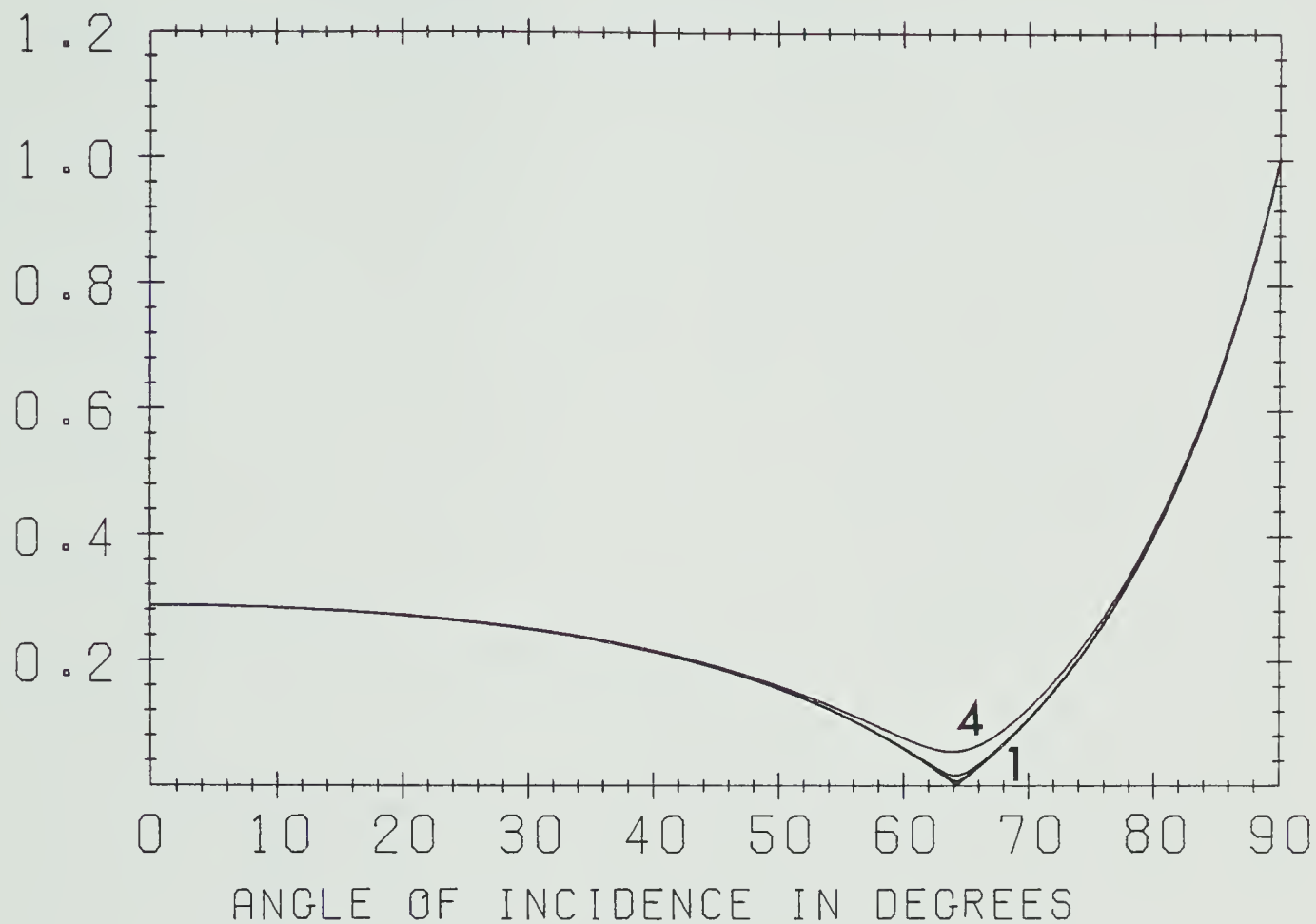
RQ2= 0.02222

DEN1= 2.100

DEN2= 2.600

VH1= 2.400

VH2= 3.500



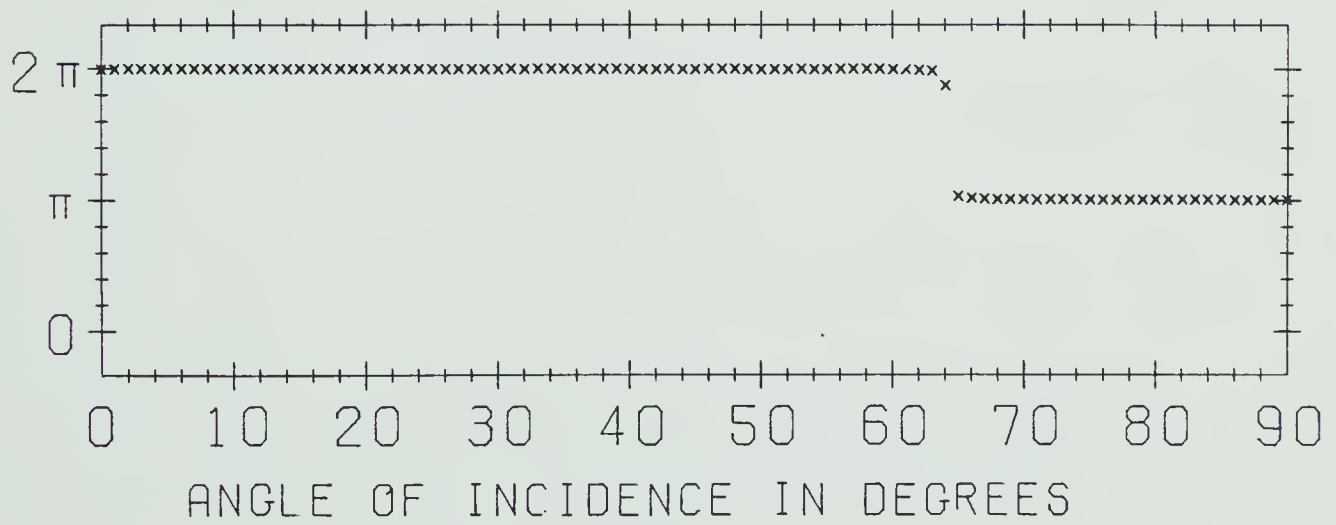
(a)





H2H2

RQ1= 0.03333	RQ2= 0.02222
DEN1= 2.100	DEN2= 2.600
VH1= 2.400	VH2= 3.500



(b)



H2H2

RQ1= 0.03333

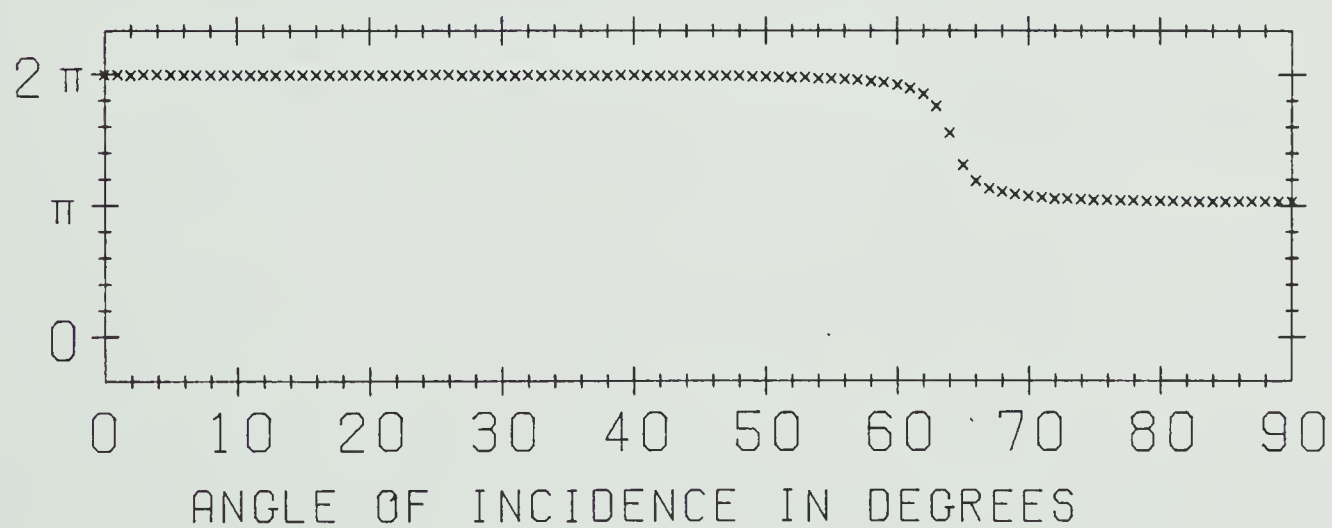
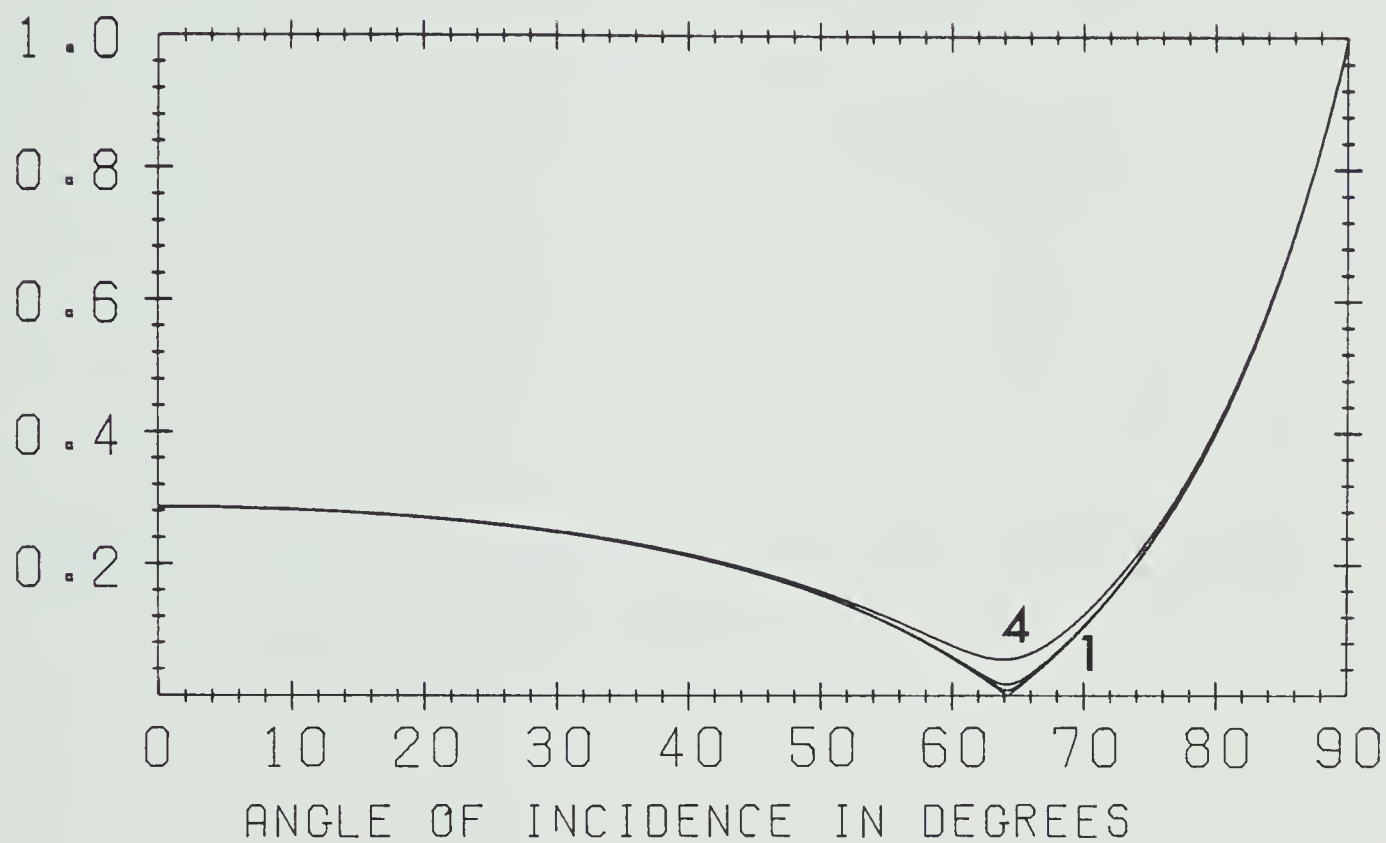
RQ2= 0.02222

DEN1= 2.100

DEN2= 2.600

VH1= 2.400

VH2= 3.500



(c)



FIGURE 7: H2H1 transmission coefficients. For details,  
see caption of Figure 4.



H2H1

RQ1= 0.03333

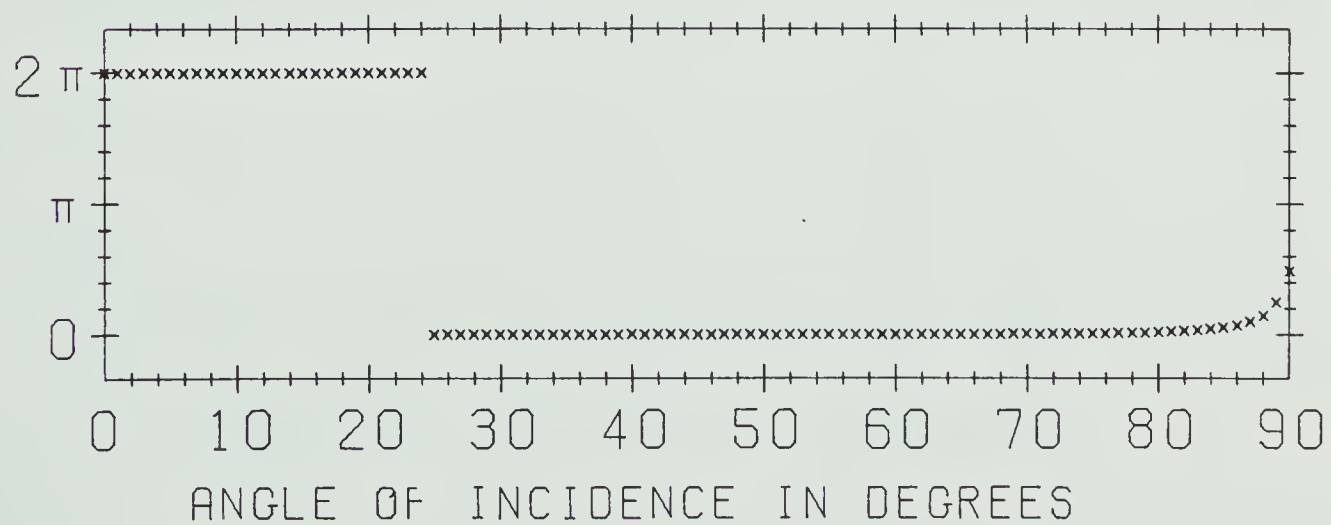
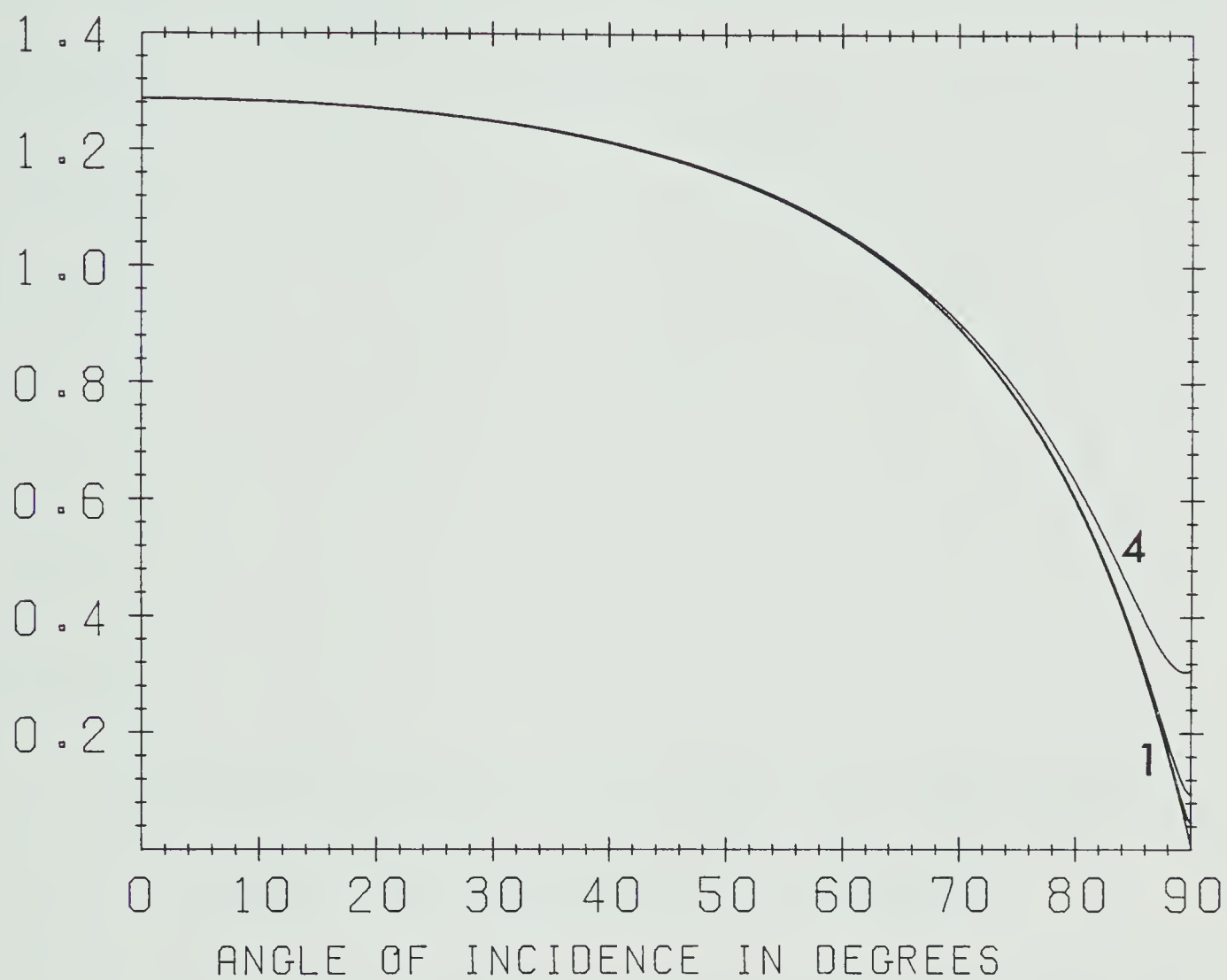
RQ2= 0.02222

DEN1= 2.100

DEN2= 2.600

VH1= 2.400

VH2= 3.500



(a)





H2H1

RQ1= 0.03333

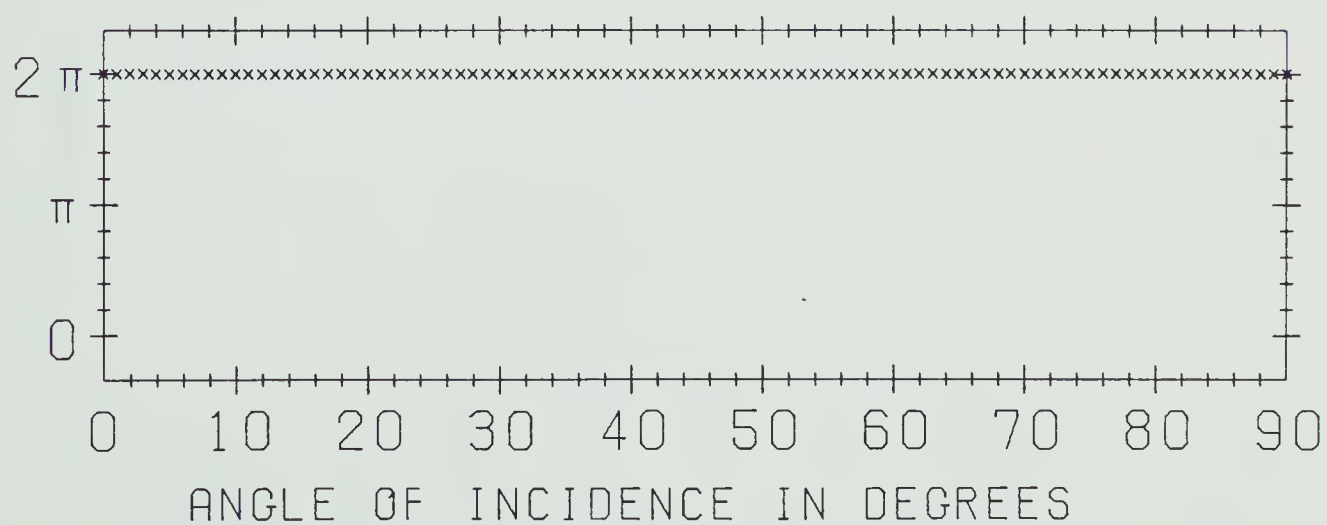
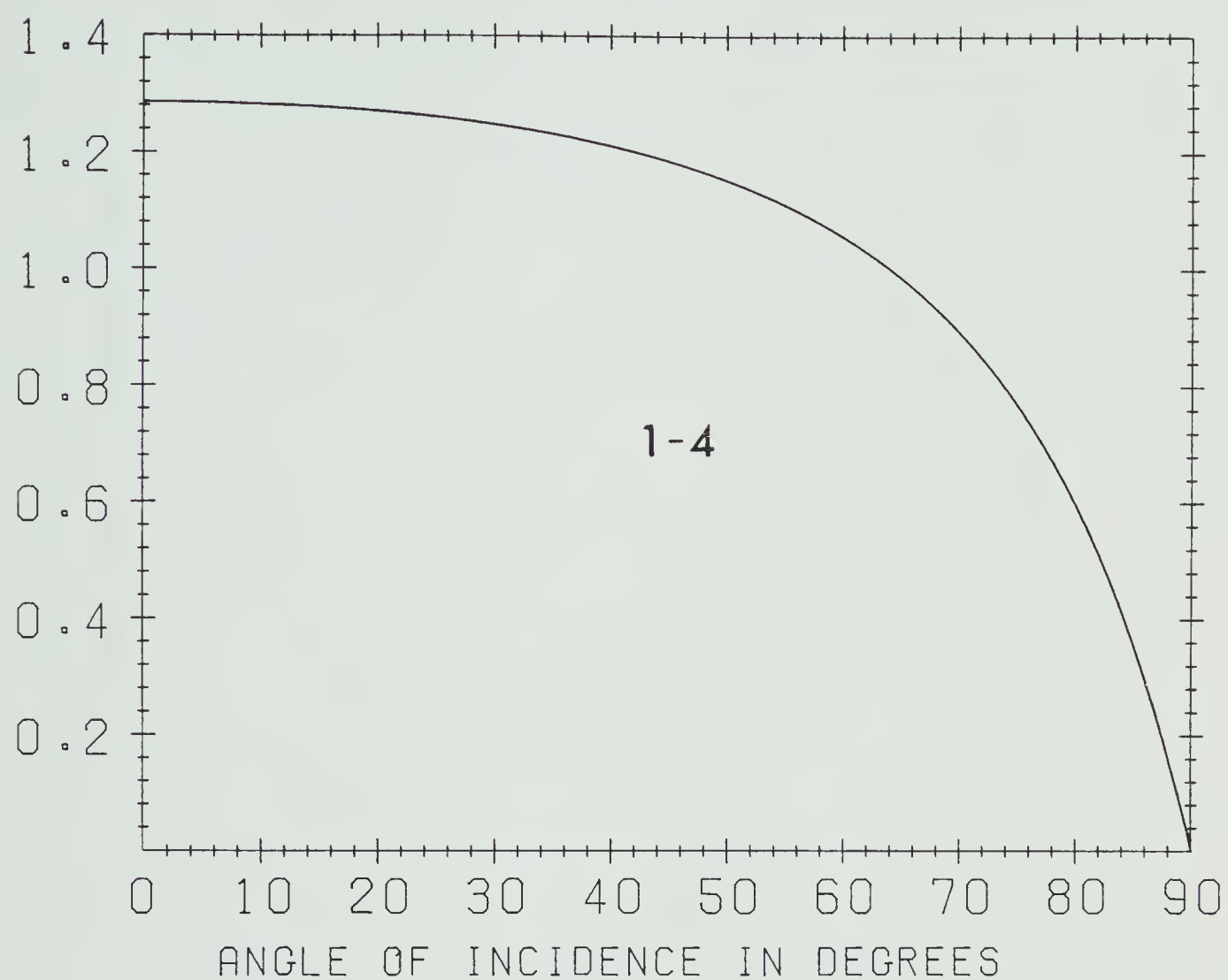
RQ2= 0.02222

DEN1= 2.100

DEN2= 2.600

VH1= 2.400

VH2= 3.500



(b)



H2H1

RQ1= 0.03333

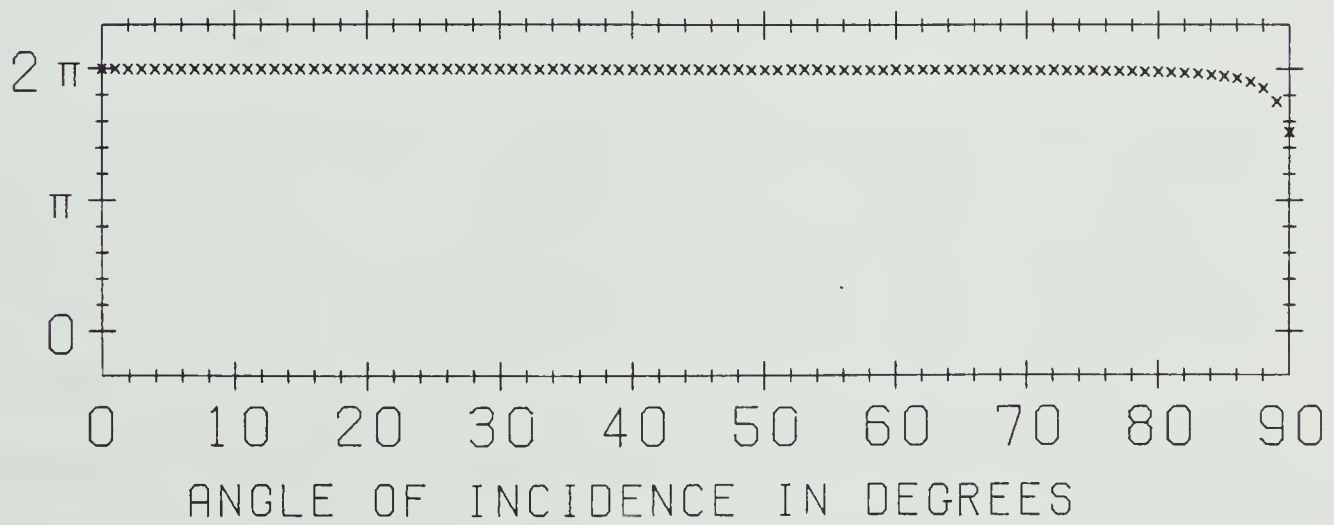
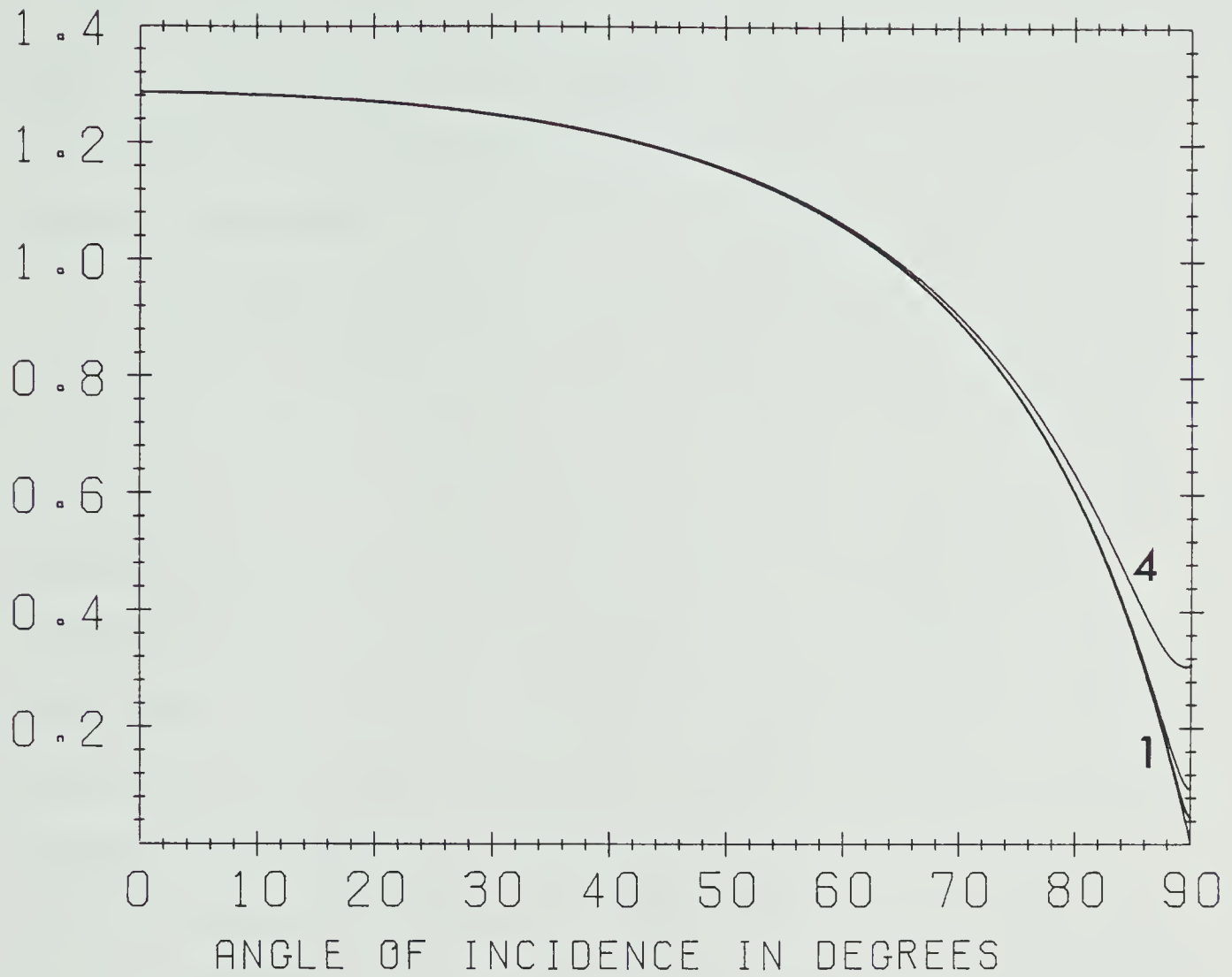
RQ2= 0.02222

DEN1= 2.100

DEN2= 2.600

VH1= 2.400

VH2= 3.500



(c)



Figure 1). In each plot, the phase curve corresponds to amplitude curve #3. Only one phase curve has been plotted in each diagram to avoid unnecessary cluttering. The three phase curves for each reflection/transmission coefficient correspond to  $\gamma_{inc} = -60^\circ$ ,  $0^\circ$  and  $+60^\circ$  and illustrate the general behaviour of the phases as a function of  $\gamma_{inc}$ .

When the incident ray is in medium 1 (H1H1 and H1H2, i.e. Figures 4 and 5) critical angles for the transmitted ray occur only for values of  $\gamma_{inc}$  greater than or equal to about  $+17.43^\circ$ . For lesser values of  $\gamma_{inc}$ , the transmitted propagation vector ( $\vec{P}'$  in Figure 1) never quite becomes parallel to the interface. No critical angles occur when the incident ray is in medium 2. As we have previously seen, the numerical values of these critical angles vary with  $\gamma_{inc}$ . For the perfectly elastic case, the critical angle for the transmitted ray is  $43.29^\circ$ . For the anelastic case, critical angles occur in Figures 4b, 4c, 5b and 5c for  $\gamma_{inc} = 20^\circ$ ,  $40^\circ$ ,  $60^\circ$  and  $80^\circ$ , and are  $44.74^\circ$ ,  $56.70^\circ$ ,  $69.63^\circ$  and  $83.14^\circ$  respectively. At  $\gamma_{inc} = \gamma_m \approx 17.43^\circ$ , the value of  $\gamma_{inc}$  for which critical angles begin to appear, the critical angle has the same value as for the perfectly elastic case, i.e.  $\dot{\theta}_c(\gamma_m) = \theta_c(\text{elastic}) = 43.29^\circ$ . The exact value of  $\gamma_m$  can be determined by substituting  $\sin \theta_1 = v_H / v'_H$  (the formula for the critical angle in the perfectly elastic case) into (4.15). One obtains



$$\tan \gamma_m = (1-G) \tan \theta_1 = \frac{(v_H/v_H') (1-G)}{\sqrt{1-(v_H/v_H')^2}} \quad (4.28)$$

where

$$G = (v_H'/v_H)^2 \xi = \frac{Q'^{-1} (1 + \sqrt{1 + Q'^{-2}})}{Q^{-1} (1 + \sqrt{1 + Q'^{-2}})} \quad (4.29)$$

With the medium parameters shown in Figures 4-7, i.e.  $v_H = 2.4$  km/s,  $v_H' = 3.5$  km/s, etc., we get  $\gamma_m = 17.42866...^\circ$ . We can see that unlike the perfectly elastic amplitude curve which exhibits a sharp transition when going from sub-critical to super-critical incident angles, the anelastic amplitude curves show a smooth, rapid transition. This, combined with the discrete nature of critical angles shown previously, shows that in linear viscoelasticity, the concept of a critical angle is somewhat vague or degraded. Other authors, for example, Cooper (1967), Buchen (1971b), Kennett (1975), Borchardt (1977) and Fryer (1978) have arrived at similar conclusions. In Figures 6 and 7, where the incident ray is in medium 2 (no critical angles occur) the curves do not deviate from the perfectly elastic curve (#1) as much as in Figures 4 and 5.

#### 4.2 P-SV Waves

The theoretical development of the reflection/transmission problem for P-SV waves is very similar to the development for SH waves. All the equations and discussions





presented for the SH case have analogies in the P-SV case. It is more complicated only in the sense that there are more waves to handle.

Since the treatment of the P-SV case is analogous to the SH case, we will not expound it in detail. Instead, we will confine ourselves to the derivation of the systems of equations describing the boundary conditions, whose solutions are the reflection and transmission coefficients for P-SV plane waves impinging upon a plane boundary separating two linear viscoelastic media. Free surface reflection coefficients will also be treated. The notation will be the same as in the previous section except, in this case, we add the subscripts P,  $\phi$  or  $\alpha$  and S,  $\psi$  or  $\beta$  to denote quantities associated with P or S waves.

From equation (3.42) we see that the displacement vector for the incident and reflected P waves can be written as

$$\vec{u}_{Pj} = D_{Pj} e^{i(\omega t - \vec{k}_{Pj} \cdot \vec{r})} \hat{t}_{Pj}, \quad j=1,2 \quad (4.30)$$

where, as in (4.1),

$$\vec{k}_{Pj} = k_x \hat{x} + (-1)^j d_\alpha \hat{z} \quad (4.31)$$

$$\text{and} \quad d_\alpha = \pm \text{p.v.} \sqrt{k_P^2 - k_x^2} \quad (4.32)$$

The vector  $\hat{t}_{Pj}$  is a complex unit vector representing the particle motion, and is given by



$$\hat{t}_{Pj} = \hat{k}_{Pj} = \frac{\vec{k}_{Pj}}{k_P} \quad (4.33)$$

with

$$\hat{t}_{Pj} \cdot \hat{t}_{Pj} = 1 \quad (4.34)$$

As before,  $j=1$  and  $2$  are associated with the incident and reflected waves, respectively. The relative displacement amplitude  $D_{Pj}$  is given in terms of the relative potential amplitude  $B_{Pj}$  as

$$D_{Pj} = -i |\vec{k}_{Pj}| B_{Pj} = -i k_P B_{Pj} \quad (4.35)$$

For the transmitted P wave, we have, in the same way,

$$\vec{u}'_P = D'_P e^{i(\omega t - \vec{k}'_P \cdot \vec{r})} \hat{t}'_P \quad (4.36)$$

where

$$\begin{aligned} \vec{k}'_P &= k'_x \hat{x} - d'_\alpha \hat{z} \\ d'_\alpha &= \pm \text{p.v.} \sqrt{k'^2_P - k_x^2} \\ \hat{t}'_P &= \hat{k}'_P = \frac{\vec{k}'_P}{k'_P} \\ \hat{t}'_P \cdot \hat{t}'_P &= 1 \\ D'_P &= -i k'_P B'_P \end{aligned} \quad (4.37)$$

The x-component of the complex wave vector is the same for all waves, since, as before, we will require that the relative amplitudes are space independent, i.e.



$$k_{Px1} \text{ (or } k_{Sx1}) = k_{Px2} = k_{Sx2} = k'_{Px} = k'_{Sx} \equiv k_x \quad (4.38)$$

As in the previous section, this leads to the complex form of Snell's law:

$$\begin{aligned} k_{xR} &= P_{\phi 1} \sin \theta_{P1} \text{ (or } P_{\psi 1} \sin \theta_{S1}) = P_{\phi 2} \sin \theta_{P2} = P_{\psi 2} \sin \theta_{S2} \\ &= P'_{\phi} \sin \theta'_P = P'_{\psi} \sin \theta'_S \end{aligned} \quad (4.39)$$

$$\begin{aligned} -k_{xI} &= A_{\phi 1} \sin(\theta_{P1} - \gamma_{P1}) \text{ (or } A_{\psi 1} \sin(\theta_{S1} - \gamma_{S1})) = A_{\phi 2} \sin(\theta_{P2} - \gamma_{P2}) \\ &= A_{\psi 2} \sin(\theta_{S2} - \gamma_{S2}) = A'_{\phi} \sin(\theta'_P - \gamma'_P) = A'_{\psi} \sin(\theta'_S - \gamma'_S) \end{aligned}$$

The first equation can be written in the same familiar form as (4.14) by using  $\vec{P} = \omega / |\vec{V}|$ .

From equations (3.75) and (3.76), noting that  $\hat{n} = \hat{y}$ , we see that the displacement vector for the incident and reflected SV waves can be written as

$$\vec{u}_{Sj} = D_{Sj} e^{i(\omega t - \vec{k}_{Sj} \cdot \vec{r})} \hat{t}_{Sj}, \quad j=1,2 \quad (4.40)$$

where  $\vec{k}_{Sj} = k_x \hat{x} + (-1)^j d_{\beta} \hat{z}$

$$d_{\beta} = \pm \text{p.v.} \sqrt{k_S^2 - k_x^2}$$

$$\hat{t}_{Sj} = (-1)^j \hat{y} \times \hat{k}_{Sj}, \quad \hat{k}_{Sj} = \frac{\vec{k}_{Sj}}{k_S} \quad (4.41)$$

$$\hat{t}_{Sj} \cdot \hat{t}_{Sj} = 1$$

$$\hat{t}_{Sj} \cdot \hat{k}_{Sj} = 0$$

$$D_{Sj} = (-1)^j k_S B_{Sj}$$



For the transmitted S wave,

$$\vec{u}'_S = D'_S e^{i(\omega t - \vec{k}'_S \cdot \vec{r})} \hat{t}'_S \quad (4.42)$$

with  $\vec{k}'_S = k'_x \hat{x} - d'_\beta \hat{z}$

$$d'_\beta = \pm \text{p.v.} \sqrt{k'^2_S - k'^2_x}$$

$$\hat{t}'_S = -\hat{y} \times \hat{k}'_S, \quad \hat{k}'_S = \frac{\vec{k}'_S}{k'_S} \quad (4.43)$$

$$\hat{t}'_S \cdot \hat{t}'_S = 1$$

$$\hat{t}'_S \cdot \hat{k}'_S = 0$$

$$D'_S = -ik'_S B'_S$$

The complex unit vectors can be written in terms of  $\hat{x}$  and  $\hat{z}$  as

$$\begin{aligned} \hat{t}_{Pj} &= \frac{k_x}{k_P} \hat{x} + \frac{(-1)^j d_\alpha}{k_P} \hat{z} \\ \hat{t}'_P &= \frac{k_x}{k'_P} \hat{x} - \frac{d'_\alpha}{k'_P} \hat{z} \\ \hat{t}_{Sj} &= \frac{d_\beta}{k_S} \hat{x} - \frac{(-1)^j k_x}{k_S} \hat{z} \\ \hat{t}'_S &= \frac{d'_\beta}{k_S} \hat{x} + \frac{k_x}{k'_S} \hat{z} \end{aligned} \quad (4.44)$$

In the case of perfect elasticity, defining the unit vectors  $\hat{t}_{Pj}$ , etc. (which are real for perfect elasticity) in such a way that their x-components are positive, makes the reflection/transmission boundary condition equations independent of the direction of the z-axis (e.g., upwards





or downwards in Figure 1), i.e. the equations will look the same for both directions. This convention has been extended here to the anelastic case. For instance,  $\hat{t}'_S$  has been defined as  $-\hat{y} \times \hat{k}'_S$  rather than  $+\hat{y} \times \hat{k}'_S$ .

The welded contact boundary conditions imply that  $u_1$ ,  $u_3$ ,  $\sigma_{31}$  and  $\sigma_{33}$  are continuous across the boundary. In the boundary condition equations, the factor  $e^{i(\omega t - \vec{k} \cdot \vec{r})} \big|_{z=0} = e^{i(\omega t - k_x x)}$  will appear in every term, and hence we cancel it out from the start. Using (4.44) in the displacements and stresses, the boundary condition equations can be written in their x and z components.

For the x-component, the condition  $u_1 = u'_1$  at  $z=0$  yields

$$\frac{k_x}{k_P} (D_{P1} + D_{P2}) + \frac{d_\beta}{k_S} (D_{S1} + D_{S2}) = \frac{k_x}{k'_P} D'_P + \frac{d'_\beta}{k'_S} D'_S \quad (4.45)$$

and for the z-component,  $u_3 = u'_3$  at  $z=0$  yields

$$-\frac{d_\alpha}{k_P} (D_{P1} - D_{P2}) + \frac{k_x}{k_S} (D_{S1} - D_{S2}) = -\frac{d'_\alpha}{k'_P} D'_P + \frac{k_x}{k'_S} D'_S \quad (4.46)$$

The horizontal stress is given by

$$\sigma_{31} = 2Me_{31} = M(u_{3,1} + u_{1,3})$$

For  $\vec{u}$  in the general form

$$\vec{u} = D e^{i(\omega t - \vec{k} \cdot \vec{r})} \hat{t}$$

we then have



$$\sigma_{31} = -iMD[k_x \hat{t}_z + k_z \hat{t}_x] e^{i(\omega t - \vec{k} \cdot \vec{r})}$$

Hence the condition  $\sigma_{31} = \sigma'_{31}$  at  $z=0$  leads to

$$\begin{aligned} -2Mk_x \left(\frac{d_\alpha}{k_P}\right) (D_{P1} - D_{P2}) - M \left(\frac{d_\beta^2 - k_x^2}{k_S}\right) (D_{S1} - D_{S2}) \\ = -2M'k_x \left(\frac{d'_\alpha}{k'_P}\right) D'_P - M' \left(\frac{d'^2_\beta - k'^2_x}{k'_S}\right) D'_S \end{aligned} \quad (4.47)$$

The vertical stress is given by

$$\sigma_{33} = \Lambda \theta + 2Me_{33} = \Lambda(u_{1,1} + u_{3,3}) + 2Mu_{3,3}$$

For  $\vec{u}$  in the general form

$$\vec{u} = D e^{i(\omega t - \vec{k} \cdot \vec{r})} \hat{t}$$

we then have,

$$\sigma_{33} = -i\{\Lambda D[k_x \hat{t}_x + k_z \hat{t}_z] + 2MDk_z \hat{t}_z\} e^{i(\omega t - \vec{k} \cdot \vec{r})}$$

Using the relation

$$\begin{aligned} \Lambda &= \rho \alpha^2 - 2M = (M/\beta^2) \alpha^2 - 2M \\ &= M(\alpha/\beta)^2 - 2M \\ &= M(k_S/k_P)^2 - 2M \end{aligned}$$

to eliminate  $\Lambda$ , the condition  $\sigma_{33} = \sigma'_{33}$  at  $z=0$  gives, after some calculation,



$$\begin{aligned}
M \left( \frac{d_\beta^2 - k_x^2}{k_P} \right) (D_{P1} + D_{P2}) - 2M d_\beta \left( \frac{k_x}{k_S} \right) (D_{S1} + D_{S2}) \\
= M' \left( \frac{d_\beta'^2 - k_x^2}{k_P'} \right) D_P' - 2M' d_\beta' \left( \frac{k_x}{k_S'} \right) D_S'
\end{aligned} \tag{4.48}$$

Equations (4.45)-(4.48) are the equations describing the P-SV boundary conditions. They can be split into two systems of 4 linear equations in 4 unknowns, for the case of incident P waves, and the case of incident S waves. For incident P waves, we must set  $D_{S1} \equiv 0$ . The resulting  $4 \times 4$  system can then be solved for the reflection and transmission coefficients, i.e.  $(D_{P2}/D_{P1})$ ,  $(D_{S2}/D_{P1})$ ,  $(D_P'/D_{P1})$  and  $(D_S'/D_{P1})$ . Similarly, for incident S waves, we must set  $D_{P1} \equiv 0$ . The resulting  $4 \times 4$  system can then be solved for  $(D_{S2}/D_{S1})$ ,  $(D_{P2}/D_{S1})$ ,  $(D_P'/D_{S1})$  and  $(D_S'/D_{S1})$ .

The reflection coefficients for a free surface are obtained from the condition of vanishing stress at the surface. For a P wave incident on a free surface ( $D_{S1} \equiv 0$ ), equations (4.47) and (4.48) give

$$\begin{aligned}
\frac{2k_x d_\alpha}{k_P} (D_{P1} - D_{P2}) - \left( \frac{d_\beta^2 - k_x^2}{k_S} \right) D_{S2} &= 0 \\
\left( \frac{d_\beta^2 - k_x^2}{k_P} \right) (D_{P1} + D_{P2}) - \left( \frac{2d_\beta k_x}{k_S} \right) D_{S2} &= 0
\end{aligned} \tag{4.49}$$

The solution of this system gives the reflection coefficients for a P wave incident on a free surface, and they are



$$\frac{D_{P2}}{D_{P1}} = \frac{4k_x^2 d_\alpha d_\beta - (d_\beta^2 - k_x^2)^2}{g(k_x)} \quad (4.50)$$

$$\frac{D_{S2}}{D_{P1}} = \frac{4k_x d_\alpha (k_S/k_P) (d_\beta^2 - k_x^2)}{g(k_x)}$$

$$\text{where } g(k_x) = 4k_x^2 d_\alpha d_\beta + (d_\beta^2 - k_x^2)^2 \quad (4.51)$$

For an S wave incident on a free surface ( $D_{P1} \equiv 0$ ), equations (4.47) and (4.48) give

$$\left(\frac{2k_x d_\alpha}{k_P}\right) D_{P2} - \left(\frac{d_\beta^2 - k_x^2}{k_S}\right) (D_{S1} - D_{S2}) = 0 \quad (4.52)$$

$$\left(\frac{d_\beta^2 - k_x^2}{k_P}\right) D_{P2} - \frac{2d_\beta k_x}{k_S} (D_{S1} + D_{S2}) = 0$$

Solving this system for the reflection coefficients gives

$$\frac{D_{P2}}{D_{S1}} = \frac{4k_x d_\beta (k_P/k_S) (d_\beta^2 - k_x^2)}{g(k_x)} \quad (4.53)$$

$$\frac{D_{S2}}{D_{S1}} = \frac{-4k_x^2 d_\alpha d_\beta + (d_\beta^2 - k_x^2)^2}{g(k_x)}$$

where  $g(k_x)$  is given by (4.51).

As mentioned in the previous section, one must choose the signs of  $d_\alpha$ ,  $d_\beta$ ,  $d'_\alpha$  and  $d'_\beta$  properly if one is computing reflection/transmission coefficients in super-critical regions.





## CHAPTER 5

### ASYMPTOTIC RAY THEORY FOR LINEAR VISCOELASTIC MEDIA

In this chapter, we apply asymptotic ray theory to the problem of body-wave propagation in a layered homogeneous isotropic linear viscoelastic medium. Our main goal is to calculate an expression for the geometrical spreading of a given viscoelastic wave generated by a point source on the surface. We develop only the relevant aspects of the theory which are necessary for our purposes. The development will parallel standard applications of asymptotic ray theory to elastic wave propagation (see, for example, Červený and Ravindra (1971) and Hron and Kanasevich (1971)).

The equation of motion for linear viscoelastic waves in a homogeneous isotropic medium is given by equation (2.6), which is repeated here for convenience, i.e.

$$[\lambda(t) + \mu(t)] * d(\nabla(\nabla \cdot \vec{u})) + \mu(t) * d(\nabla^2 \vec{u}) = \rho \ddot{\vec{u}} \quad (5.1)$$

A general solution of this equation may be written as

$$\vec{u}(\vec{r}, t) = \frac{1}{2\pi} \int_{-\infty}^{\infty} \vec{W}(\vec{r}, \omega) S(\omega) e^{i\omega[t - \tau(\vec{r}, \omega)]} d\omega \quad (5.2)$$

where  $S(\omega)$  is the spectrum of the source pulse, and  $\tau$  is the complex phase function whose real and imaginary parts correspond to the arrival time and the attenuation of a ray, respectively.  $\vec{W}$  includes quantities pertaining to reflection and transmission at boundaries, geometrical



spreading, etc. To solve equation (5.1) in the sense of asymptotic ray theory, we expand  $\vec{W}$  as a power series in  $(1/i\omega)$  with coefficients  $\vec{W}_n(\vec{r}, \omega)$ , which, in general, depend on frequency for viscoelastic waves. We then have<sup>†</sup>

$$\vec{u}(\vec{r}, t) = \frac{1}{\pi} \text{Re} \int_{\omega_1}^{\infty} \sum_{n=0}^{\infty} \vec{W}_n(\vec{r}, \omega) s_n(\xi, \omega) d\omega \quad (5.3)$$

where

$$s_n(\xi, \omega) = \frac{S(\omega)}{(i\omega)^n} e^{i\omega\xi} \quad (5.4)$$

$$\xi = t - \tau(\vec{r}, \omega)$$

Substituting (5.3) into (5.1), and using the facts

$$s'_n = \frac{ds_n}{d\xi} = s_{n-1} \quad (5.5)$$

$$\nabla s_n = -s_{n-1} \nabla \tau$$

and multiplying through by  $\pi$ , we obtain, after some calculation,

$$\begin{aligned} \rho \text{Re} \int_{\omega_1}^{\infty} \sum_n \vec{W}_n s_{n-2} d\omega = & \text{Re} \left[ [\lambda + \mu] * d \left\{ \int_{\omega_1}^{\infty} \sum_n [s_{n-2} (\vec{W}_n \cdot \nabla \tau) \nabla \tau \right. \right. \\ & - s_{n-1} (\nabla (\vec{W}_n \cdot \nabla \tau) + (\nabla \cdot \vec{W}_n) \nabla \tau) + s_n \nabla (\nabla \cdot \vec{W}_n)] d\omega \} \\ & + \mu * d \left\{ \int_{\omega_1}^{\infty} \sum_n [s_{n-2} \vec{W}_n (\nabla \tau)^2 - s_{n-1} (2 \nabla \tau \cdot \nabla \vec{W}_n + \vec{W}_n \nabla^2 \tau) \right. \\ & \left. \left. + s_n \nabla^2 \vec{W}_n] d\omega \right\} \right] \quad (5.6) \end{aligned}$$

The general term in this equation has the form



$$\ell(t) * d\left\{\int_{\omega_1}^{\infty} s_{n-m}(\xi, \omega) F_n(\vec{r}, \omega) d\omega\right\} \quad , \quad m=0,1,2 \quad (5.7)$$

and can be simplified as follows:

$$\begin{aligned} \ell * d\{\} &= \int_{-\infty}^t \ell(t-\eta) \frac{\partial}{\partial \eta} \left\{ \int_{\omega_1}^{\infty} s_{n-m}(\eta-\tau, \omega) F_n(\vec{r}, \omega) d\omega \right\} d\eta \\ &= \int_{-\infty}^t \ell(t-\eta) \left\{ \int_{\omega_1}^{\infty} s_{n-m-1}(\eta-\tau, \omega) F_n(\vec{r}, \omega) d\omega \right\} d\eta \\ &= \int_0^{\infty} \ell(\phi) \left\{ \int_{\omega_1}^{\infty} s_{n-m-1}(t-\phi-\tau, \omega) F_n(\vec{r}, \omega) d\omega \right\} d\phi \\ &\quad \text{(where } \phi=t-\eta\text{)} \\ &= \int_{\omega_1}^{\infty} \left\{ i\omega \int_0^{\infty} \ell(\phi) e^{-i\omega\phi} d\phi \right\} s_{n-m}(\xi, \omega) F_n(\vec{r}, \omega) d\omega \\ &\quad \text{(where (5.4) was used)} \end{aligned}$$

Letting

$$L(\omega) \equiv i\omega \int_0^{\infty} \ell(t) e^{-i\omega t} dt$$

as in (2.8), we then have

$$\begin{aligned} \ell(t) * d\left\{\int_{\omega_1}^{\infty} s_{n-m}(\xi, \omega) F_n(\vec{r}, \omega) d\omega\right\} \\ = \int_{\omega_1}^{\infty} s_{n-m}(\xi, \omega) L(\omega) F_n(\vec{r}, \omega) d\omega \end{aligned} \quad (5.8)$$

Hence, using (5.8) and (2.8), equation (5.6) becomes



$$\begin{aligned}
& \operatorname{Re} \sum_n \left\{ \int_{\omega_1}^{\infty} s_{n-2} (\rho \vec{W}_n) d\omega \right\} = \operatorname{Re} \sum_n \left\{ \int_{\omega_1}^{\infty} s_{n-2} (\Lambda+M) (\vec{W}_n \cdot \nabla \tau) \nabla \tau d\omega \right. \\
& - \int_{\omega_1}^{\infty} s_{n-1} (\Lambda+M) [\nabla (\vec{W}_n \cdot \nabla \tau) + (\nabla \cdot \vec{W}_n) \nabla \tau] d\omega \\
& + \int_{\omega_1}^{\infty} s_n (\Lambda+M) \nabla (\nabla \cdot \vec{W}_n) d\omega + \int_{\omega_1}^{\infty} s_{n-2} M \vec{W}_n (\nabla \tau)^2 d\omega \\
& \left. - \int_{\omega_1}^{\infty} s_{n-1} M (2 \nabla \tau \cdot \nabla \vec{W}_n + \vec{W}_n \nabla^2 \tau) d\omega + \int_{\omega_1}^{\infty} s_n M \nabla^2 \vec{W}_n d\omega \right\}
\end{aligned}$$

Gathering terms, we can write this equation as

$$\operatorname{Re} \sum_{n=0}^{\infty} \int_{\omega_1}^{\infty} [s_{n-2} \vec{N}(\tau, \vec{W}_n) - s_{n-1} \vec{M}(\tau, \vec{W}_n) + s_n \vec{L}(\vec{W}_n)] d\omega = 0 \quad (5.9)$$

where

$$\begin{aligned}
\vec{N}(\tau, \vec{W}_n) &= (\Lambda+M) (\vec{W}_n \cdot \nabla \tau) \nabla \tau + [M (\nabla \tau)^2 - \rho] \vec{W}_n \\
\vec{M}(\tau, \vec{W}_n) &= (\Lambda+M) [(\nabla \cdot \vec{W}_n) \nabla \tau + \nabla (\vec{W}_n \cdot \nabla \tau)] \\
&\quad + M [2 (\nabla \tau \cdot \nabla) \vec{W}_n + \vec{W}_n \nabla^2 \tau] \\
\vec{L}(\vec{W}_n) &= (\Lambda+M) \nabla (\nabla \cdot \vec{W}_n) + M \nabla^2 \vec{W}_n
\end{aligned} \quad (5.10)$$

Expanding the sum in (5.9) and defining  $\vec{W}_{-1} = \vec{W}_{-2} = 0$ , we see that (5.9) can be written as

$$\operatorname{Re} \sum_{n=-2}^{\infty} \int_{\omega_1}^{\infty} s_n (\xi, \omega) [\vec{N}(\tau, \vec{W}_{n+2}) - \vec{M}(\tau, \vec{W}_{n+1}) + \vec{L}(\vec{W}_n)] d\omega = 0 \quad (5.11)$$

In order for (5.11) to be generally true, we must then have

$$\vec{N}(\tau, \vec{W}_{n+2}) - \vec{M}(\tau, \vec{W}_{n+1}) + \vec{L}(\vec{W}_n) = 0 \quad , \quad n=-2, -1, \dots \quad (5.12)$$





or,

$$\vec{N}(\tau, \vec{W}_0) = 0$$

$$\vec{N}(\tau, \vec{W}_1) - \vec{M}(\tau, \vec{W}_0) = 0 \quad (5.13)$$

$$\vec{N}(\tau, \vec{W}_{n+2}) - \vec{M}(\tau, \vec{W}_{n+1}) + L(\vec{W}_n) = 0, \quad n=0,1,2,\dots$$

Equations (5.13) could have been more easily obtained by substituting a Fourier-transformed displacement solution, such as

$$\vec{u} = \sum_{n=0}^{\infty} \vec{W}_n(\vec{r}, \omega) \frac{e^{-i\omega\tau(\vec{r}, \omega)}}{(i\omega)^n} S(\omega)$$

into the Fourier-transformed equation of motion (2.7), however, it was felt that the above approach was more generally valid.

The first equation in (5.13) implies

$$\begin{aligned} \vec{N}(\tau, \vec{W}_0) \cdot \nabla\tau &= (\Lambda+M)(\vec{W}_0 \cdot \nabla\tau)(\nabla\tau)^2 + [M(\nabla\tau)^2 - \rho](\vec{W}_0 \cdot \nabla\tau) \\ &= [(\Lambda+2M)(\nabla\tau)^2 - \rho](\vec{W}_0 \cdot \nabla\tau) = 0 \end{aligned} \quad (5.14)$$

$$\text{and} \quad \vec{N}(\tau, \vec{W}_0) \times \nabla\tau = [M(\nabla\tau)^2 - \rho](\vec{W}_0 \times \nabla\tau) = 0 \quad (5.15)$$

In general,  $\vec{W}_0 \cdot \nabla\tau$  and  $\vec{W}_0 \times \nabla\tau$  are not zero simultaneously. Similarly,  $(\Lambda+2M)(\nabla\tau)^2 - \rho$  and  $M(\nabla\tau)^2 - \rho$  are not simultaneously zero, hence (5.14) and (5.15) have two solutions, i.e.

$$\begin{aligned} (\nabla\tau)^2 &= \frac{\rho}{\Lambda+2M} = \frac{1}{\alpha^2}, \quad \vec{W}_0 \times \nabla\tau = 0 \\ (\nabla\tau)^2 &= \frac{\rho}{M} = \frac{1}{\beta^2}, \quad \vec{W}_0 \cdot \nabla\tau = 0 \end{aligned} \quad (5.16)$$



These are the eikonal equations. In terms of previous notation,  $\tau$  is given by

$$\tau = \frac{\vec{k} \cdot \vec{r}}{\omega} = \frac{\vec{P} \cdot \vec{r}}{\omega} - i \frac{\vec{A} \cdot \vec{r}}{\omega} \quad (5.17)$$

for either P or S waves, hence

$$\begin{aligned} \nabla \tau &= \frac{\vec{k}}{\omega} = \frac{\vec{P}}{\omega} - i \frac{\vec{A}}{\omega} \\ \Rightarrow (\nabla \tau)^2 &= \frac{\vec{k} \cdot \vec{k}}{\omega^2} = \frac{k^2}{\omega^2} \end{aligned} \quad (5.18)$$

and so equations (5.16) are the same as equations (2.11).

The amplitude coefficients  $\vec{W}_n$  can be extracted from equations (5.13). Since we will be taking a plane wave approach, it will not be necessary to determine  $\vec{W}_n$  for all  $n$ , rather only for  $n=0$ , i.e. we consider only the zeroth order of the theory. We now calculate  $\vec{W}_0$  for P waves.

### 5.1 P Waves

For plane P waves, we can write

$$\vec{W}_0 = W_0 \hat{t}_P \quad (5.19)$$

where  $\hat{t}_P$  is the complex unit vector for P waves, discussed in section 4.2, and is given by

$$\hat{t}_P = \hat{k}_P = \alpha \nabla \tau \quad (5.20)$$

To determine  $\vec{W}_0$ , we first compute  $\vec{M}(\tau, \vec{W}_0) \cdot \nabla \tau$ .



$$\begin{aligned}\vec{M}(\tau, \vec{W}_0) \cdot \nabla \tau &= (\Lambda + M) [(\nabla \cdot \vec{W}_0) (\nabla \tau)^2 + \nabla(\vec{W}_0 \cdot \nabla \tau) \cdot \nabla \tau] \\ &+ M[\nabla^2 \tau (\vec{W}_0 \cdot \nabla \tau) + 2\{(\nabla \tau \cdot \nabla) \vec{W}_0\} \cdot \nabla \tau]\end{aligned}$$

We have

$$(\nabla \tau)^2 = 1/\alpha^2$$

$$\nabla \cdot \vec{W}_0 = \nabla \cdot (W_0 \alpha \nabla \tau) = \alpha \nabla \tau \cdot \nabla W_0 + \alpha W_0 \nabla^2 \tau$$

$$\vec{W}_0 \cdot \nabla \tau = W_0 \alpha (\nabla \tau)^2 = W_0 / \alpha$$

$$(\nabla \tau \cdot \nabla) \vec{W}_0 = (\nabla \tau \cdot \nabla) W_0 \hat{t}_P = (\nabla \tau \cdot \nabla W_0) \hat{t}_P$$

(since the medium is homogeneous)

$$\Rightarrow \nabla \tau \cdot \{(\nabla \tau \cdot \nabla) \vec{W}_0\} = (1/\alpha) \nabla \tau \cdot \nabla W_0$$

Hence

$$\begin{aligned}\vec{M}(\tau, \vec{W}_0) \cdot \nabla \tau &= (\Lambda + M) \left[ \frac{1}{\alpha} \nabla \tau \cdot \nabla W_0 + \frac{1}{\alpha} W_0 \nabla^2 \tau + \frac{1}{\alpha} \nabla \tau \cdot \nabla W_0 \right] \\ &+ M \left[ \frac{W_0}{\alpha} \nabla^2 \tau + \frac{2}{\alpha} \nabla \tau \cdot \nabla W_0 \right] \\ &= \left( \frac{\Lambda + 2M}{\alpha} \right) [W_0 \nabla^2 \tau + 2 \nabla \tau \cdot \nabla W_0] \\ &= \rho \alpha [W_0 \nabla^2 \tau + 2 \nabla \tau \cdot \nabla W_0]\end{aligned}\tag{5.21}$$

$$\text{Hence } [\vec{M}(\tau, \vec{W}_0) \cdot \nabla \tau] W_0 = \rho \alpha \nabla \cdot [(W_0)^2 \nabla \tau] \tag{5.22}$$

Now, from (5.10), we have

$$\begin{aligned}\vec{N}(\tau, \vec{W}_n) \cdot \nabla \tau &= (\Lambda + M) (\vec{W}_n \cdot \nabla \tau) (\nabla \tau)^2 + [M (\nabla \tau)^2 - \rho] (\vec{W}_n \cdot \nabla \tau) \\ &= \left[ \left( \frac{\Lambda + M}{\alpha} \right) + \frac{M}{\alpha} - \rho \right] (\vec{W}_n \cdot \nabla \tau) \\ &= \left[ \frac{\Lambda + 2M}{\alpha} - \rho \right] (\vec{W}_n \cdot \nabla \tau) = 0\end{aligned}\tag{5.23}$$



Hence, the second equation of (5.13) then shows that

$\vec{M}(\tau, \vec{W}_0) \cdot \nabla \tau = 0$ . Therefore, equation (5.22) becomes

$$\nabla \cdot [(W_0)^2 \nabla \tau] = 0 \quad (5.24)$$

Let us now use the concept of a ray tube about a central ray connecting two wavefronts of the central ray at different times  $t_0$  and  $t$  with  $t_0 < t$  (see, for example, Červený and Ravindra (1971)). Let  $s$  be the length along the ray path in the direction of propagation  $\vec{P}$ . The ray tube is bounded by rays adjacent to the central ray and infinitesimally distant from it, and by the infinitesimal wavefront surfaces at  $s=s_0$  and  $s$ , i.e.,  $d\sigma(s_0)$  and  $d\sigma(s)$ . Integrating over the volume  $V$  of the ray tube, and using Gauss' divergence theorem, we have

$$\int_{\sigma} (W_0)^2 \nabla \tau \cdot \vec{d\sigma} = 0 \quad (5.25)$$

where  $d\sigma$  is the element of area on the ray tube. Writing  $\nabla \tau$  as

$$\nabla \tau = \frac{1}{\omega} (\vec{P} - i\vec{A}) = \frac{1}{\omega} (\hat{P}\hat{P} - i\hat{A}\hat{A}) \quad (5.26)$$

where  $\hat{P}$  and  $\hat{A}$  are real unit vectors, we obtain

$$\begin{aligned} \int_{\sigma} (W_0)^2 \nabla \tau \cdot \vec{d\sigma} &= \frac{P}{\omega} \{ [(W_0)^2 d\sigma]_s - [(W_0)^2 d\sigma]_{s_0} \} \\ &\quad - \frac{iA \cos \gamma}{\omega} \{ [(W_0)^2 d\sigma]_s - [(W_0)^2 d\sigma]_{s_0} \} \\ &= 0 \end{aligned} \quad (5.27)$$





Hence

$$[(W_0)^2 d\sigma]_s - [(W_0)^2 d\sigma]_{s_0} = 0 \quad (5.28)$$

which leads to

$$W_0(s) = \sqrt{\frac{d\sigma(s_0)}{d\sigma(s)}} W_0(s_0) \quad (5.29)$$

This equation gives  $W_0$  at any point  $s$  on the ray, assuming we know it at  $s_0$ . It has the same form as the analogous elastic result (see Červený and Ravindra (1971)), which is what one would expect since (5.29) is a purely geometrical result which describes the geometrical spreading of waves. Intuitively, one would also expect an attenuation term to be present, however, this is accounted for by the imaginary part of  $\tau$ .

## 5.2 S Waves

For S waves, we can write

$$\vec{W}_0 = W_0^2 \vec{t}_2 + W_0^3 \vec{t}_3 \quad (5.30)$$

where the complex unit vectors  $\vec{t}_2$  and  $\vec{t}_3$  are given by

$$\vec{t}_2 = \hat{y} \times \hat{k}_S, \quad \vec{t}_3 = \hat{y} \quad (5.31)$$

as discussed in section 4.2. The vectors  $\hat{t}_p$ ,  $\vec{t}_2$  and  $\vec{t}_3$  are orthogonal. To determine  $\vec{W}_0$ , we compute  $\vec{M}(\tau, \vec{W}_0) \cdot \vec{t}_i$ ,  $i=2,3$ . Since  $\vec{t}_i \cdot \nabla \tau = 0$ , and  $\vec{W}_0 \cdot \nabla \tau = 0$ , we have

$$\vec{M}(\tau, \vec{W}_0) \cdot \vec{t}_i = M[W_0^i \nabla^2 \tau + 2\{(\nabla \tau \cdot \nabla) \vec{W}_0\} \cdot \vec{t}_i] \quad , \quad i=2,3$$



Now,

$$\begin{aligned} \{(\nabla\tau \cdot \nabla)\vec{W}_0\} \cdot \vec{t}_i &= (\nabla\tau \cdot \nabla W_0^2) \vec{t}_2 \cdot \vec{t}_i + (\nabla\tau \cdot \nabla W_0^3) \vec{t}_3 \cdot \vec{t}_i \\ &= \nabla\tau \cdot \nabla W_0^i, \quad i=2,3 \end{aligned}$$

Hence

$$\vec{M}(\tau, \vec{W}_0) \cdot \vec{t}_i = M[W_0^i \nabla^2 \tau + 2\nabla\tau \cdot \nabla W_0^i] \quad (5.32)$$

$$\text{and } [\vec{M}(\tau, \vec{W}_0) \cdot \vec{t}_i] W_0^i = M \nabla \cdot [(W_0^i)^2 \nabla \tau] \quad (5.33)$$

Now, since  $(\nabla\tau)^2 = 1/\beta^2 = \rho/M$ , we have for S waves,

$$\vec{N}(\tau, \vec{W}_n) = (\Lambda + M) (\vec{W}_n \cdot \nabla \tau) \nabla \tau \quad (5.34)$$

$$\text{Hence } \vec{N}(\tau, \vec{W}_1) \cdot \vec{t}_i = 0, \quad i=2,3 \quad (5.35)$$

Therefore, the second equation of (5.13) shows that

$\vec{M}(\tau, \vec{W}_0) \cdot \vec{t}_i = 0$ . Hence, equation (5.33) gives

$$\nabla \cdot [(W_0^i)^2 \nabla \tau] = 0 \quad (5.36)$$

As in the previous section, this leads to

$$W_0^i(s) = \sqrt{\frac{d\sigma(s_0)}{d\sigma(s)}} W_0^i(s_0), \quad i=2,3 \quad (5.37)$$

as in equation (5.29). It again has the same form as the analogous elastic result (see Červený and Ravindra (1971)).

### 5.3 Geometrical Spreading

We now calculate the geometrical spreading factor for a ray propagating through a layered homogeneous isotropic linear viscoelastic medium. Let us consider a typical ray



consisting of  $m$  segments, as in Figure 8 and define  $O_j$  to be the endpoint of the  $j$ th ray segment, at an interface. Using equations (5.29) or (5.37) to compute the amplitude coefficient of the ray anywhere along its path, we obtain at the endpoint  $K$

$$W(K) = \frac{1}{L(K, K_O)} \prod_{j=1}^{m-1} R_j \quad (5.38)$$

where

$$L(K, K_O) = \sqrt{\frac{d\sigma(K)}{d\sigma(K_O)}} \prod_{j=1}^{m-1} \sqrt{\frac{d\sigma(O_j)}{d\sigma'(O_j)}} \quad (5.39)$$

We assume that  $K_O$  is at a unit distance from the source.

$R_j$  is the reflection/transmission coefficient at  $O_j$ . We use the prime to denote quantities associated with the reflected or transmitted wave at  $O_j$ , and an unprimed quantity is associated with the incident wave at  $O_j$ .

$L(K, K_O)$  is the geometrical spreading factor of the ray.

To evaluate (5.39), we first get an expression for  $d\sigma(K)/d\sigma(K_O)$ . Referring to Figure 9, we see that

$$d\sigma(K) = (\cos\theta(K) dx) (x d\phi_O)$$

where  $\phi_O$  is the azimuthal coordinate at  $K_O$ , and  $x$  is the epicentral distance. Now since  $x = x(z, \theta_O, \gamma_O)$  where  $\theta_O = \theta(K_O)$  and  $\gamma_O = \gamma(K_O)$  are the propagation and attenuation angles at the source, we have

$$dx = \frac{\partial x}{\partial \theta_O} d\theta_O + \frac{\partial x}{\partial \gamma_O} d\gamma_O + \frac{\partial x}{\partial z} dz$$



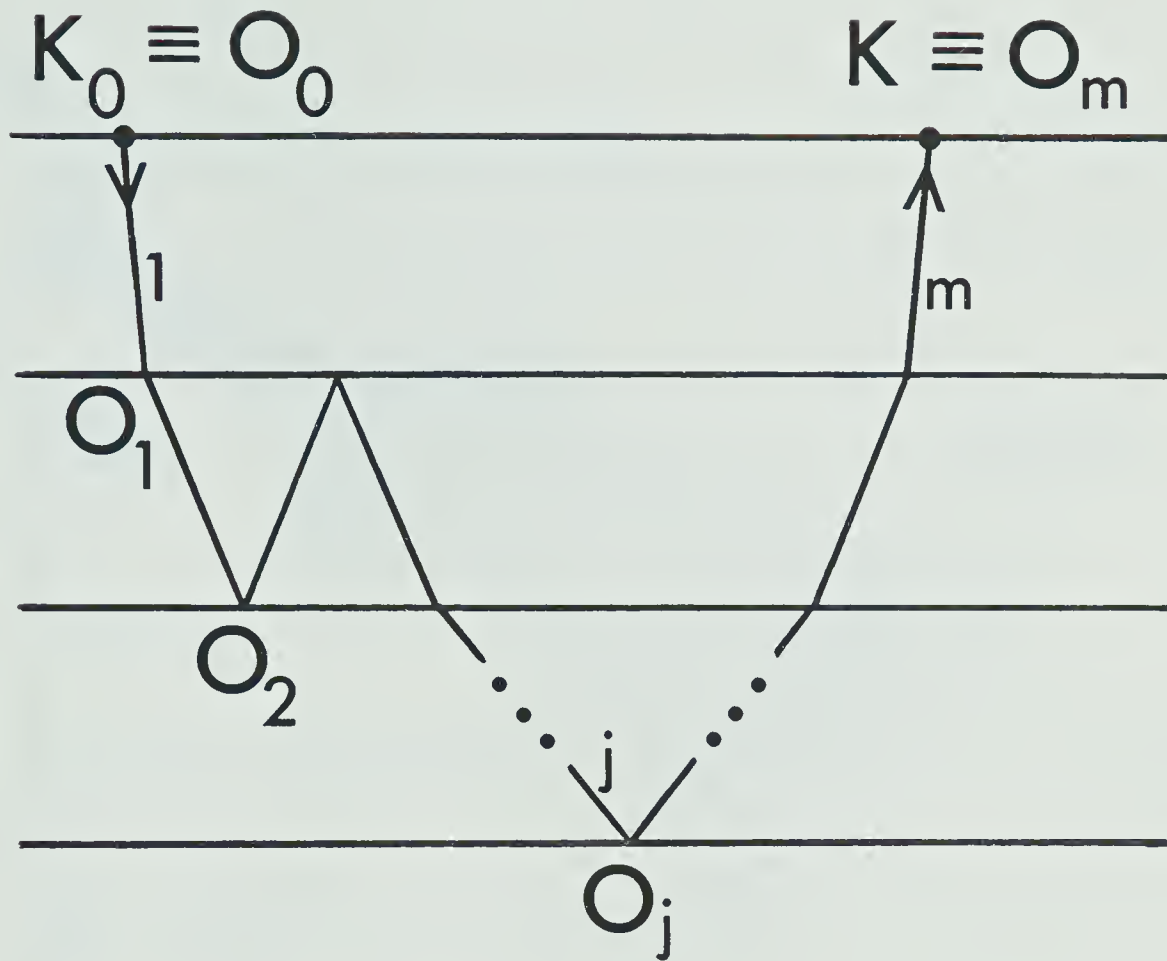


FIGURE 8: Typical ray in a homogeneous layered medium.  $K_0$  and  $K$  are the source and receiver points, respectively.  $O_j$ ,  $j = 1, \dots, m$  is the endpoint of the  $j$ th ray segment, at an interface.





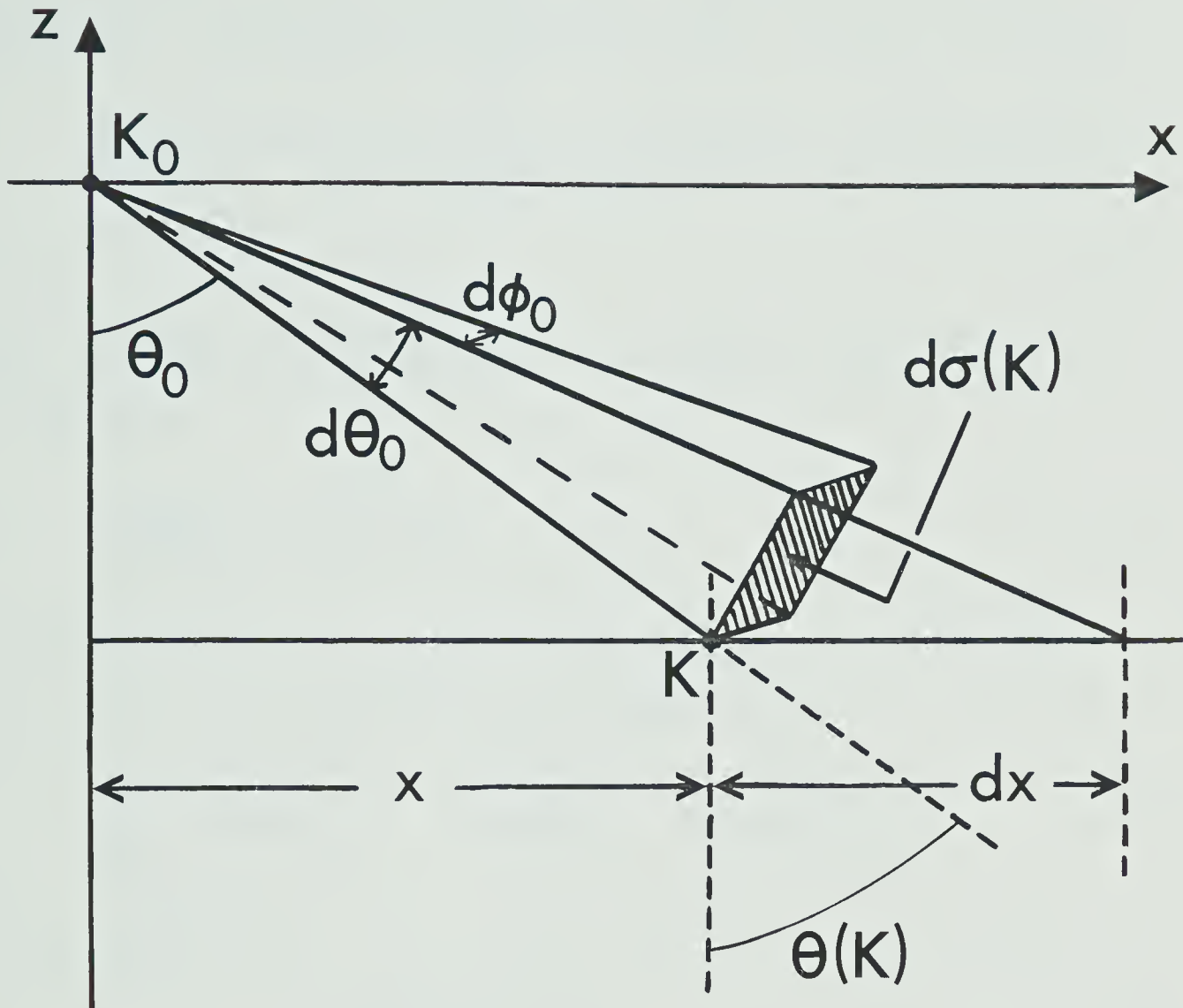


FIGURE 9: Ray tube between  $K_0$  and  $K$  for a homogeneous medium.  $d\sigma(K)$  is the cross-sectional area at  $K$ . The diagram is partially schematic - there may be, in actuality, an arbitrary number of reflections and transmissions at interfaces between  $K_0$  and  $K$ .



From Figure 9,  $dz=0$ . Also, we will assume that the source rays all have the same value of  $\gamma_o$ , which implies  $d\gamma_o=0$ . The cross-section of the spherical wave at the source,  $d\sigma_o=d\sigma(K_o)$ , is given by  $d\sigma_o=\sin\theta_o d\theta_o d\phi_o$ . Hence, we have

$$\frac{d\sigma(K)}{d\sigma(K_o)} = \frac{x(\partial x/\partial \theta_o) \cos\theta(K) d\theta_o d\phi_o}{\sin\theta_o d\theta_o d\phi_o} = \frac{x(\partial x/\partial \theta_o) \cos\theta(K)}{\sin\theta_o} \quad (5.40)$$

Next, we simplify the product in (5.39). From Figure 10, we see that

$$\frac{d\sigma(O_j)}{d\sigma'(O_j)} = \frac{\cos\theta(O_j)}{\cos\theta'(O_j)} \quad (5.41)$$

Now, for homogeneous media,  $\theta'(O_j)=\theta(O_{j+1})$ . Using this in (5.41) and then expanding the product in (5.39), we obtain

$$\prod_{j=1}^{m-1} \sqrt{\frac{d\sigma(O_j)}{d\sigma'(O_j)}} = \sqrt{\frac{\cos\theta(O_1)}{\cos\theta(O_m)}} = \sqrt{\frac{\cos\theta_o}{\cos\theta(K)}} \quad (5.42)$$

Hence, using (5.40) and (5.42), equation (5.39) becomes

$$L(K, K_o) = \sqrt{x \frac{\partial x}{\partial \theta_o} \cot\theta_o} \quad (5.43)$$

The epicentral distance  $x$  is given by

$$x = \sum_{j=1}^m x_j \quad (5.44)$$

$$\text{where } x_j = h_j \tan \theta_j \quad (5.45)$$

where  $h_j$  is the thickness of the layer containing the  $j$ th ray segment,  $\theta_j=\theta(O_j)$ , and  $x_j$  is the horizontal distance traversed by the  $j$ th ray segment.



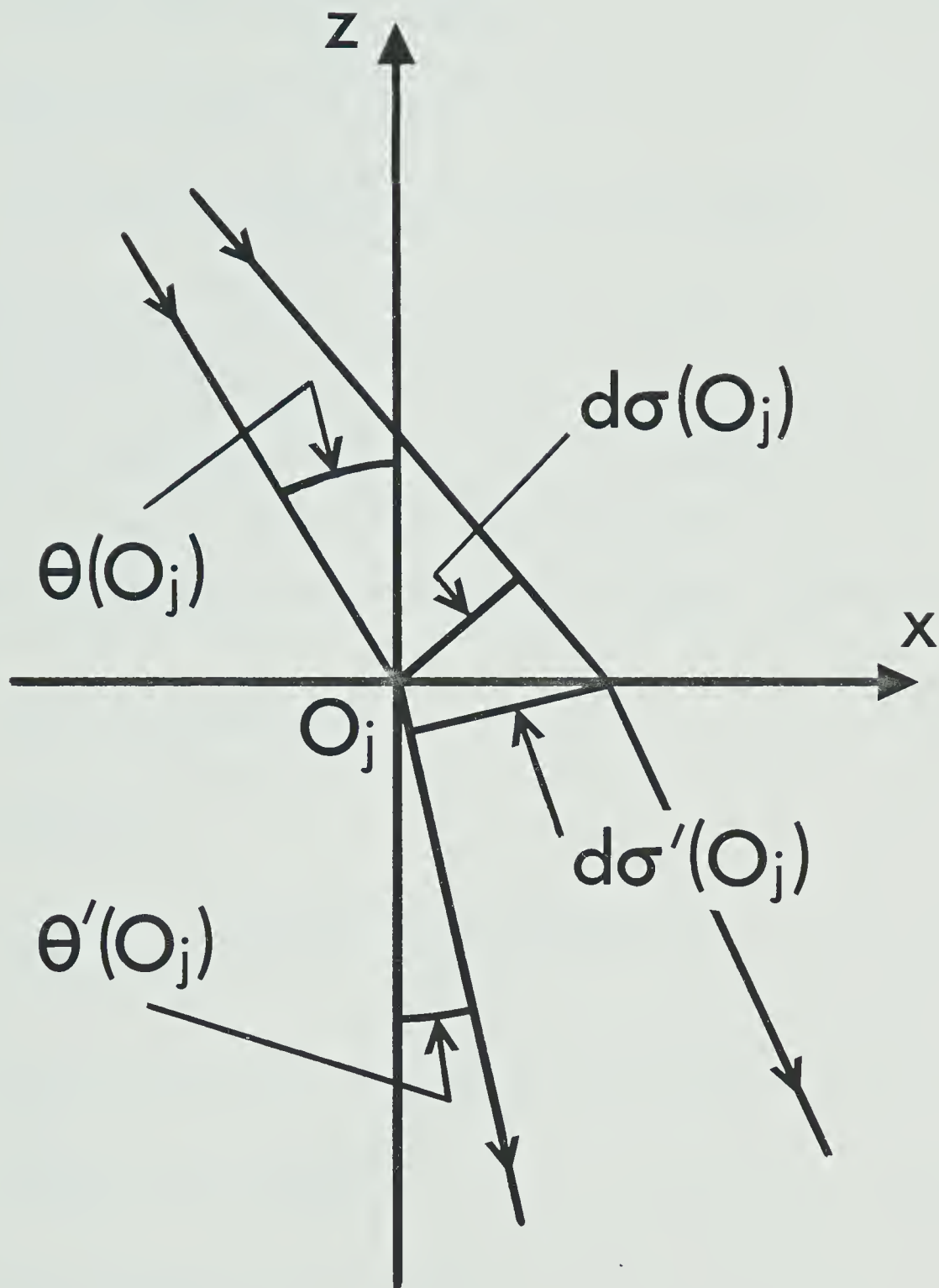


FIGURE 10: Change in the cross-sectional area of the ray tube at an interface.



We now evaluate  $\partial x_j / \partial \theta_o$ . We have

$$\tan \theta_j = \frac{x_j}{h_j} = \frac{|P_{jx}|}{|P_{jz}|} = \frac{k_{xR}}{d_{jR}} \quad (5.46)$$

where  $k_{xR} = P_j \sin \theta_j = P_o \sin \theta_o$  (5.47)

$$d_j = + \text{p.v.} \sqrt{k_j^2 - k_x^2} \quad (\text{P, SV or SH waves})$$

We have suppressed the subscripts P, S,  $\alpha, \beta$  etc. so that the analysis holds for P, SV and SH waves. The subscript "o" denotes quantities at  $K_o$ . The "+" sign was chosen for  $d_j$  since we are dealing only with body waves, i.e. ray segments propagating at sub-critical angles. Hence, we have

$$x_j = h_j P_o \sin \theta_o / d_{jR} \quad (5.48)$$

which implies

$$\frac{\partial x_j}{\partial \theta_o} = h_j P_o \left[ \frac{d_{jR} \cos \theta_o - \sin \theta_o (\partial d_{jR} / \partial \theta_o)}{d_{jR}^2} \right] \quad (5.49)$$

For  $(\partial d_{jR} / \partial \theta_o)$  we have, suppressing the symbol "p.v.",

$$\frac{\partial d_{jR}}{\partial \theta_o} = \text{Re} \left[ - \frac{k_x}{d_j} \frac{\partial k_x}{\partial \theta_o} \right] \quad (5.50)$$

Now  $k_x$  and  $\partial k_x / \partial \theta_o$  are given by

$$k_x = P_o \sin \theta_o - i A_o \sin(\theta_o - \gamma_o) \quad (5.51)$$

$$\frac{\partial k_x}{\partial \theta_o} = P_o \cos \theta_o - i A_o \cos(\theta_o - \gamma_o)$$





Substituting these into (5.50), and then using the resulting equation for  $\partial d_{jR}/\partial \theta_o$  in (5.49), we obtain

$$\begin{aligned} \frac{\partial x_j}{\partial \theta_o} = \frac{h_j P_o}{d_{jR}} \{ \cos \theta_o + \frac{\frac{1}{2} [P_o^2 \sin 2\theta_o - A_o^2 \sin 2(\theta_o - \gamma_o)] \sin \theta_o}{|d_j^2|} \\ - \frac{P_o A_o \sin(2\theta_o - \gamma_o) \sin \theta_o d_{jI}}{d_{jR} |d_j^2|} \} \end{aligned} \quad (5.52)$$

Hence, we can write

$$\frac{\partial x}{\partial \theta_o} = \sum_{j=1}^m \frac{\partial x_j}{\partial \theta_o} = (P_o \cos \theta_o) Z \quad (5.53)$$

where

$$\begin{aligned} Z = \sum_{j=1}^m \frac{h_j}{d_{jR}} + \frac{1}{2} [P_o^2 \sin 2\theta_o - A_o^2 \sin 2(\theta_o - \gamma_o)] \tan \theta_o \sum_{j=1}^m \frac{h_j}{d_{jR} |d_j^2|} \\ - P_o A_o \sin(2\theta_o - \gamma_o) \tan \theta_o \sum_{j=1}^m \frac{h_j d_{jI}}{d_{jR}^2 |d_j^2|} \end{aligned} \quad (5.54)$$

$$\text{Using } x = \sum_{j=1}^m x_j = P_o \sin \theta_o \sum_{j=1}^m \frac{h_j}{d_{jR}} \quad (5.55)$$

implies

$$x \cot \theta_o = P_o \cos \theta_o \sum_{j=1}^m \frac{h_j}{d_{jR}} \quad (5.56)$$

Hence, the final expression for the geometrical spreading factor  $L$  is

$$L(K, K_o) = P_o \cos \theta_o \sqrt{\left( \sum_{j=1}^m \frac{h_j}{d_{jR}} \right) Z} \quad (5.57)$$

where  $Z$  is given by (5.54). We can show that this reduces to the correct expression for  $L$  in the perfectly elastic



case, as follows. For perfect elasticity, we have

$$d_{jR} = d_j = \frac{\omega}{v_j} \cos \theta_j$$

$$A_o = 0$$

Hence (5.54) becomes

$$\begin{aligned} z_{el} &= \frac{1}{\omega} \sum_{j=1}^m \frac{v_j h_j}{\cos \theta_j} + \frac{1}{\omega} \frac{\sin^2 \theta_o}{v_o^2} \sum_{j=1}^m \frac{v_j^3 h_j}{\cos^3 \theta_j} \\ &= \frac{1}{\omega} \sum_{j=1}^m \left[ \frac{v_j h_j}{v_o^2 \cos^3 \theta_j} (v_o^2 \cos^2 \theta_j + v_j^2 \sin^2 \theta_o) \right] \end{aligned}$$

where  $P_o = \omega/v_o$  was used. Now, Snell's law in elastic media implies  $v_j \sin \theta_o = v_o \sin \theta_j$ , hence, using  $\cos^2 \theta_j + \sin^2 \theta_j = 1$ ,  $Z$  becomes

$$z_{el} = \frac{1}{\omega} \sum_{j=1}^m \frac{v_j h_j}{\cos^3 \theta_j}$$

and finally, (5.57) becomes

$$L_{el} = \frac{\cos \theta_o}{v_o} \sqrt{\left( \sum_{j=1}^m \frac{v_j h_j}{\cos \theta_j} \right) \left( \sum_{j=1}^m \frac{v_j h_j}{\cos^3 \theta_j} \right)} \quad (5.58)$$

This agrees with the expression for  $L$  in perfectly elastic media given by Červený and Ravindra (1971, equation 2.143).

The expression (5.57) for  $L$  will be used in the next chapter for the computation of body-wave synthetic seismograms for a point source at the surface.



## CHAPTER 6

### SYNTHETIC SEISMOGRAMS

In this chapter, we use the theory developed in the previous chapters to compute synthetic seismograms for body waves in a layered anelastic medium. Both the teleseismic case, and the case of a point source at the surface are treated. Hron et al. (1974) developed a computer program to calculate synthetic seismograms for teleseismic body waves in a plane layered homogeneous isotropic elastic medium via a ray theory approach. A similar program to compute synthetic seismograms for waves generated by a point source at the surface was developed by Hron and Kanasewich (1971). These programs automatically generate all rays which arrive at the receiver, including multiples, up to a given maximum number of segments per ray, and can automatically identify the rays that make up a given event on the synthetic seismogram. The program for the teleseismic case can also handle dipping interfaces. The program for the surface point source case groups all generated rays into kinematic and dynamic analogs, which significantly improves the computing efficiency. For the purposes of this thesis, these programs have been modified to compute synthetic seismograms for SH body waves propagating through a layered homogeneous isotropic linear viscoelastic medium. In order to be able to compute synthetic seismograms for a layered medium consisting of elastic layers embedded



among anelastic layers, all six computational cases of reflection/transmission at a boundary discussed in Chapter 4 have been incorporated into the programs.

The medium we use is a model of the Berkeley crust due to Silva (1976), and is shown in Table 1. The parameters  $v_{HP}$  and  $v_{HS}$  are the homogeneous phase speeds for P and S waves and the parameter  $h$  is the thickness of a layer. The model consists of three anelastic layers over an elastic half-space. The interfaces are plane and horizontal.

### 6.1 Teleseismic Case

For teleseismic waves, each ray originates in the elastic half-space, which means that  $A_x$  will be zero for the incident ray segment, and since  $A_x$  must be continuous across a boundary,  $A_x$  will be zero for every ray segment, i.e.  $\vec{A}$  will be in the  $\pm z$  direction for every ray segment.

For SH waves, the displacement of a given ray at the receiver is in the  $y$  direction, and the amplitude of motion of the ray is given by an inverse Fourier transform as

$$\begin{aligned}
 W &= \frac{1}{\pi} \operatorname{Re} \int_0^{\infty} Y(\omega) e^{i\phi(\omega)} S(\omega) e^{i\omega(t-\tau(\omega))} d\omega \\
 &= \frac{1}{\pi} \operatorname{Re} \int_0^{\infty} Y e^{i\phi} S(\omega) e^{\omega\tau} I e^{i\omega(t-\tau_R)} d\omega
 \end{aligned} \tag{6.1}$$

We may use the above form rather than  $(1/2\pi) \int_{-\infty}^{\infty}$  because  $W$  is the response and is a real number (see Appendix 2).





TABLE 1

CRUSTAL MODEL

Layer Number	$v_{HP}$ (km/s)	$v_{HS}$ (km/s)	$\rho$ (g/cc)	$Q_P$	$Q_S$	$h$ (km)
1	4.2	2.4	2.1	67	30	1.4
2	6.1	3.5	2.6	100	45	8.2
3	7.3	4.2	3.0	180	80	12.9
4	7.8	4.5	3.3	$\infty$	$\infty$	$\infty$



The quantity  $Y(\omega)e^{i\phi(\omega)}$  is the product of the anelastic reflection and transmission coefficients for the ray,  $Y$  and  $\phi$  being the relative magnitude and phase.  $S(\omega)$  is the spectrum of the source pulse.  $\tau = \tau_R + i\tau_I$  is the complex phase function, where  $\tau_R$  is its real part and is the arrival time of the ray, and  $\tau_I$  is its imaginary part and corresponds to the attenuation of the ray. For a given ray segment,  $\tau$  is given by

$$\tau = \frac{\vec{k} \cdot \vec{r}}{\omega} = \frac{\vec{P} \cdot \vec{r}}{\omega} - i \frac{\vec{A} \cdot \vec{r}}{\omega} \quad (6.2)$$

hence,

$$\tau_R = \vec{P} \cdot \vec{r} / \omega, \quad \tau_I = -\vec{A} \cdot \vec{r} / \omega \quad . \quad (6.3)$$

We suppress the subscript "S", since we are dealing only with SH waves.

Since we are considering teleseismic waves, no geometrical spreading factor appears in (6.1).

In our computations, we assume that  $Q$  is independent of frequency. This means that we are neglecting velocity dispersion in our calculations, i.e. we are using one constant velocity  $v_H$  for all frequencies. It is well known that this assumption introduces an acausality in the response (Futterman (1962)). However, this will not be an important effect in our case, due to the nature of our source pulse, whose spectrum exhibits a large, narrow peak at a dominant frequency  $f_0$ . Thus, most of the contribution to the integral in (6.1) will come from a narrow frequency



interval centered about  $\omega = \omega_o = 2\pi f_o$ , and the dispersion in this interval will be negligible. This also means that choosing our constant velocity  $v_H$  to be the velocity at the dominant frequency of our source pulse, i.e.  $v_H = v_H(\omega_o)$  (which can be obtained from dispersion data), and similarly choosing  $Q = Q(\omega_o)$ , should considerably reduce the errors in arrival time that would be introduced by neglecting dispersion. Finally, if we restrict ourselves to values of  $Q$  which are not too low, and ray paths which are not too long, we should, by the above frequency-independent approach, be able to obtain a good approximation to the actual dispersive response. These arguments would not be as valid in the case of a  $\delta$ -function source pulse, whose spectrum is a constant for all frequencies.

An added computational advantage in using the above frequency-independent approach, is that by choosing an appropriate source pulse, we will be able to calculate the response in (6.1) analytically, i.e. in closed form, as we shall see below.

The arrival time  $\tau_R$  is obtained by summing up the travel times of each segment of the ray. The speed and length of each ray segment are calculated from the viscoelastic theory presented in the previous chapters.

The attenuation term  $\tau_I$  is obtained in a similar fashion. For a given ray segment, from (6.3) we have

$$\nabla \tau_I = -\vec{A}/\omega \quad (6.4)$$



Letting  $s$  be the length along the ray path in the direction of propagation  $\vec{P}$ , and using (2.16) and (6.4) we then obtain for a given segment

$$\begin{aligned} \frac{d\tau_I}{ds} &= \hat{P} \cdot \nabla \tau_I = |\nabla \tau_I| \cos(\hat{P}, \nabla \tau_I) \\ &= \frac{A}{\omega} \cos(\pi - \gamma) = -\frac{A}{\omega} \cos \gamma \\ &= \frac{\text{Im}(k^2)}{2\omega P} \end{aligned} \quad (6.5)$$

Hence, for the entire ray,  $\tau_I$  is given by a sum over the ray segments:

$$\tau_I(\text{receiver}) = \sum_j \int \left[ \frac{\text{Im}(k^2)}{2\omega P} \right]_j ds \quad (6.6)$$

where the limits of the integral are the beginning and end points of the  $j$ -th ray segment. Using (2.15), and the fact that the medium is homogeneous, (6.6) becomes

$$\tau_I(\text{rec.}) = \sum_j \left[ \frac{1}{2} (k_j^2 / \omega^2)_I (v_j \ell_j) \right] \quad (6.7)$$

where  $v_j = \omega/P_j$  is the phase speed of the  $j$ -th ray segment, and  $\ell_j$  is its length. Employing (2.21), equation (6.7) finally becomes

$$\tau_I(\text{rec.}) = - \sum_j \left[ \frac{Q_j^{-1} v_j \ell_j}{v_{Hj}^2 (1 + \sqrt{1 + Q_j^{-2}})} \right] \quad (6.8)$$

If  $Q_j$  is frequency-independent, then so are  $v_j$  and  $v_{Hj}$ , hence  $\tau_I$  is frequency-independent. Also,  $Y(\omega)$  and  $\phi(\omega)$





are frequency-independent. Letting  $\xi = t - \tau_R$ , (6.1) becomes

$$\begin{aligned}
 W &= \frac{Y}{\pi} \operatorname{Re} \left\{ e^{i\phi} \int_0^{\infty} S(\omega) e^{\omega \tau_I} e^{i\omega \xi} d\omega \right\} \\
 &= Y \operatorname{Re} \{ e^{i\phi} f(\xi, \tau_I) \} \\
 &= Y [f_R(\xi, \tau_I) \cos \phi - f_I(\xi, \tau_I) \sin \phi]
 \end{aligned} \tag{6.9}$$

where

$$f(\xi, \tau_I) = \frac{1}{\pi} \int_0^{\infty} S(\omega) e^{\omega \tau_I} e^{i\omega \xi} d\omega \tag{6.10}$$

The subscripts R and I refer to the real and imaginary parts.

It would be a definite computational advantage to be able to evaluate (6.10) analytically, i.e. in closed form, since then the response could also be evaluated in closed form. With this in mind, we choose our source pulse to be

$$s(t) = \frac{\sin(\omega_0 t)}{1 + (\omega_0 t / \eta)^2} \tag{6.11}$$

The spectrum for this pulse is given by

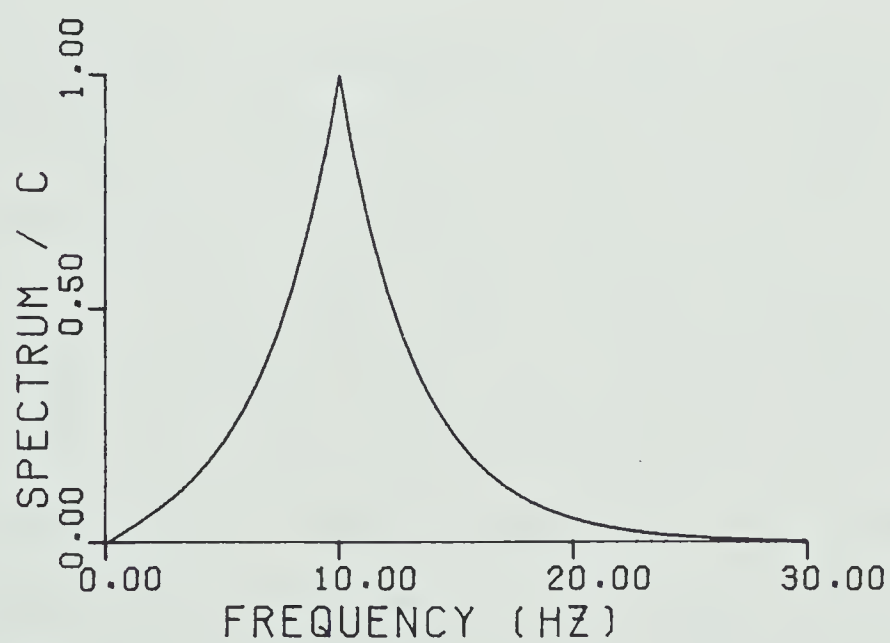
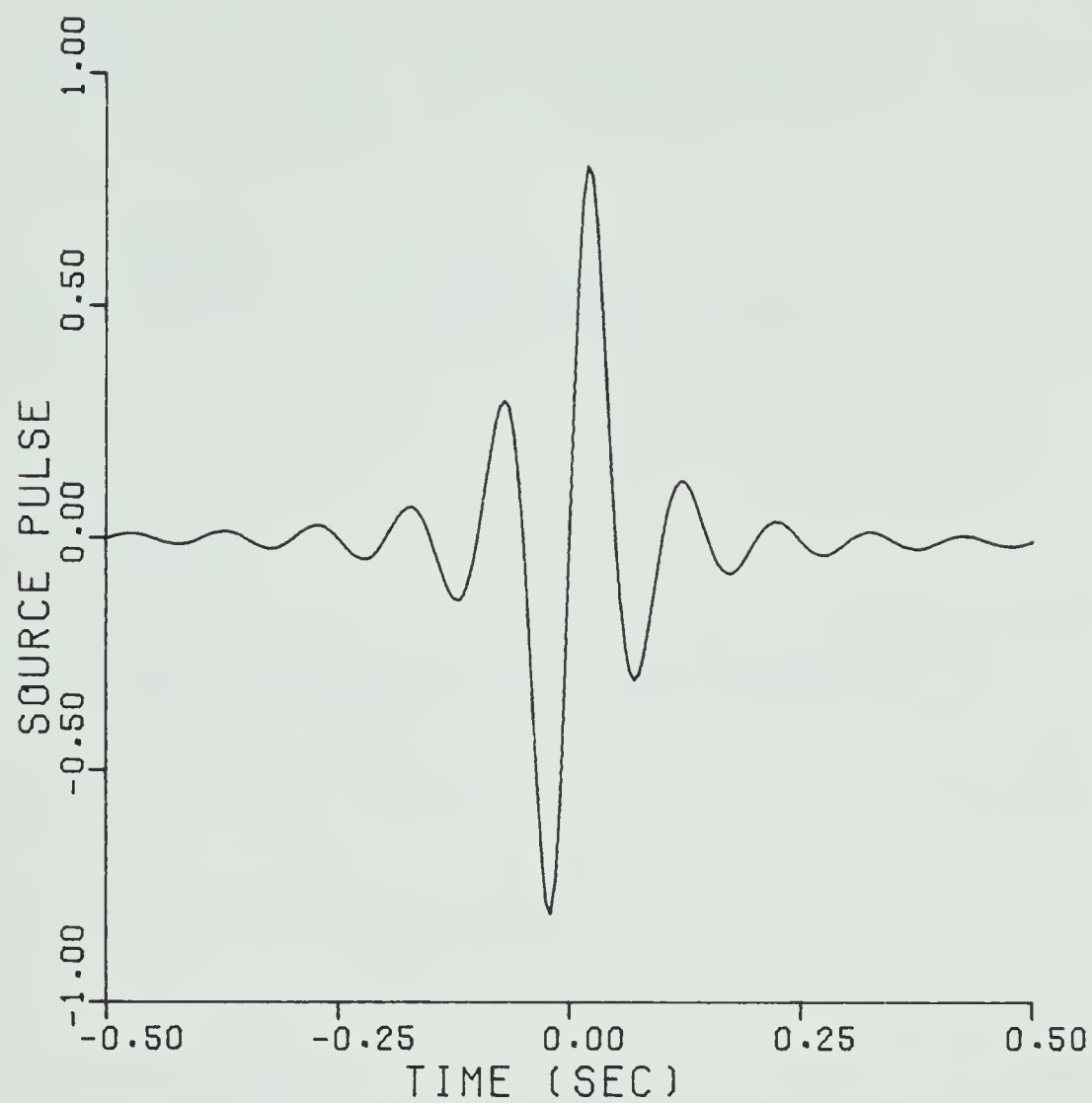
$$S(\omega) = -\frac{i\pi\eta}{2\omega_0} \left\{ \exp\left[-\frac{\eta}{\omega_0} |\omega - \omega_0| \right] - \exp\left[-\frac{\eta}{\omega_0} (\omega + \omega_0) \right] \right\} \tag{6.12}$$

The pulse and spectrum are shown in Figure 11. As required, the spectrum has a peak at  $\omega = \omega_0$ . Since  $\tau_I$  and  $\xi$  are independent of  $\omega$ , we can see that the integrand in (6.10) involves a product of exponential and trigonometric functions whose arguments are linear in  $\omega$ , which is easy to integrate. The result is



FIGURE 11: Source pulse, and absolute value of spectrum divided by  $C$ , where  $C = \pi\eta/2\omega_0$ . In this diagram,  $\eta = 3$  and  $f_0 = 10$  Hz.







$$f_R(\xi, \tau_I) = \frac{t_o^2 \{ e^{\omega_o \tau_I} [ (t_o^2 + \xi^2 - \tau_I^2) \sin \omega_o \xi + 2\tau_I \xi \cos \omega_o \xi ] - 2\tau_I \xi e^{-\eta} \}}{[ (t_o + \tau_I)^2 + \xi^2 ] [ (t_o - \tau_I)^2 + \xi^2 ]} \quad (6.13)$$

$$f_I(\xi, \tau_I) = - \frac{t_o^2 \{ e^{\omega_o \tau_I} [ (t_o^2 + \xi^2 - \tau_I^2) \cos \omega_o \xi - 2\tau_I \xi \sin \omega_o \xi ] - (t_o^2 + \xi^2 - \tau_I^2) e^{-\eta} \}}{[ (t_o + \tau_I)^2 + \xi^2 ] [ (t_o - \tau_I)^2 + \xi^2 ]}$$

where

$$t_o = \eta / \omega_o \quad (6.14)$$

For  $\tau_I = 0$ , i.e. no attenuation, these reduce to

$$f_R(\xi, 0) = \frac{\sin \omega_o \xi}{1 + (\omega_o \xi / \eta)^2} \quad (6.15)$$

$$f_I(\xi, 0) = - \frac{(\cos \omega_o \xi - e^{-\eta})}{1 + (\omega_o \xi / \eta)^2}$$

As is expected,  $f_R(\xi, 0)$  is the same as (6.11), where  $\xi$  corresponds to  $t$ .

The synthetic seismograms for the crustal model in Table 1 are shown in Figure 12. Figure 12a shows the results for the case of perfect elasticity ( $Q^{-1}$  is set equal to zero in each layer), and Figure 12b shows the results for the anelastic case. The source parameters used are  $\eta=3$  and  $f_o=10$  Hz. The interfaces in the crustal model are horizontal. From the top down, the traces in Figures 12a and 12b correspond to teleseismic waves impinging upon the deepest interface at incident angles of  $0^\circ$ ,  $15^\circ$ ,  $30^\circ$ ,  $45^\circ$ ,  $60^\circ$  and  $75^\circ$ . In each figure, the





FIGURE 12: Synthetic seismograms for teleseismic SH body waves

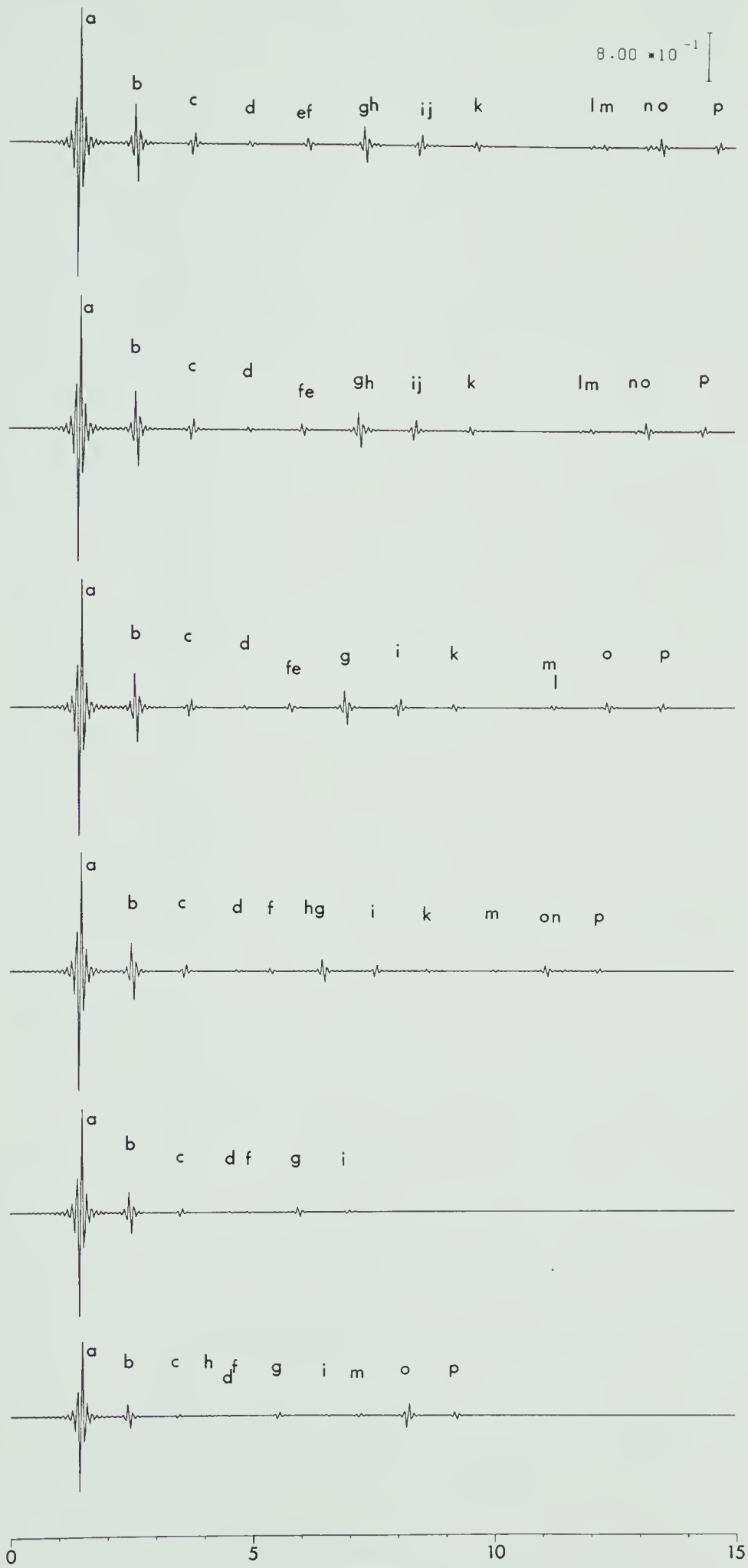
(a) for the perfectly elastic crustal model

( $Q^{-1} = 0$  in each layer, and

(b) for the anelastic crustal model.

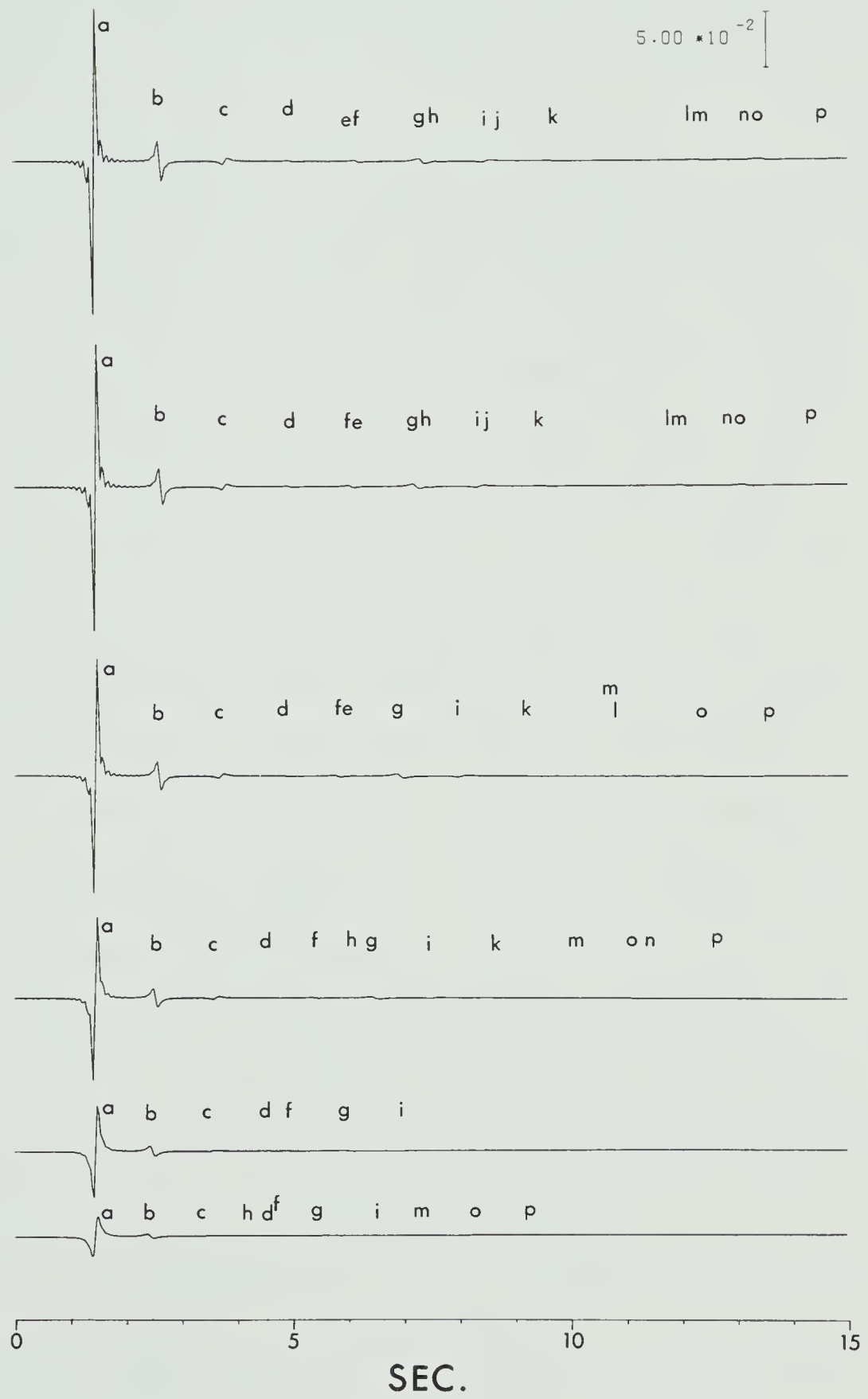
In each figure, from the top down, the angles of incidence for the incoming ray in the half-space are  $0^\circ$ ,  $15^\circ$ ,  $30^\circ$ ,  $45^\circ$ ,  $60^\circ$  and  $75^\circ$ . The scales are shown in the upper right-hand corners. The letters a, b, c, etc., identify the phases contributing the most to the events (see Table 2). The source parameters are  $\eta = 3$  and  $f_0 = 10$  Hz.





(a)





(b)



scale for each trace is shown in the upper right-hand corner. The letters a, b, c, etc., identify the rays contributing the most to the events on the trace, and are listed in Table 2. The numerical code is such that 4 3 2 1 stands for  $S_4 S_3 S_2 S_1$ , etc.

The traces in Figure 12 show the effects of attenuation: the amplitudes are reduced, the oscillations are smoothed out, and the waveform spreads. Many of the later arrivals which appear in the elastic traces do not show up in the anelastic traces, and also, in a given trace, the ratio of the amplitude of a given later arrival to the amplitude of the first arrival is significantly smaller in the anelastic case than in the elastic case. This is to be expected because the amplitude reduction is not only due to reflection/transmission losses, but also to attenuation, which increases monotonically with the ray path length.

## 6.2 Surface Point Source Case

In this case, the SH waves propagating through the medium are generated by a point source situated at the surface, and hence, the expression for the displacement of a given SH ray at the receiver, i.e., equation (6.1), must contain an extra factor  $L$ , representing the geometrical spreading of a ray generated by a point source, i.e.,

$$W = \frac{1}{\pi} \operatorname{Re} \int_0^{\infty} \frac{Y e^{i\phi}}{L} S(\omega) e^{\omega \tau_I} e^{i\omega(t-\tau_R)} d\omega \quad (6.16)$$





TABLE 2  
 RAY CODES FOR THE TELESEISMIC  
 SYNTHETIC SEISMOGRAMS

Letter Code	Numerical Code
a	4 3 2 1
b	4 3 2 1 1 1
c	4 3 2 1 1 1 1 1
d	4 3 2 1 1 1 1 1 1 1
e	4 3 2 1 1 1 1 1 1 1 1 1
f	4 3 2 2 2 1
g	4 3 2 1 1 2 2 1
h	4 3 3 3 2 1
i	4 3 2 1 1 1 1 2 2 1
j	4 3 3 3 2 1 1 1
k	4 3 2 1 1 1 1 1 1 2 2 1
l	4 3 2 2 2 1 1 2 2 1
m	4 3 2 2 3 3 2 1
n	4 3 2 1 1 2 2 1 1 2 2 1
o	4 3 2 1 1 2 3 3 2 1
p	4 3 2 1 1 1 1 2 3 3 2 1
q	4 3 2 1 1 1 1 2 2 1 1 1
r	4 3 2 1 1 2 3 3 2 1 1 1



where  $L$  is given by (5.57) for a linear viscoelastic medium. The expressions for  $\tau_R$ ,  $\tau_I$ ,  $S(\omega)$ , etc. are the same as in the previous section, and we again assume that  $Q$  is independent of frequency (which implies that  $L$  is also frequency-independent).

Since the initial ray segment is located in the first layer, which is an anelastic layer, we are faced with the choice of the value of  $\gamma_0$ , the attenuation angle of the initial ray segment. Intuitively, one would expect that the source would generate homogeneous rays, for which  $\gamma_0=0$ , however, in general,  $\gamma_0$  is an arbitrary parameter. We assume only that each ray generated by the source has the same value of  $\gamma_0$ . The expression for the geometrical spreading factor  $L$  in (5.57), gives  $L$  for any value of  $\gamma_0$ . In the examples below, we compute seismograms for three different values of  $\gamma_0$ , and examine their differences.

The synthetic seismograms for the crustal model of Table 1 are shown in Figure 13. Figure 13a shows the results for the case of perfect elasticity ( $Q_S^{-1}$  is equal to zero for each layer) and Figures 13b, 13c and 13d show the results for the anelastic case for  $\gamma_0=-60^\circ$ ,  $0^\circ$  and  $+60^\circ$ , respectively. The source parameters are  $\eta=3$  and  $f_0=15$  Hz. Traces for eight epicentral distances (0-3.5 km) are shown. In each figure the scale is shown in the upper right-hand corner. The letters a to f identify the rays contributing the most to the events on the traces, and are



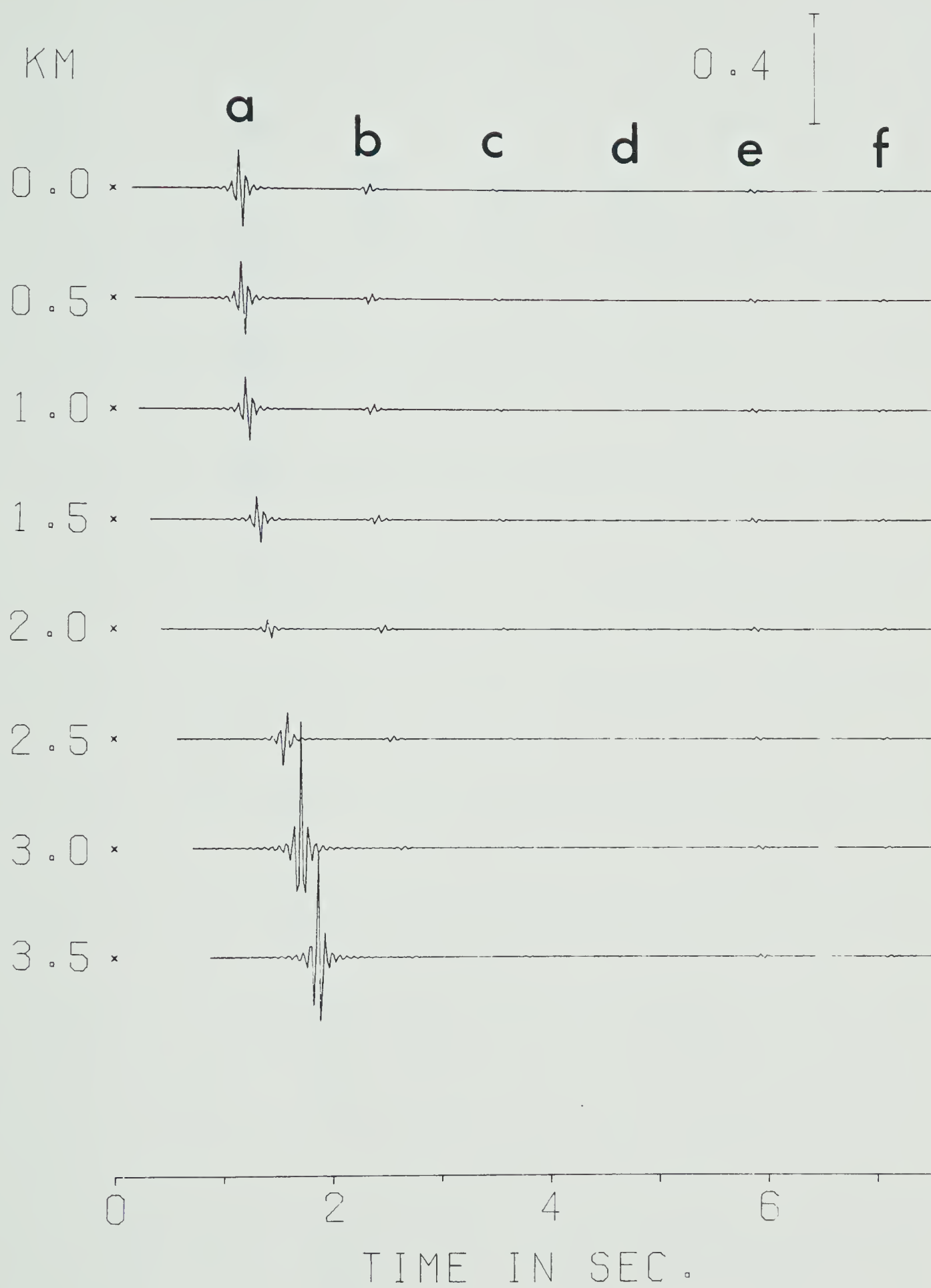
FIGURE 13: Synthetic seismograms for SH body waves generated by a surface point source

(a) for the perfectly elastic crustal model ( $Q^{-1} = 0$  in each layer), and

(b) - (d) for the anelastic crustal model.

The attenuation angle  $\gamma_0$  of the incident ray segment is  $\gamma_0 = -60^\circ$ ,  $0^\circ$  and  $+60^\circ$  in (b), (c) and (d), respectively. Traces for eight epicentral distances from 0 to 3.5 km are shown. The scales are shown in the upper right-hand corners. The letters a, b, c, etc., identify the phases which contribute the most to the events (see Table 3). The source parameters are  $\eta = 3$  and  $f_0 = 15$  Hz.

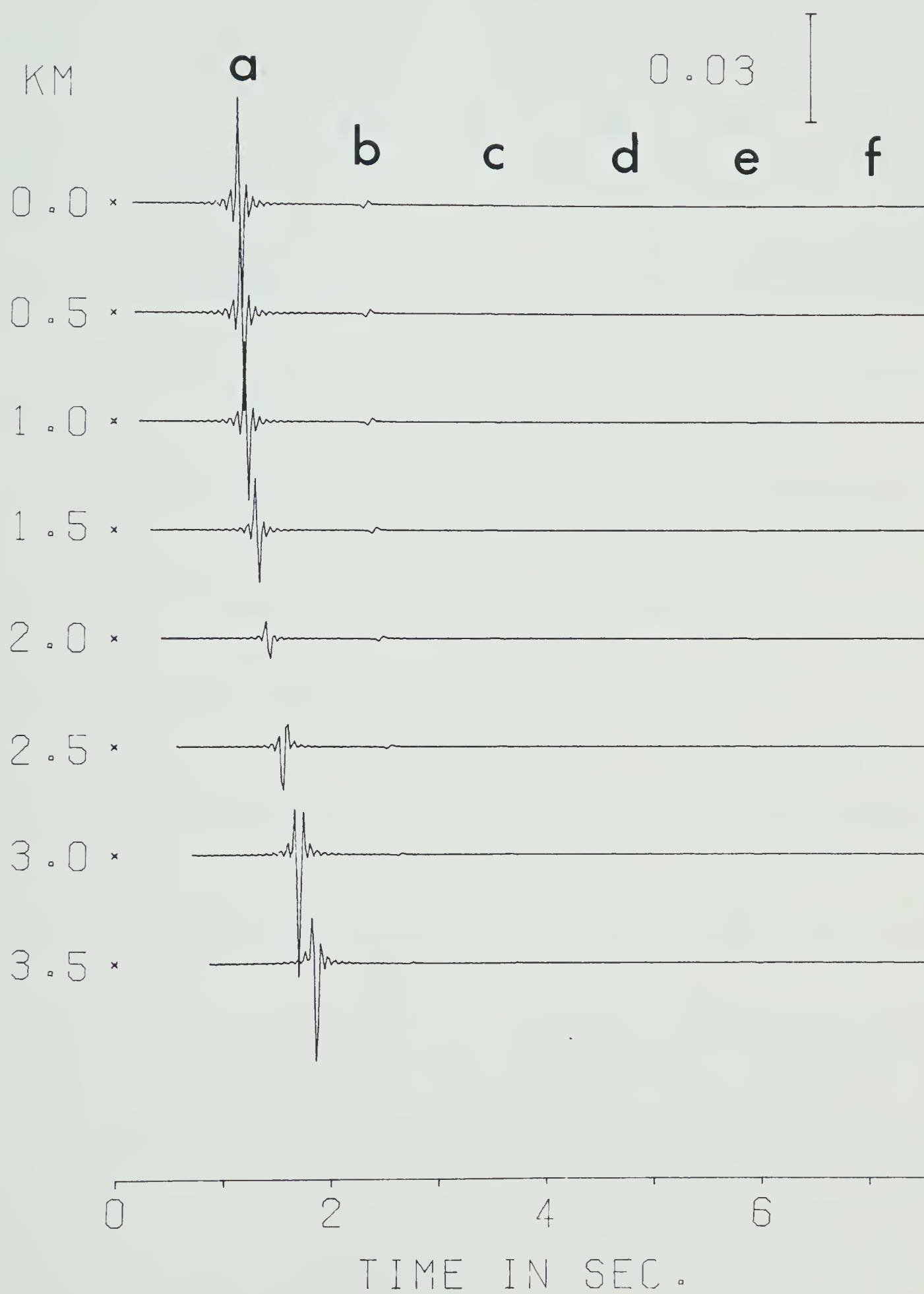




(a)

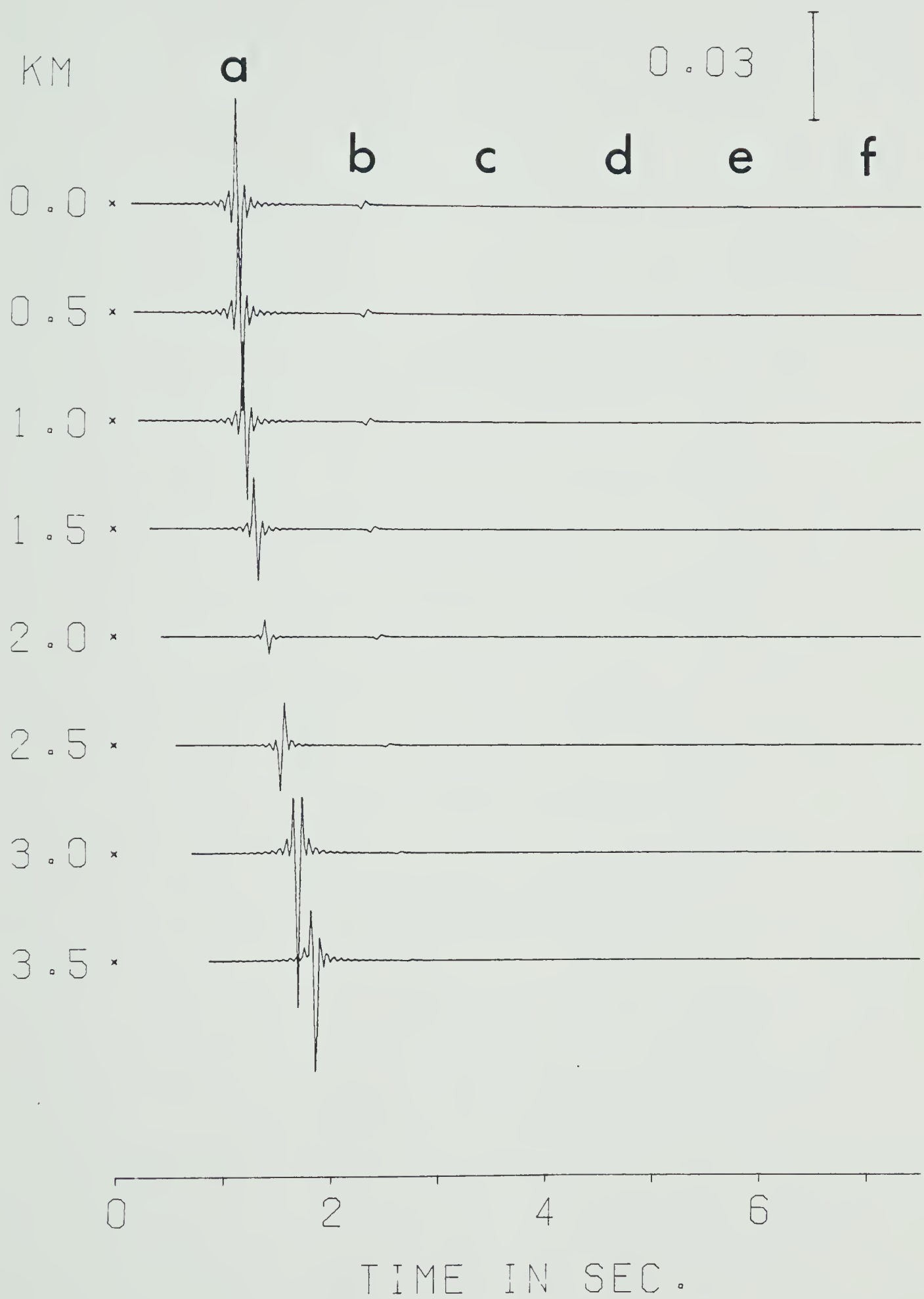






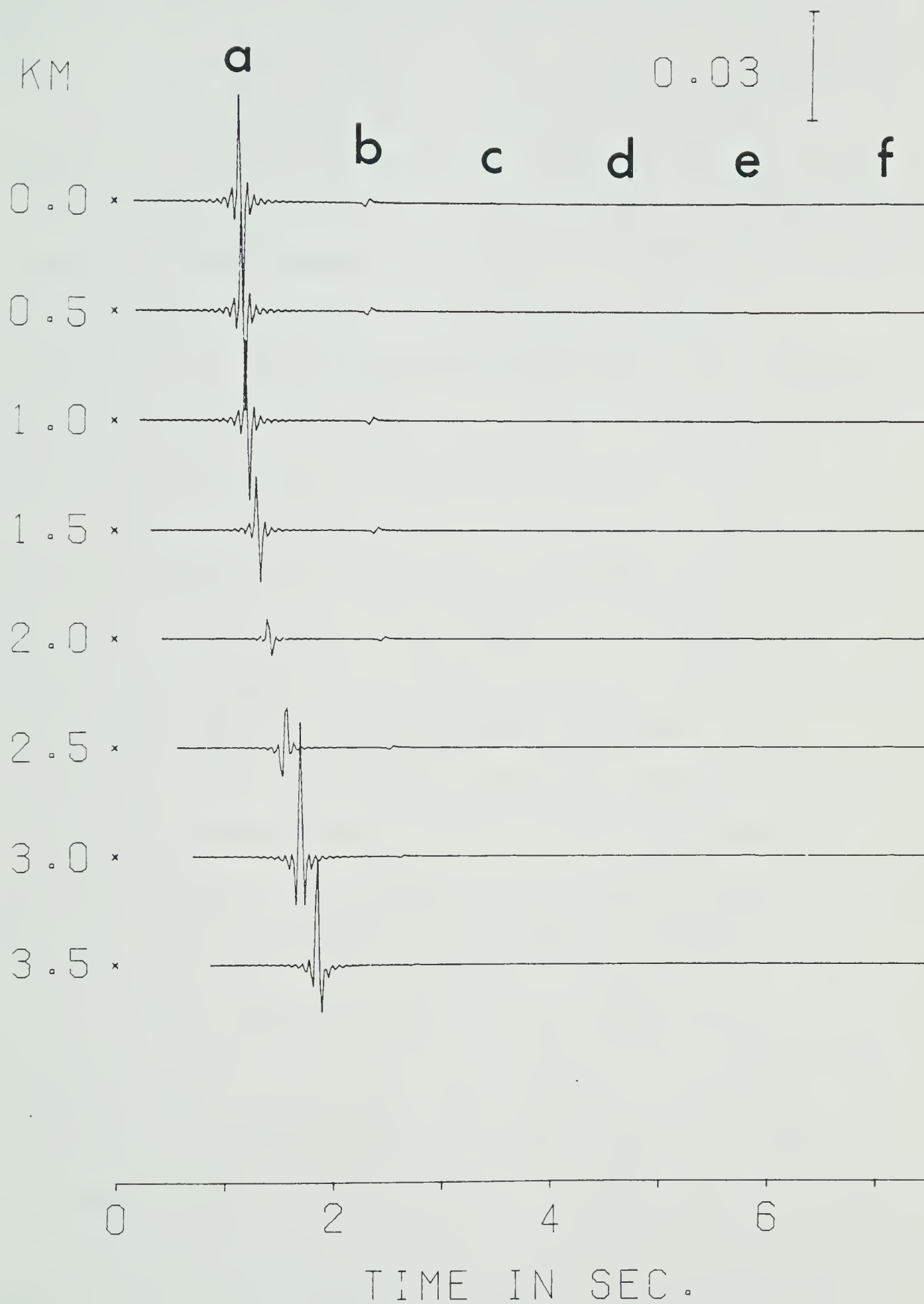
(b)





(c)





(d)



listed in Table 3. The numerical code is the same as for Table 2, i.e., for example, 1 2 2 1 stands for  $S_1 S_2 S_2 S_1$ .

In these seismograms, we do not see as many significant arrivals beyond the initial arrival as we did in the teleseismic case, due to the presence of geometrical spreading, which reduces the amplitudes of the rays. As for the teleseismic case, we can see the effects of attenuation in the reduction of amplitudes, and, for the rays with longer ray paths, the spreading of the waveform and the smoothing-out of the oscillations.

The arrival labelled "a" in the four figures is the primary reflection off the first interface, i.e. the  $S_1 S_1$  ray, and the behaviour of its amplitude and phase for increasing epicentral distances illustrates the behaviour of the HlHl reflection coefficients of Figure 4 for increasing angles of incidence. For the larger epicentral distances, we note a curious behaviour of the phase of the  $S_1 S_1$  arrival. For example, for the epicentral distance of 3 km, which corresponds to an angle of incidence of  $46.97^\circ$  for the  $S_1 S_1$  ray, the phase of  $S_1 S_1$  for the traces with  $\gamma_0 = -60^\circ$  and  $0^\circ$  is roughly  $-\pi/2$  (or  $3\pi/2$ ), whereas the phase of  $S_1 S_1$  for the trace with  $\gamma_0 = +60^\circ$  is roughly  $+\pi/2$ . This can be predicted from the phase curves in Figure 4. The phase of  $S_1 S_1$  in the perfectly elastic case is roughly  $+\pi/2$  at the 3 km mark, which can also be predicted from the phase curve for the perfectly elastic HlHl coefficient,





TABLE 3  
RAY CODES FOR THE SURFACE POINT SOURCE  
SYNTHETIC SEISMOGRAMS

<u>Letter Code</u>	<u>Numerical Code</u>
a	1 1
b	1 1 1 1
c	1 1 1 1 1 1
d	1 1 1 1 1 1 1 1
e	1 2 2 1
f	1 1 1 2 2 1



shown in Figure 14. Hence, if we assume that  $\gamma_0$  must be zero, then we must also be prepared to accept a phase of roughly  $-\pi/2$  for the anelastic  $S_1S_1$  arrival as compared to a phase of roughly  $+\pi/2$  for the elastic  $S_1S_1$  arrival.

Another fact pertaining to the  $S_1S_1$  arrival, obtained from the results of Chapter 4, is that for  $\gamma_0=0^\circ$ , there is no critical angle for the transmitted SH ray. As the angle of incidence  $\theta_0$  increases, the angle of transmission also increases, nearing  $90^\circ$  for  $\theta_0$  greater than about  $43.29^\circ$ , the elastic critical angle, but never quite reaching  $90^\circ$  as  $\theta_0$  increases beyond  $43.29^\circ$ . In other words, no  $S_1S_2S_1$  head wave would be produced for  $\gamma_0=0^\circ$ . Critical angles begin to exist only for  $\gamma_0 \geq 17.43^\circ$  in this case.

We also note that the amplitude of the  $S_1S_1$  arrival at 3 km in the three anelastic cases (Figure 13b-d) is largest for  $\gamma_0=0^\circ$ , which again reflects the behaviour of the HlHl coefficients in Figure 4.



FIGURE 14: HlHl reflection coefficient for the perfectly elastic case. The amplitude curve is the same as curve #1 in Figure 4.



H1H1

RQ1= 0.00000

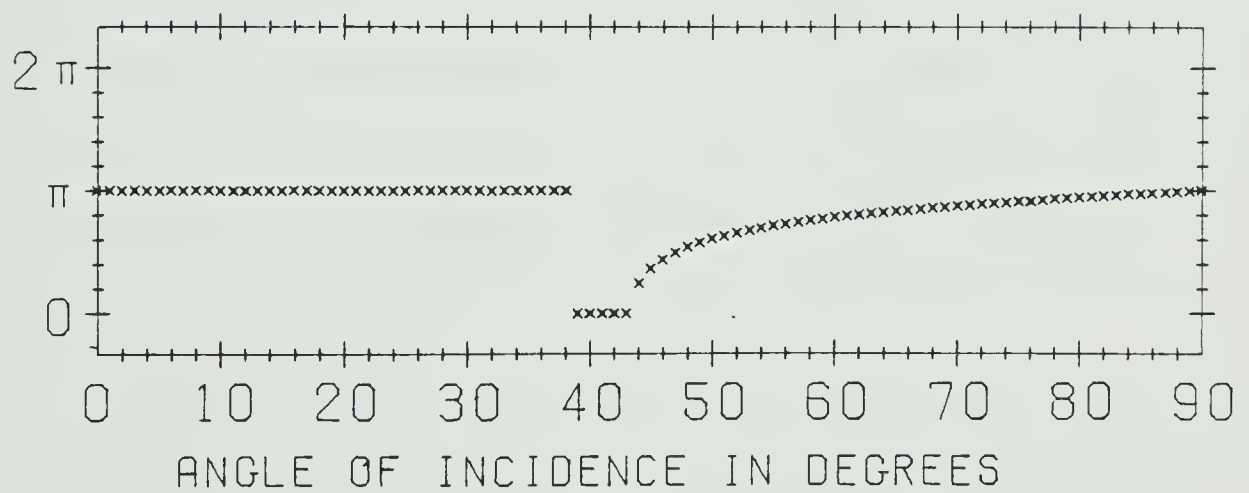
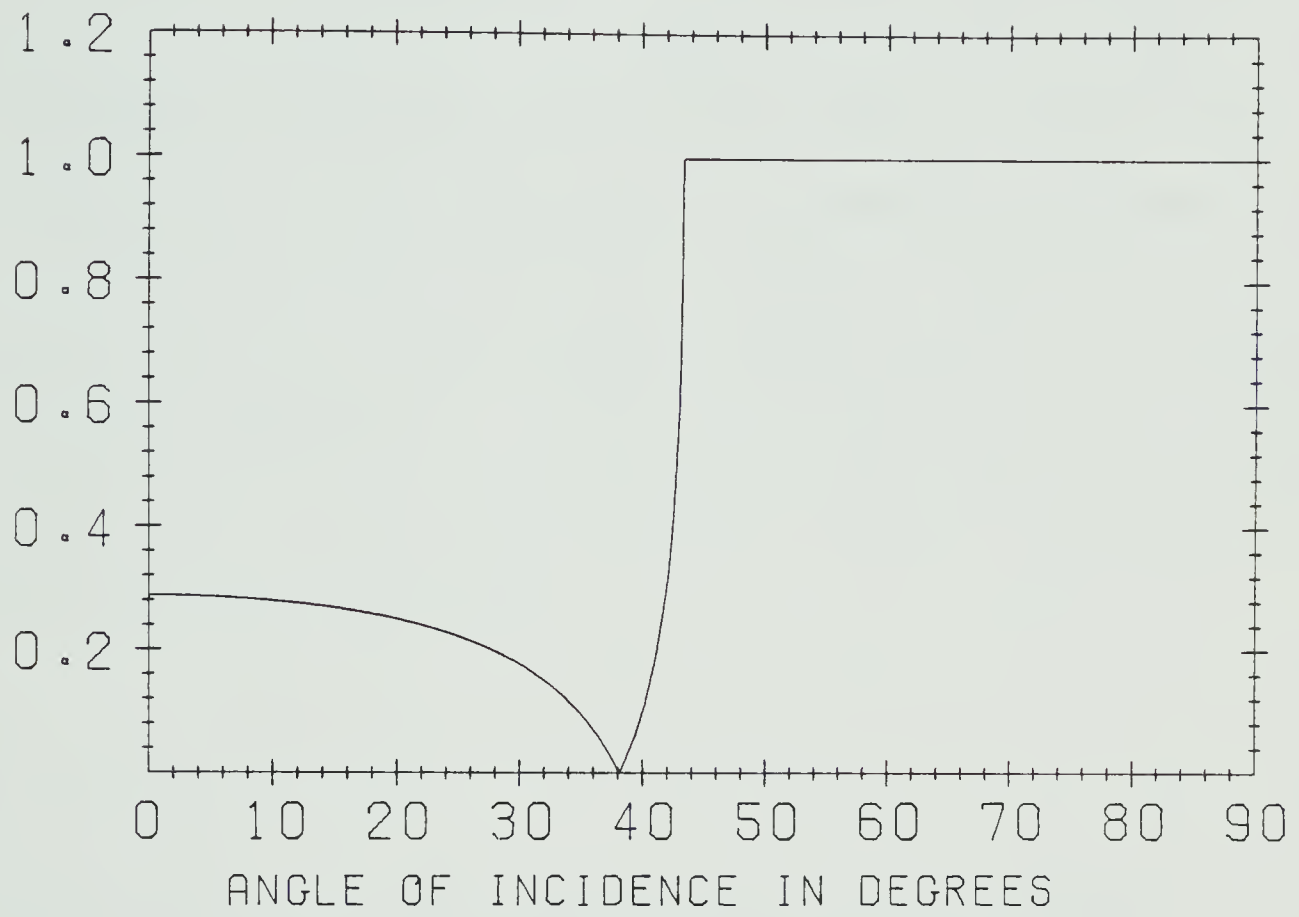
RQ2= 0.00000

DEN1= 2.100

DEN2= 2.600

VH1= 2.400

VH2= 3.500







## FOOTNOTES

[Page 47]

We assume that jump discontinuities in the amplitude and phase curves of reflection/transmission coefficients, such as in Figure 2a, are unphysical because, referring to the amplitude curve, they imply a discontinuous change in the amplitude of the reflected/transmitted wavefront emanating from the interface, which cannot be accounted for by any physical process, since the assumption of homogeneity, isotropy and plane interfaces should guarantee a continuous wavefront. Hence, it is unacceptable physical behaviour.

[Page 89]

Since  $\vec{u}(\vec{r}, t)$  is the real response, we can replace  $(1/2\pi) \int_{-\infty}^{\infty}$  by  $(1/\pi) \operatorname{Re} \int_0^{\infty}$  (see Appendix 2). Also, to avoid divergence problems at  $\omega = 0$ , we replace the lower limit of the integral by  $\omega_1$ , where  $\omega_1$  is small, but greater than zero (see Hron and Kanasewich (1971)).



## REFERENCES

- Borcherdt, R.D. (1973). Energy and plane waves in linear viscoelastic media, *J. Geophys. Res.* 78, 2442-2453.
- Borcherdt, R.D. (1977). Reflection and refraction of type-II S waves in elastic and anelastic media, *Bull. Seism. Soc. Am.* 67, 43-67.
- Buchen, P.W. (1971a). Plane waves in linear viscoelastic media, *Geophys. J.* 23, 531-542.
- Buchen, P.W. (1971b). Reflection, transmission and diffraction of SH-waves in linear viscoelastic solids, *Geophys. J.* 25, 97-113.
- Červený, V. and Ravindra, R. (1971). *Theory of Seismic Head Waves*, U. of Toronto Press, 312 pp.
- Christensen, R.M. (1971). *Theory of Viscoelasticity: an Introduction*, Academic Press, New York, 245 pp.
- Cooper, H.F. Jr. and Reiss, E. L. (1966). Reflection of plane viscoelastic waves from plane boundaries, *J. Acoust. Soc. Am.* 39, 1133-1138.
- Cooper, H.F. Jr. (1967). Reflection and transmission of oblique plane waves at a plane interface between viscoelastic media, *J. Acoust. Soc. Am.* 42, 1064-1069.
- Flügge, W. (1975). *Viscoelasticity*, second edition, Springer-Verlag, New York, 194 pp.
- Fryer, G.J. (1978). Reflectivity of the ocean bottom at low frequency  $\alpha$ , *J. Acoust. Soc. Am.* 63, 35-42.
- Fung, Y.C. (1965). *Foundations of Solid Mechanics*, Prentice-Hall, Inc., New Jersey, 525 pp.
- Futterman, W.I. (1962). Dispersive body waves, *J. Geophys. Res.* 67, 5279-5291.
- Hron, F. and Kanasewich, E.R. (1971). Synthetic seismograms for deep seismic sounding studies using asymptotic ray theory, *Bull. Seism. Soc. Am.* 61, 1169-1200.
- Hron, F., Kanasewich, E.R. and Alpaslan, T. (1974). Partial ray expansion required to suitably approximate the exact wave solution, *Geophys. J.* 36, 607-625.



- Kennett, B.L.N. (1975). The effects of attenuation on seismograms, Bull. Seism. Soc. Am. 65, 1643-1651.
- Lockett, F.J. (1962). The reflection and refraction of waves at an interface between viscoelastic materials, J. Mech. Phys. Solids 10, 53-64.
- Lockett, F.J. (1972). Nonlinear Viscoelastic Solids, Academic Press, New York, 195 pp.
- Schoenberg, M. (1971). Transmission and reflection of plane waves at an elastic-viscoelastic interface, Geophys. J. 25, 35-47.
- Shaw, R.P. and Bugl, P. (1969). Transmission of plane waves through layered linear viscoelastic media, J. Acoust. Soc. Am. 46, 649-654.
- Silva, W. (1976). Body waves in a layered anelastic solid, Bull. Seism. Soc. Am. 66, 1539-1554.



# APPENDIX 1

## FOURIER TRANSFORM OF $f(t)*dg(t)$

Let  $f(t)$  and  $g(t)$  be two arbitrary functions of time  $t$ . The Stieltjes convolution of  $f(t)$  and  $g(t)$  is given by

$$f(t)*dg(t) = \int_{-\infty}^t f(t-\tau) \frac{dg(\tau)}{d\tau} d\tau \quad (A1.1)$$

and its Fourier transform is

$$\begin{aligned} \overline{f*dg} &= \int_{-\infty}^{\infty} f(t)*dg(t) e^{-i\omega t} dt \\ &= \int_{-\infty}^{\infty} \left[ \int_{-\infty}^t f(t-\tau) \frac{dg(\tau)}{d\tau} d\tau \right] e^{-i\omega t} dt \end{aligned} \quad (A1.2)$$

Changing the order of integration, we get

$$\overline{f*dg} = \int_{-\infty}^{\infty} \left[ \int_{\tau}^{\infty} f(t-\tau) e^{-i\omega t} dt \right] \frac{dg(\tau)}{d\tau} d\tau \quad (A1.3)$$

Letting  $t-\tau=\xi$ , the  $t$ -integral becomes

$$\int_{\tau}^{\infty} f(t-\tau) e^{-i\omega t} dt = e^{-i\omega \tau} \int_0^{\infty} f(\xi) e^{-i\omega \xi} d\xi \quad (A1.4)$$

Hence

$$\begin{aligned} \overline{f*dg} &= \left[ \int_0^{\infty} f(t) e^{-i\omega t} dt \right] \int_{-\infty}^{\infty} e^{-i\omega \tau} \frac{dg(\tau)}{d\tau} d\tau \\ &= [\dots] \left\{ e^{-i\omega \tau} g(\tau) \Big|_{-\infty}^{\infty} - (-i\omega) \int_{-\infty}^{\infty} g(\tau) e^{-i\omega \tau} d\tau \right\} \\ &= F\overline{g} \end{aligned} \quad (A1.5)$$

where





$$F = F(\omega) = i\omega \int_0^{\infty} f(t) e^{-i\omega t} dt$$
$$\bar{g} = \bar{g}(\omega) = \int_{-\infty}^{\infty} g(t) e^{-i\omega t} dt$$
(A1.6)



APPENDIX 2

THE INVERSE FOURIER TRANSFORM  
FOR A REAL RESPONSE

Let us assume that the response  $f(t)$  at the receiver is a real function of time  $t$ , i.e.

$$f(t) = f^*(t) \quad (\text{A2.1})$$

where the  $*$  denotes the complex conjugate. Then, from its Fourier transform

$$\bar{f}(\omega) = \int_{-\infty}^{\infty} f(t) e^{-i\omega t} dt \quad (\text{A2.2})$$

we have

$$\begin{aligned} \bar{f}^*(\omega) &= \int_{-\infty}^{\infty} f^*(t) e^{i\omega t} dt \\ &= \int_{-\infty}^{\infty} f(t) e^{i\omega t} dt \\ &= \bar{f}(-\omega) \end{aligned} \quad (\text{A2.3})$$

Hence

$$\begin{aligned} f(t) &= \frac{1}{2\pi} \int_{-\infty}^{\infty} \bar{f}(\omega) e^{i\omega t} d\omega \\ &= \frac{1}{2\pi} \left[ \int_{-\infty}^0 (\dots) + \int_0^{\infty} (\dots) \right] \\ &= \frac{1}{2\pi} \left[ \int_0^{\infty} \bar{f}(-\omega) e^{-i\omega t} d\omega + \int_0^{\infty} \bar{f}(\omega) e^{i\omega t} d\omega \right] \\ &= \frac{1}{2\pi} \int_0^{\infty} [\bar{f}^*(\omega) e^{-i\omega t} + \bar{f}(\omega) e^{i\omega t}] d\omega \end{aligned}$$



$$\begin{aligned}
&= \frac{1}{2\pi} \int_0^{\infty} [\{\bar{f}(\omega) e^{i\omega t}\}^* + \{\bar{f}(\omega) e^{i\omega t}\}] d\omega \\
&= \frac{1}{2\pi} \int_0^{\infty} [2 \operatorname{Re}\{\bar{f}(\omega) e^{i\omega t}\}] d\omega \\
&= \frac{1}{\pi} \operatorname{Re} \int_0^{\infty} \bar{f}(\omega) e^{i\omega t} d\omega \tag{A2.4}
\end{aligned}$$

Hence, if  $f(t)$  is real, we can use the form  $(1/\pi) \operatorname{Re} \int_0^{\infty}$  rather than the form  $(1/2\pi) \int_{-\infty}^{\infty}$ . The integrand of (5.1) satisfies (A2.3) if the various terms are defined appropriately for negative frequencies.





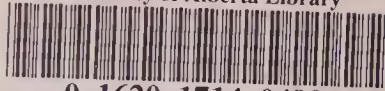








University of Alberta Library



0 1620 1714 0490

**B30276**